

BIOBUTANOL DEHYDRATION USING OAT HULL BASED BIOSORBENT

A Thesis Submitted to the
College of Graduate and Postdoctoral Studies
In Partial Fulfillment of the Requirements
For the Degree of Doctor of Philosophy
In the Department of Chemical & Biological Engineering
University of Saskatchewan
Saskatoon

By

Qian Huang

© Copyright Qian Huang, October, 2020. All rights reserved.
Unless otherwise noted, copyright of the material in this thesis belongs to the author.

PERMISSION TO USE

In presenting this thesis in partial fulfillment of the requirements for a Postgraduate degree from the University of Saskatchewan, I agree that the Libraries of this University may make it freely available for inspection. I further agree that permission for copying of this thesis in any manner, in whole or in part, for scholarly purposes may be granted by Dr. Catherine Niu and Dr. Ajay Dalai who supervised my thesis work or, in their absence, by the Head of the Department or the Dean of the College in which my thesis work was done. It is understood that any copying or publication or use of this thesis or parts thereof for financial gain shall not be allowed without my written permission. It is also understood that due recognition shall be given to me and to the University of Saskatchewan in any scholarly use which may be made of any material in my thesis.

DISCLAIMER

Reference in this thesis to any specific commercial products, process, or service by trade name, trademark, manufacturer, or otherwise, does not constitute or imply its endorsement, recommendation, or favoring by the University of Saskatchewan. The views and opinions of the author expressed herein do not state or reflect those of the University of Saskatchewan, and shall not be used for advertising or product endorsement purposes.

Requests for permission to copy or to make other uses of materials in this thesis in whole or part should be addressed to:

Head of the Department of Chemical & Biological Engineering

57 Campus Dr.

University of Saskatchewan

Saskatoon, Saskatchewan S7N 5A9 Canada

OR

Dean

College of Graduate and Postdoctoral Studies

University of Saskatchewan

116 Thorvaldson Building, 110 Science Place

Saskatoon, Saskatchewan S7N 5C9 Canada

ABSTRACT

Biobutanol has gained increasing interest due to its application in fuel industry. Butanol has lower vapor pressure, higher energy content, and less corrosive character than ethanol, which makes butanol a superior fuel additive. Usually, biobutanol is produced by the acetone-butanol-ethanol (ABE) fermentation process from renewable feedstock. To obtain pure butanol from the fermentation broth, preliminary distillation is usually applied to remove acetone and ethanol from butanol. Then, the decantation and two-column distillation are used to separate butanol from heterogeneous azeotrope of butanol and water (butanol composition of 55.5 wt%). This leads to high energy consumption to break the butanol and water azeotrope. Therefore, efforts have been made to develop various approaches to separate water from the butanol-water azeotrope. Among these approaches, adsorption is known as an effective method for separation and purification due to its low cost, high efficiency, and easy operation.

With regard to the reasons mentioned above, the goal of this research is to develop an alternative technology of sorption to remove water directly from the butanol-water azeotrope vapor generated from the distillation in the biobutanol industry in to reduce or replace the downstream decantation and distillations in the biobutanol industry. This work also aims to investigate the isotherm, mechanisms, and kinetics aspects of water and butanol sorption by natural material based biosorbents.

The overall research is divided into 5 phases:

In Phase I, a biosorbent was developed from the oat hull, and the biosorbent was characterized by various methods. In addition, the water sorption on the biosorbent was visualized with the aid of microscope imaging. The oat hull based biosorbent was used to dehydrate butanol in a packed column in order to produce biofuel products. The sorption performance and the separation factors of water over butanol on the biosorbent were determined. Through the dehydration process

developed for this work, high purity butanol products (95.3%, 97.1%, 98.1%, and 99.0%) were achieved from low-grade butanol-water mixtures (56.6%, 69.1%, 79.7%, and 90.3%). The highest water sorption capacity is 146 ± 8 mg/g, and the highest separation factor of water over butanol is 2.94 ± 0.13 . The results indicate the oat hull based biosorbent has the capability for butanol dehydration. The effects of parameters were investigated, and the effects of temperature and feed concentration are significant.

In Phase II, the water sorption equilibrium data obtained from the single component system and butanol-water binary system was simulated by the Dubinin-Polanyi model. Besides, the equilibrium data of butanol sorption on the biosorbent was studied. The results indicate the large pore Dubinin-Polanyi model is able to describe water and butanol sorption equilibrium data. The approximate adsorption site energy distribution was calculated to further analyze the equilibrium data. The site energy distribution shows the maximum water sorption capacity is much higher than that of butanol in either the single or binary system. The weighted mean site energy for water sorption in the butanol-water binary system is 2378 J/mol, which is higher than that of butanol (2105 J/mol), showing water has a higher affinity on the biosorbent. The thermodynamic study provided evidence of the physical and exothermic nature of the sorption process. The dipole-dipole attraction may suggest the mechanism of water and butanol molecules sorption on the biosorbent.

To better understand the fundamentals of water and butanol sorption, Phase III investigated the sorption dynamics of pure butanol and pure water. The Klinkenberg model simulated the sorption breakthrough curves obtained in pure water or pure butanol single component sorption system satisfactorily. The mass transfer coefficient and mass transfer resistances were investigated from the modeling results. The sorption of pure water or butanol on the oat hull based biosorbent was controlled by mass transfer. The values of overall mass transfer resistance of pure water

sorption are lower than those of butanol at the same conditions, which suggests that water has more favorable sorption performance than butanol.

In Phase IV, the dynamics of water sorption from butanol-water vapor mixtures in a fixed bed column were investigated. Water sorption breakthrough curves in the binary system were simulated by the Bohart-Adams model and Klinkenberg model. The Klinkenberg model is better for simulating the breakthrough curves. This implies that the water sorption mechanism and dynamics are more likely to follow the Klinkenberg model's theory. The rate of water sorption was controlled by mass transfer resistance based on the estimated values of mass transfer resistances. The kinetically driven competitive sorption of butanol and water was discussed to explain the basis of the separation of the butanol-water mixture by the oat hull biosorbent. Compared to butanol, water has a more favorable sorption performance on the oat hull biosorbent. Thus, this biosorbent is able to dehydrate butanol solutions.

Phase V involved the reusability study of the oat hull based biosorbent. The biosorbent was regenerated and reused in the same column without being changed. It was demonstrated that the biosorbent derived from the oat hull used in this study was regenerated and reused successfully for more than 20 cycles with satisfactory performance and high stability. The oat hull based biosorbent used in this work is able to be used continually. The preliminary economic analysis shows the production of anhydrous biobutanol by pressure swing adsorption process using the oat hull based biosorbent is more economical with 29% lower utilities cost than using the traditional adsorbent molecular sieves.

The aforementioned studies demonstrated that the oat hull based biosorbent is able to dehydrate the water/butanol binary azeotrope (butanol composition of 55.5 wt%) and the feed of higher butanol concentrations of 56.6–90.3 wt.% through the dynamic sorption process.

ACKNOWLEDGEMENTS

Foremost, I would like to express my sincere gratitude to my supervisors Dr. Catherine Niu and Dr. Ajay Dalai for their great support and guidance throughout the program. They led me to start this research and helped me carry out research professionally.

My genuine thanks also go to my advisory committee members: Dr. Jaffar Soltan, Dr. Lifeng Zhang, Dr. Oon-Doo Baik, and Dr. Renfei Feng for their guidance and suggestions in this work. I really appreciate their help.

This work was supported by MITACS, Natural Sciences and Engineering Research Council of Canada, Canada Foundation for Innovation, Saskatchewan Ministry of Agriculture and the Canada-Saskatchewan Growing Forward 2-bilateral agreement, Saskatchewan Canola Development Commission, and the Western Grains Research Foundation. All these financial supports are highly appreciated.

I sincerely thank Richardson Milling Ltd. for providing free oat hull samples. I also greatly appreciate the help from the Nano-Science Technology Center (University of Central Florida) for technical assistance in microscope imaging.

Last but not least, I would like to thank all members of the Chemical and Biological Engineering Department and all the members of the Biosorption Group for their kindness and support. My special thanks go to Mr. Richard Blondin and Mr. RLee Prokopishyn for their technical support. I sincerely thank all my friends throughout this journey for their advice, encouragement, and love.

DEDICATION

To my dear parents, Mr. Yong Huang and Mrs. Jianbo Liu, for their selfless true love and support throughout my life.

To my beloved husband, Mr. Qiwei Yu, for his company throughout the program and his dedication to our family. To my beloved daughter, Lyra Yu, for her inspiration every day.

TABLE OF CONTENTS

PERMISSION TO USE.....	i
ABSTRACT.....	iii
ACKNOWLEDGEMENTS.....	vi
DEDICATION.....	vii
TABLE OF CONTENTS.....	viii
LIST OF TABLES.....	xiii
LIST OF FIGURES.....	xv
ABBREVIATIONS AND NOMENCLATURE.....	xx
CHAPTER 1. INTRODUCTION AND THESIS OUTLINE.....	1
1.1 Research motivation.....	1
1.2 Knowledge gaps.....	4
1.3 Hypothesis.....	5
1.4 Research Objectives.....	5
1.5 Research phases.....	6
1.6 Thesis Outline.....	8
1.7 Publications.....	9
CHAPTER 2. LITERATURE REVIEW.....	11
2.1 Biobutanol.....	11
2.2 Production and purification of biobutanol.....	13
2.3 Methods for biobutanol recovery.....	16
2.3.1 Distillation.....	17
2.3.2 Gas stripping.....	18
2.3.3 Extraction.....	18

2.3.4 Membrane pervaporation	19
2.3.5 Adsorption	20
2.4 Adsorption for alcohols dehydration	22
2.4.1 Pressure swing adsorption in a packed column	23
2.4.2 Inorganic adsorbents	24
2.4.3 Biosorbents	25
2.5 Adsorption equilibrium in alcohols dehydration	29
2.5.1 Isotherms and modeling.....	29
2.5.2 Site energy distribution analysis	31
2.6 Dynamics study in alcohols dehydration in packed columns	33
2.7 Mechanisms of alcohols dehydration using biosorbents	35
CHAPTER 3. MATERIALS AND METHODS	38
3.1 Materials	38
3.2 Characterization methods used for oat hull based biosorbent	38
3.3 Experimental apparatuses	40
3.4 Dehydration and sorption experiments	42
3.4.1 Sorption of pure water or butanol in the single component system.....	44
3.4.2 Dehydration in the butanol-water binary system.....	44
3.5 Desorption.....	45
CHAPTER 4. PREPARATION AND CHARACTERIZATION OF AN OAT HULL BASED BIOSORBENT	46
4.1 Preparation of oat hull based biosorbent.....	46
4.2 Characterization results of the biosorbent.....	47

4.2.1 Surface properties and particle size distribution	47
4.2.2 Thermal stability	48
4.2.3 FTIR spectra	49
4.2.4 SEM analysis	51
4.2.5 Coomassie blue staining and optical microscopy imaging	52
4.3 Chapter summary	54
CHAPTER 5. PRODUCTION OF ANHYDROUS BIOBUTANOL USING THE OAT HULL BASED BIOSORBENT	56
5.1 Performance of oat hull biosorbent for pure water or pure butanol sorption.....	56
5.2 Performance of oat hull biosorbent for butanol dehydration	59
5.3 Effects of the operation parameters of the butanol-water binary system.....	64
5.3.1 Effect of temperature	64
5.3.2 Effect of pressure	65
5.3.3 Effect of feed concentration.....	67
5.3.4 Effect of particle size	68
5.3.5 Effect of different batches of oat hulls.....	70
5.4 Chapter summary	72
CHAPTER 6. EQUILIBRIUM AND MODELING STUDY OF WATER AND BUTANOL SORPTION.....	74
6.1 Equilibrium and modeling study of water sorption	74
6.1.1 Equilibrium study of pure water sorption	76
6.1.2 Water sorption equilibrium study in binary mixture system	78
6.2 Site energy distribution analysis of the biosorbent for water sorption	82

6.3 Equilibrium and modeling study of butanol sorption	87
6.3.1 Equilibrium study of pure butanol sorption	87
6.3.2 Butanol sorption equilibrium study in binary mixture system	89
6.4 Site energy distribution analysis of the biosorbent for butanol sorption	92
6.5 Thermodynamic study	95
6.6 Chapter summary	96
CHAPTER 7. DYNAMIC AND MODELING STUDY OF PURE WATER AND PURE BUTANOL SORPTION.....	98
7.1 Dynamic study and models considered in this chapter	98
7.2 Sorption of water and butanol at different temperatures	102
7.3 Sorption of water and butanol at different feed concentrations	107
7.4 Chapter summary	111
CHAPTER 8. DYNAMICS OF WATER SORPTION FROM BUTANOL-WATER VAPOR	112
8.1 Dynamic models	112
8.1.1 Bohart-Adams model	114
8.1.2 Klinkenberg model	115
8.2 Simulation of water breakthrough curves and comparisons	117
8.3 Interpretation of water sorption data obtained at different sorption temperatures	120
8.4 Simulation of water breakthrough curves at different feed concentrations	122
8.5 Discussion of competitive sorption between water and butanol.....	124
8.6 Discussion on sorption mechanism.....	126
8.7 Chapter summary	128
CHAPTER 9. REUSABILITY STUDY OF THE OAT HULL BIOSORBENT.....	129

9.1 Reusability of the biosorbent in the binary system.....	129
9.2 Reusability of the biosorbent in pure water or pure butanol system.....	131
9.3 Economic analysis of butanol dehydration.....	132
9.3.1 Butanol dehydration in a pressure swing adsorption process	132
9.3.2 Total capital cost and manufacturing cost estimation.....	134
9.4 Chapter summary	137
CHAPTER 10. CONCLUSIONS, ORIGINAL CONTRIBUTIONS AND	
RECOMMENDATIONS	139
10.1 Overall conclusions and original contributions to knowledge development	139
10.2 Recommendations for future work	143
REFERENCES	145
APPENDIX A. FREUNDLICH MODELING RESULTS OF WATER AND BUTANOL	
SORPTION.....	164
APPENDIX B. THE MEAN FREE ENERGY.....	167
APPENDIX C. ECONOMIC ANALYSIS FOR BUTANOL DEHYDRATION BY	
DISTILLATION.....	169

LIST OF TABLES

Table 2.1 Comparison of butanol with other biofuels and conventional fossil fuels (Rathour et al., 2018).	13
Table 2.2 Different types of substrates and microorganisms used in butanol production (Rathour et al., 2018).	15
Table 5.1 Sorption capacities of water and butanol on oat hull and separation factors (135 kPa, 110 °C, 0.425–1.18 mm).	61
Table 5.2 Comparison of water sorption capacity of different biosorbents at similar conditions.	62
Table 5.3 Sorption capacities of water and butanol on oat hull at different temperatures (135 kPa, 0.425–1.18 mm).	64
Table 5.4 Sorption capacities and separation factor of water and butanol on oat hull at different pressure (110 °C, 0.425–1.18 mm particle size).	66
Table 5.5 Sorption capacities of water and butanol on oat hull at different particle sizes (110 °C, 135 kPa).	69
Table 5.6 Sorption capacities of water and butanol on the biosorbent with different batches (110 °C, 135 kPa, 0.425–1.18 mm particle size).	71
Table 6.1 Fitting results of the Dubinin-Polanyi models of pure water sorption.	78
Table 6.2 Fitting results of the Dubinin-Polanyi models of water sorption in binary system.	82
Table 6.3 Fitting results of the Dubinin-Polanyi models of pure butanol sorption.	89
Table 6.4 Fitting results of the Dubinin-Polanyi models of butanol sorption in the binary system.	91
Table 6.5 Thermodynamic parameters for water and butanol sorption on the biosorbent.	96

Table 7.1 Fitting results of the Klinkenberg model at different temperatures.	105
Table 7.2 Fitting results of the Klinkenberg model at different feed concentrations.....	110
Table 8.1 Fitting results of water breakthrough curves by the Bohart-Adams model and the Klinkenberg model (135 kPa, 44 wt% water and 56 wt% butanol in the feed).....	120
Table 8.2 Results of water mass transfer study for water sorption in the binary system at different sorption temperatures based on the Klinkenberg modeling results.	121
Table 8.3 Results of mass transfer study for water sorption in the binary system at different feed concentrations based on the Klinkenberg modeling results.....	124
Table 9.1 Summary of economic analysis for butanol dehydration by PSA using different adsorbents.	137
Table A.1 Fitting results of the Freundlich model for pure butanol and pure water sorption....	166
Table B.1 Fitting results of the Freundlich model for pure butanol and pure water sorption....	167
Table C.1 Summary of economic analysis for butanol dehydration by adsorption.	169
Table C.2 Summary of economic analysis for butanol dehydration by distillation.....	170

LIST OF FIGURES

Figure 3.1 Schematic diagram of the experimental setup.....	41
Figure 4.1 Particle size distribution of the biosorbent.	48
Figure 4.2 Thermogravimetric curves of the oat hull based biosorbent (0.425–1.18 mm particle size).	49
Figure 4.3 (a) FTIR spectra of oat hull based biosorbent; (b) FTIR spectra of two different batch oat hull based biosorbent.	50
Figure 4.4 SEM images of oat hull based biosorbent (a) before sorption; (b) after sorption and regeneration.....	51
Figure 4.5 Coomassie blue stained oat hull (a) imaged using a 20x objective; (b) imaged using a 100x objective (Scale bars, 50 μ m).	52
Figure 4.6 Optical microscopy image of oat hull particles after water-dye solution sorption.....	53
Figure 4.7 Time lapse images of an oat hull particle upon the addition of the solution using a 50x objective (Scale bar, 50 μ m).	54
Figure 5.1 The breakthrough curves of water sorption on the biosorbent at 120 °C, 135 kPa at different feed concentrations. Error bars represent standard deviations.	57
Figure 5.2 The breakthrough curves of butanol sorption on the biosorbent at 120 °C, 135 kPa at different feed concentrations.....	58
Figure 5.3 The equilibrium sorption capacity of water and butanol on the biosorbent at 120 °C, 135 kPa.....	59
Figure 5.4 Butanol product concentration profiles during dehydration at 110 °C, 135 kPa, and 3 mL/min liquid feed rate with different feeding concentrations.	63

Figure 5.5 Butanol product concentration profiles at different sorption temperatures (135 kPa, 56 wt.% butanol in feeding concentration, 0.425–1.18 mm particle size).	65
Figure 5.6 Butanol product concentration profiles at different pressure (110 °C, 56 wt.% butanol in feeding concentration, 0.425–1.18 mm particle size).....	67
Figure 5.7 Butanol product concentration profiles using different particle sizes (110 °C, 135 kPa, 56 wt.% butanol in feeding concentration).	70
Figure 5.8 Butanol product concentration profiles on the biosorbent with different batch (110 °C, 135 kPa, 56.6 wt.% butanol in feeding concentration, 0.425–1.18 mm particle size)...	72
Figure 6.1 (a) Water sorption isotherm in the pure water system, (b) Equilibrium water sorption data in the pure water system and fitting results of the large pore Dubinin-Polanyi model. Pressure of 135 kPa, temperature of 120 °C, carrier gas flow rate 680 mL/min.	77
Figure 6.2 Equilibrium water sorption data in the pure water system and fitting results of the micropore Dubinin-Polanyi model (pressure of 135 kPa, temperature of 120 °C, carrier gas flow rate 680 mL/min).	78
Figure 6.3 Water sorption characteristic curve based on the Polanyi adsorption potential theory (pressure of 135 kPa, temperature of 110–120 °C, carrier gas flow rate 680 mL/min).	79
Figure 6.4 Equilibrium water sorption data in the binary butanol-water system and fitted curve of large pore Dubinin-Polanyi model (pressure of 135 kPa, temperature of 110–120 °C, carrier gas flow rate 680 mL/min).....	80
Figure 6.5 Equilibrium water sorption data in the binary butanol-water system and fitted curve of micropore Dubinin-Polanyi model (pressure of 135 kPa, temperature of 110–120 °C, carrier gas flow rate 680 mL/min).....	81

Figure 6.6 Site energy distribution of oat hull biosorbent for water sorption according to the large pore Dubinin-Polanyi model.....	85
Figure 6.7 Butanol sorption data in the single system and fitting curve of the large pore Dubinin-Polanyi model (pressure of 135 kPa, temperature of 120 °C, carrier gas flow rate 680 mL/min).	88
Figure 6.8 Butanol sorption data in the single system and fitting curve of the micropore Dubinin-Polanyi model (pressure of 135 kPa, temperature of 120 °C, carrier gas flow rate 680 mL/min).	88
Figure 6.9 Butanol sorption data in the butanol-water binary system and fitting curve of the large pore Dubinin-Polanyi model (pressure of 135 kPa, temperature of 110–120 °C, carrier gas flow rate 680 mL/min).	90
Figure 6.10 Butanol sorption data in the butanol-water binary system and fitting curve of the micropore Dubinin-Polanyi model (pressure of 135 kPa, temperature of 110–120 °C, carrier gas flow rate 680 mL/min).	91
Figure 6.11 Site energy distribution of oat hulls for butanol sorption according to the large pore Dubinin-Polanyi model.	94
Figure 7.1 Breakthrough curves of water sorption on the biosorbent at different temperatures and the simulation curves of the Klinkenberg model (feed water concentration of 0.65 mol/mol, 135 kPa).	103
Figure 7.2 Breakthrough curves of butanol sorption on the biosorbent at different temperatures and the simulation curves of the Klinkenberg model (feed concentration of 0.65 mol/mol, 135 kPa).	104

Figure 7.3 Breakthrough curves of water sorption on the biosorbent at different feed concentrations and the simulation curves of the Klinkenberg model (120 °C, 135 kPa).	107
Figure 7.4 Breakthrough curves of butanol sorption on the biosorbent at different feed concentrations and the simulation curves of the Klinkenberg model (120 °C, 135 kPa).	108
Figure 8.1 Breakthrough curves of water sorption on the biosorbent (pressure of 135 kPa, 44 wt% water and 56 wt% butanol in the feed, carrier gas flow rate 680 mL/min) at different temperatures, and simulation curves of the Bohart-Adams model.	118
Figure 8.2 Breakthrough curves of water sorption on the biosorbent (pressure of 135 kPa, 44 wt% water and 56 wt% butanol in the feed, carrier gas flow rate 680 mL/min) at different temperatures, and simulation curves of the Klinkenberg model.....	119
Figure 8.3 Breakthrough curves of butanol dehydration at different feed concentrations (pressure of 135 kPa, temperature of 110 °C, carrier gas flow rate 680 mL/min) and the simulation curves of the Klinkenberg model.	124
Figure 8.4 The water and butanol uptake versus time (56 wt.% butanol feed concentration, 120 °C, 135 kPa).	126
Figure 9.1 The profile of butanol concentration in effluent on the fresh and regenerated bed at 110 °C, 135 kPa, and 56 wt% butanol feed concentration.	130
Figure 9.2 FTIR spectra of the fresh oat hull biosorbent and FTIR spectra of reused and regenerated oat hull biosorbent.	130
Figure 9.3 Breakthrough curves of the fresh and regenerated bed at 120 °C, 135 kPa: (a) water sorption; (b) butanol sorption.....	132
Figure 9.4 Simulation in Aspen Adsorption.	133

Figure A.1 Fit curves of the Freundlich model for pure water and pure butanol sorption on the biosorbent..... 165

ABBREVIATIONS AND NOMENCLATURE

Abbreviations

ABE	Acetone 1-butanol and ethanol
BET	Brunner-Emmet-Teller
BJH	Barrett–Joyner–Halenda
FTIR	Fourier transform infrared spectroscopy
LDF	Linear driving force
PSA	Pressure swing adsorption
RSS	Residual sum of squares
SEM	Scanning electron microscopy
TGA	Thermogravimetric analysis

List of symbols

c	Adsorbate concentration, mol/m ³
c_0	Adsorbate concentration in the feed, mol/m ³
c_{ef}	Adsorbate concentration in effluent, mol/m ³
c^*	The equilibrium concentration, mol/m ³
D_e	Effective diffusivity, m ² /s
D_i	Molecular diffusivity, m ² /s
D_L	Axial dispersion coefficient, m ² /s
D_p	The diameter of adsorbent particles, m
E	Adsorption energy difference between the solute and solvent for a given sorption site, J/mol

E_m	Weighted mean site energy, J/mol
E_s	Lowest physically realizable sorption energy, J/mol
E^*	The difference between E and lowest physically realizable sorption energy, J/mol
$F(E)$	Site energy frequency distribution over a range of energies, dimensionless
$F(E^*)$	Approximate site energy distribution over a range of energies, g·mol/(g·J)
ΔG^0	The standard free energy change, kJ/mol
ΔH^0	The standard enthalpy change, kJ/mol
K	Equilibrium constant in the linear isotherm, (mol/m ³ adsorbent)/(mol/m ³ fluid phase)
K_f	Freundlich coefficient, (mmol/g)/(Pa ^{1/n})
k_{BA}	Bohart-Adams rate constant, m ³ /(kg·min)
k_c	External mass transfer coefficient, m/s
k_{LDF}	Overall mass transfer coefficient, s ⁻¹
P	Pressure, kPa
$1/n$	Empirical constant, dimensionless
P_i	Partial pressure of the adsorbate, kPa
P^s	Saturated vapor pressure of the adsorbate, kPa
q	Mass adsorbed per unit mass of dry biosorbent, g/g adsorbent

q^*	Adsorbate loading in adsorbent in equilibrium with the concentration in bulk fluid, mol/m ³
\bar{q}	Average loading of adsorbate in the adsorbent, mol/m ³
q_0	Limiting mass for sorption, g/g biosorbent
q_e	Equilibrium sorption capacity, g/g biosorbent
q_h	Energetically homogeneous isotherm, g/g biosorbent
q_s	Saturated adsorbate loading in adsorbent, mol/m ³
R	Universal gas constant, J/(mol·K)
Re	Reynolds number, dimensionless
R_p	Equivalent radius of the adsorbent particles, m
R^2	Correlation coefficient, dimensionless
ΔS^0	The standard entropy change, kJ/mol·K
Sc	Schmidt number, dimensionless
Sh	Sherwood number, dimensionless
T	Temperature, °C
t	Time, min or s
u	Interstitial velocity, m/s
X_b	Mass concentration of butanol in the biosorbent, g/cm ³
X_w	Mass concentration of water in the biosorbent, g/cm ³
Y_b	Mass concentration of butanol in vapor phase, g/cm ³
Y_w	Mass concentration of water in vapor phase, g/cm ³
z	Distance from the bed entrance, m

Z Length of the column, m

Greek letters

α Separation factor, dimensionless

β Affinity coefficient, dimensionless

ε Adsorption potential, J/mol

ε_b Bed porosity, dimensionless

κ_1 Constant of micropore Dubinin-Polanyi model, (mol/J)²

κ_2 Constant of large pore Dubinin-Polanyi model, mol/J

ξ Dimensionless distance, dimensionless

τ Dimensionless time, dimensionless

CHAPTER 1. INTRODUCTION AND THESIS OUTLINE

Contribution of this chapter to overall Ph.D. work

This chapter provides the research motivation, the problem that will be investigated in biobutanol production, and the relative research progress. The research plan was designed based on knowledge gaps, hypothesis, and objectives. The outline of this thesis was also provided in this chapter.

1.1 Research motivation

The development of biofuels is increasingly important due to limited availability and rapid depletion of fossil fuels, and the need for reduction in greenhouse gas emissions (Huang et al., 2014). Biofuels are renewable energy, competitive additives and alternatives to fossil fuel. Biobutanol is a biofuel source, which can be produced from acetone-butanol-ethanol (ABE) fermentation. One of the key steps of this process is the recovery of low concentrated butanol from fermentation broth. The total concentration of butanol, acetone, and ethanol is no more than 20 g/L in the fermentation broth due to inhibition caused by butanol (Bankar et al., 2013; Cai et al., 2016; Faisal et al., 2018; Ladisch, 1991; Qureshi et al., 2005; Thirmal & Dahman, 2012). Acetone and ethanol are coproduced, so these components are needed to be separated from the product stream from the fermentation. Hence, the recovery of butanol involves two steps: removing acetone and ethanol from the fermentation product, and separating butanol from water (Mariano & Filho, 2012).

In industrial biobutanol facilities, a series of five distillation columns are involved to recover butanol (Mariano & Filho, 2012; van der Merwe et al., 2013), because a heterogeneous azeotrope of butanol and water (approx. 55.5 wt.% butanol) forms during the distillation (Mariano & Filho,

2012). The azeotrope product is condensed into two phases with 79.9 wt.% butanol in the upper phase, and 7.7 wt.% butanol in the lower phase. Thus, the distillation columns combined with a decanter are responsible for the separation of the butanol-water system (Friedl, 2016; Mariano & Filho, 2012). This leads to high energy consumption to break the butanol and water azeotrope (Xu et al., 2015).

Efforts have been made to develop various approaches to recover butanol in biobutanol production. These separation techniques include adsorption (Lin et al., 2012; Oudshoorn et al., 2009a; Qureshi et al., 2005; Saravanan et al., 2010), gas stripping (Groot et al., 1989), membrane pervaporation (Liu et al., 2005), extraction and supercritical extraction (Davison & Thompson, 1993; Groot et al., 1990), and hybrid recovery technologies (Kraemer et al., 2011; Xue et al., 2014).

Currently, adsorption is known as an effective method for separation and purification due to its low cost, high efficiency, and easy operation (Grande, 2012). Adsorption-based recovery technologies are reported to be the low energy requirement alternatives (Grande, 2012; Oudshoorn et al., 2009b; Qureshi et al., 2005; Saravanan et al., 2010). The energy requirement of butanol recovery by the adsorption process was calculated to be 1,948 kcal/kg butanol, which is much lower than that of steam stripping distillation (5,789 kcal/kg butanol) (Qureshi et al., 2005). Adsorption has been used for butanol purification in some studies (Lin et al., 2012; Oudshoorn et al., 2009a; Qureshi et al., 2005; Saravanan et al., 2010). Recently, many adsorbents such as molecular sieves and polymeric resins have been used to purify bio-alcohols (Carmo & Gubulin, 1997; Lin et al., 2012; Oudshoorn et al., 2009a; Qureshi et al., 2005; Saravanan et al., 2010). However, most of the adsorbents are expensive. In addition, the adsorption process using molecular sieves as adsorbents accompanies with high regeneration temperature and potential environmental problems.

Recently, increasing biosorbents are developed instead of traditional adsorbents for water sorption and alcohols dehydration, since they are cost-effective, biodegradable, and easily regenerated (Beery & Ladisch, 2001b; Benson & George, 2005; Ladisch, 1997; Ranjbar et al., 2013; Tajallipour et al., 2013; Yan & Niu, 2017). Dehydration of ethanol using biosorbents has been improved by the appropriate design and optimal selection of the adsorbents from starch-based and cellulose-based natural materials (Kim et al., 2011; Pruksathorn & Vitidsant, 2009). In comparison, butanol recovery and dehydration are less developed (Jayaprakash et al., 2017). Compared to starch-based adsorbents, lignocellulosic-based adsorbents could be the better choice for butanol dehydration due to better thermal stability. Thus, it is necessary to study the sorption characteristics of the potential lignocellulosic-based adsorbents and select the appropriate adsorbent for butanol dehydration. Oat hull, an agricultural by-product composed of cellulose, hemicellulose, and lignin (Paschoal et al., 2015), has potential to remove water from butanol based on the conclusions from other studies that lignocellulosic materials can be a potential option for ethanol dehydration (Quintero & Cardona, 2009; Rakshit et al., 1993). There are some studies on oat hull for dye removal (Banerjee et al., 2016); however, it has not been studied for butanol dehydration. Its sorption capability is unknown.

Thus, this work investigated the sorption of water and butanol vapor using the oat hull biosorbent. This work aimed to develop an alternative technology of sorption to directly break the azeotrope of butanol-water vapor generated from the distillation in biobutanol industry in a hope to reduce or replace the downstream decantation and distillation in the biobutanol industry, which have high energy consumption. For the interest of both industrial application and scientific research, butanol dehydration was investigated at a wider concentration range of 56-92 wt% butanol in water. The water/butanol sorption capability and characteristics in the single component

system have been carried out. The equilibrium and dynamics of water/butanol sorption from water/butanol mixture using oat hull biosorbent in a packed column were investigated in aid of experimental work and theoretical modeling. The competitive sorption of butanol and water was also discussed. Furthermore, the regeneration and reusability of the biosorbent were studied.

1.2 Knowledge gaps

Based on the literature review, the following knowledge gaps were identified:

- 1) Oat hull is cellulose-rich material and has great potential to dehydrate the biobutanol; however, it hasn't been studied for butanol dehydration. Its water/butanol sorption capability and selectivity are unknown.
- 2) The equilibrium of water/butanol sorption on the oat hull based biosorbent and their key factors are fundamental to develop a novel butanol dehydration process, however, they are not well understood.
- 3) In-depth dynamics study of water and butanol sorption on oat hull based biosorbent in a fixed bed is essential to understand the fundamentals of butanol dehydration and the process development. Such knowledge is not available.
- 4) The kinetics models which have the potential to simulate the breakthrough curves of water sorption from butanol-water vapor on the biosorbent need to be evaluated to study the sorption dynamics and mechanisms. The kinetically driven competitive sorption of butanol and water on the biosorbent needs to be further investigated.
- 5) The reusability study of oat hull based biosorbent for butanol dehydration is limited. This will provide the feasibility information for the future application of the butanol dehydration technology.

1.3 Hypothesis

Based on the literature review, the following hypotheses were proposed:

- 1) Oat hull containing rich cellulose, hemicellulose, and lignin are able to selectively separate water from biobutanol.
- 2) Adsorption potential theory model (Dubinin-Polanyi model) has the potential to describe the equilibrium data of water and butanol sorption in this process. The adsorption site energy distribution is a feasible method to describe the surface energetic characteristics of the biosorbent.
- 3) The linear driving force (LDF) model can be used to describe mass transfer in the water and butanol biosorption systems. An integrated mathematical model premised on the LDF model can be used to simulate the sorption breakthrough curves of pure water and pure sorption in the biosorbent packed column system.
- 4) The Klinkenberg model can be used to study the dynamics of water sorption from the butanol-water vapor. Compared to butanol, water has a more favorable mass transfer on the oat hull biosorbent.
- 5) The biosorbent derived from oat hull can be regenerated and reused for butanol dehydration with satisfactory performance and high stability.

1.4 Research Objectives

To address the knowledge gaps, the overall objective of this research is to develop an alternative technology of sorption to directly break the azeotrope of butanol-water vapor generated from the azeotropic distillation in a hope to reduce or replace the downstream decantation and distillation

in the biobutanol industry and investigate the fundamentals of water sorption of biosorbent. The specific sub-objectives are proposed as follows:

- 1) Develop the biosorbent based on oat hull. Characterize this biosorbent in terms of functional groups, surface area, particle size, structure, stability. Determine the sorption performance and the separation factors of water over butanol on the biosorbent.
- 2) Analyze the characteristics of water and butanol sorption equilibrium and site energy distribution of the biosorbent.
- 3) Investigate sorption dynamics of pure butanol and pure water on oat hull biosorbent in aid of mathematical modeling.
- 4) Investigate the dynamics of water sorption from butanol-water vapor mixtures through breakthrough curves of a fixed bed column system. Elucidate the dehydration mechanism based on the fundamentals of sorption and competitive sorption of butanol and water.
- 5) Evaluate the regeneration and reusability of the oat hull based biosorbent.

1.5 Research phases

The overall research progress is divided into 5 phases:

Phase I: Preparation and characterization of oat hull based biosorbent, and production of anhydrous biobutanol using oat hull based biosorbent and equilibrium study. A biosorbent developed from oat hull was prepared. Furthermore, the biosorbent was characterized by surface area analysis, particle size analysis, thermogravimetric analysis, Fourier transform infrared spectroscopy, and scanning electron microscope. These characteristics are important to design experiment conditions, and they played key roles in butanol dehydration. In addition, the water sorption on the biosorbent was visualized in aid of microscope imaging. In this phase, the oat hull based biosorbent was used to dehydrate butanol in a packed column in order to produce high purity

butanol product. The sorption performance and the separation factors of water over butanol on the biosorbent were determined. The effects of different parameters were discussed.

Phase II: Water and butanol sorption equilibrium study, and site energy distribution study. The water sorption equilibrium data in the single component sorption system and in the binary system was simulated by the Dubinin-Polanyi model. After that, the adsorption site energy distribution method was applied to describe the surface characteristics of biosorbent. The butanol sorption equilibrium data was studied by fitting to the Dubinin-Polanyi model. The site energy distribution of butanol sorption on the biosorbent was studied as well. The thermodynamics of water and butanol sorption on the biosorbent was discussed.

Phase III: Dynamic and modeling study of pure water and pure butanol sorption on the biosorbent. To better understand the fundamentals of water and butanol sorption, Phase III further investigated the sorption dynamics of butanol and water on the biosorbent in the single component sorption system. The Klinkenberg model was used to simulate the sorption breakthrough curves obtained in water or butanol single component sorption system at different conditions. The mass transfer coefficient and mass transfer resistances were investigated from the modeling results. The rate-limited step was determined.

Phase IV: Dynamics of water sorption from the butanol-water vapor. In this phase, the dynamics of water sorption from butanol-water vapor mixtures in a fixed bed column was investigated. Water sorption breakthrough curves in the binary system were simulated by the Bohart-Adams model and Klinkenberg model. The modeling results of these two models were compared to study the sorption dynamics and mechanisms. The effects of the experiment parameters were discussed according to the modeling results. The fitting results of the Klinkenberg model were further interpreted. The overall, external, and internal mass transfer resistances were

estimated by the parameters obtained from model fitting. The rate-limited step was determined. Moreover, the kinetically driven competitive sorption of butanol and water was discussed to explain the basis of the separation of the butanol-water mixture by the oat hull biosorbent.

Phase V: Reusability study of the oat hull biosorbent. This phase demonstrates the reusability study of the oat hull based biosorbent. The biosorbent was regenerated and reused in the same column without being changed. The performance and stability of the fresh biosorbent and the biosorbent, which has been reused 20 cycles, were compared. Furthermore, the preliminary economic analysis is provided to prove the economic feasibility of butanol dehydration by sorption using the biosorbent.

1.6 Thesis Outline

This thesis is produced in the traditional style. Some major results of this thesis have been published, and the detailed information of the journal publications and the conference presentations can be seen in the Publications section. The author of this thesis proposed the research working plan, designed and carried out all the experiments, collected and analyzed the experimental data, and presented all the results and discussions in the journal publications and the thesis under the general supervision of supervisors, except for the optical microscopy imaging (Figures 4.5, 4.6 and 4.7) which was done by the Nano-Science Technology Center at the University of Central Florida.

This thesis is composed of ten chapters and followed by a list of references and the appendix. Chapter 1 is the introduction of the overall thesis project, which includes the background of this research, knowledge gaps, hypothesis, objectives and research phases. Chapter 2 is the literature review, which summarizes the production of biobutanol, the alternative methods for butanol purification, and the research progress in this field. The detailed introduction of sorption-based

technologies and adsorbents were also provided in Chapter 2. Chapter 3 presents the materials, characterization methods, experimental apparatuses and procedures, and analytical methods used in this work.

Chapters 4, 5, 6, 7, 8, and 9 report the research results achieved in this work together with discussion, which are associated with the five research phases. The subjects of the research phases are described in the previous section 1.5. Chapters 4 and 5 correspond to Phase I: characterization of oat hull based biosorbent, and production of anhydrous biobutanol using the biosorbent. Chapter 6 corresponds to Phase II: water and butanol sorption equilibrium study and the site energy distribution study. Chapter 7 corresponds to Phase III: dynamic and modeling study of pure water and pure butanol sorption on the biosorbent. Chapter 8 corresponds to Phase IV: the dynamics of water sorption from butanol-water vapor on the biosorbent. Chapter 9 corresponds to Phase V: reusability study of the oat hull biosorbent.

Chapter 10 provides the overall conclusions and most significant contributions of this research and recommendations for future work. The references of all the chapters are attached at the end of the thesis.

1.7 Publications

Journal Publications:

(1) Huang, Q.; Niu, C. H.; Dalai, A. K. Production of Anhydrous Biobutanol Using a Biosorbent Developed from Oat Hulls. *Chemical Engineering Journal*. 2019, 356, 830–838.

(2) Huang, Q.; Dalai, A. K.; Parkb, J.; Diazb, A. M.; Kang, H. and Niu, C. H. Dynamics of Water Adsorption from Butanol-water Vapor in a Biosorbent Packed Column. *Industrial & Engineering Chemistry Research*. 2019, 58, 15619–15627.

(3) Huang, Q.; Niu, C. H.; Dalai, A. K. Dynamic Study of Butanol and Water Adsorption onto Oat Hull: Experimental and Simulated Breakthrough Curves. *Energy & Fuels*. 2019, 33, 9835–9842.

Conference Presentations:

(1) Huang, Q.; Niu, C. H.; Dalai, A. K. “Butanol/water Adsorption on Oat Hulls and Site Energy Distribution Analysis”, 67th Canadian Chemical Engineering Conference, Edmonton, AB, Canada, Oct 22-25, 2017.

(2) Zhou, J.; Huang, Q.; Niu, C. H. “Palletization and Characterization of Biosorbents”, 67th Canadian Chemical Engineering Conference, Edmonton, AB, Canada, Oct 22-25, 2017.

(3) Huang, Q.; Niu, C. H.; Dalai, A. K. “Dynamics and Simulation Studies of Water Adsorption on a Biosorbent”, 68th Canadian Chemical Engineering Conference, Toronto, ON, Canada, Oct 28-31, 2018.

(4) Huang, Q.; Niu, C. H.; Dalai, A. K. “Dynamic Study of Butanol and Water Adsorption on a Lignocellulosic Biosorbent in Packed-bed”, 69th Canadian Chemical Engineering Conference, Halifax, NS, Canada, Oct 20-23, 2019.

CHAPTER 2. LITERATURE REVIEW

Contribution of this chapter to overall Ph.D. work

This chapter provides an overview of biobutanol and its production. The problems and challenges for butanol recovery are described. Some alternative technologies for butanol recovery and drying are summarized. The current status of adsorption-based methods is introduced in more detail. The current research progress of biosorbent is also summarized in this chapter.

2.1 Biobutanol

Butanol (C_4H_9OH), a four-carbon straight chain alcohol, is important for its application as a solvent, an intermediate in chemical synthesis, a chemical precursor, and a fuel. The annual global demand for butanol is expected to cross 6 billion gallons (Rathour et al., 2018). The conventional chemical methods of butanol synthesis include oxo synthesis, Reppe synthesis and crotonaldehyde hydrogenation synthesis (Thirmal & Dahman, 2012). In Reppe synthesis, propylene, carbon monoxide, and water react with the aid of a catalyst. This method needs one step to produce butanol; however, it is not cost-effective. The other two methods need multiple steps to produce butanol. Petroleum or chemicals are used in the chemical methods. This will be harmful to the environment and increase the cost (Thirmal & Dahman, 2012).

Butanol can also be produced biochemically by fermentation using microorganisms (Thirmal & Dahman, 2012). The development of biofuels is increasingly important due to the limited availability and rapid depletion of fossil fuels, the need for reduction in greenhouse gas emissions, and the possible increase in the price of crude oil (Huang et al., 2014). Biobutanol is an important source of renewable biofuel, which can be produced from acetone 1-butanol and ethanol (ABE) fermentation.

One of the most important applications of butanol is a fuel additive or a replacement of gasoline. Biobutanol is a promising biofuel to be blended with gasoline due to its higher energy content, lower vapor pressure, lower flash point, and less corrosive character when compared with ethanol (Sarchami et al., 2016; Sarchami & Rehmann, 2015). Fuel additives require high octane numbers, and butanol has the octane number of 96. The properties of butanol and other biofuels can be seen in Table 2.1 (Rathour et al., 2018). Butanol can be used in butanol-gasoline blends without having major modifications in the engines (Shah & Sen, 2011). It's a great advantage for biobutanol to be used as a fuel. In addition, as a good candidate to replace fossil fuel, butanol can improve tolerance to water contamination, and it can blend with gasoline at higher concentrations compared with ethanol (Bharathiraja et al., 2017). The 85% butanol/gasoline blends are used in petrol engines without having major modifications in the engines, and it contains 22% oxygen makes it a cleaner fuel than ethanol (Bharathiraja et al., 2017). Butanol is safer to handle compared with gasoline (less flammable), and it is miscible with gasoline in any ratio (Bankar et al., 2013). Biobutanol, a suitable biofuel, has wide application in fuel industry. It can be blended with gasoline as a rich fuel extender, and converted to jet fuel (Bharathiraja et al., 2017). The other applications of butanol include its use as the industrial solvent or co-solvent, a diluent for brake fluid formulations, and the solvent for the manufacture of antibiotics, hormones, and vitamins (Bankar et al., 2013).

Table 2.1 Comparison of butanol with other biofuels and conventional fossil fuels (Rathour et al., 2018).

Fuels properties	Ethanol	Butanol	Biodiesel	Gasoline	Diesel
Energy density (MJ/L)	18.4-21.2	29.2	33.3-35.7	32-34.8	40.3
Produced by	Bacteria, fungi, yeast, and algae	Bacteria, fungi and algae	Bacteria, fungi, yeast, and algae	Refining	Distillation
Air-fuel ratio	9.0	11.1	9.2	14.6	14.7
Specific energy (MJ/kg)	26.8	36	37.8	46.4	48.1
MON	89	78	40	81-89	15-20
RON	107	96	87	91-99	25
Usage	Require engine modification	No engine modification required	Slight modification for straight veggie oil	As an automobile fuel	As an automobile fuel

MON: the motor octane number. RON: the research octane number.

2.2 Production and purification of biobutanol

Butanol can be produced by the biotechnological route using microorganisms, or by the chemical route. Currently, increased studies have been focused on butanol production from biomass due to sustainable production. Biobutanol is usually produced from the well-established acetone, butanol, and ethanol (ABE) fermentation. The main products are acetone, 1-butanol, and ethanol from this process with the ratio of 3:6:1. The performance of fermentation depends on

various parameters such as pH, temperature, incubation time, agitation, and toxicity (Kushwaha et al., 2019).

Batch reactors are usually used in biobutanol production due to its simplicity. The semi-continuous operation was also studied to increase production (Staggs & Nielsen, 2015). The more ideal reactors are under investigation to improve the yield or productivity (Kourkoutas et al., 2004; Sarchami & Rehmann, 2015). The commonly used substrate in biobutanol production includes corn, wheat, millet, rice, and so on. The cost of biobutanol production needs to be considered, so more economical substrates are developed. Some more economical substrates such as agricultural residues and energy crops are considered to produce butanol. More examples can be seen in Table 2.2 (Rathour et al., 2018). Various agricultural waste materials have been used in biobutanol production due to the lower cost (Qureshi et al., 2010; Rathour et al., 2018). ABE fermentation is achieved using microorganisms, which help to convert biomass into butanol. During the fermentation step, the various cellulosic biomasses are converted into fermentable sugars, which are subsequently converted acetone, butanol, and ethanol using specific microorganisms (Mitchell, 1998). Some microorganisms such as clostridia and Gram-positive bacteria have been used for biobutanol production. Inside the microorganism, the fermentable sugars are transported and accumulated in the cytoplasm, and then they enter the glycolytic cycle, where they are converted to pyruvate before subsequent reduction to product (Rathour et al., 2018). Various types of microorganisms can be seen in Table 2.2.

Table 2.2 Different types of substrates and microorganisms used in butanol production (Rathour et al., 2018).

Types of substrates	Examples	Microorganism
Traditional substrates	Corn, rice, potato, millet, soya, wheat, whey permeates	Pseudomonas sp., Clostridia sp., Bacillus sp., E.coli, Zymomonas
Current substrates	Corn straw, cobs, and fibers, Wheat and rice straw, banana strips, sugarcane molasses	mobilis, Monilia sp., Neurospora sp., Aspergillus sp., Trichoderma sp.

The total concentration of acetone, ethanol, and butanol in the fermentation broth is no more than 20 g/L (Ladisch, 1991; Luyben, 2008), because of the butanol inhibition to culture. The product inhibition results in high cost and large volume water removal in the purification process (Qureshi & Blaschek, 2001). In order to separate biobutanol from the fermentation broth, preliminary distillation is usually applied to remove acetone and ethanol from butanol. Then, the decantation and two-column distillation are used to separate heterogeneous azeotrope of butanol and water (approximately 56 wt % butanol in water) (Luyben, 2008), which is an energy-intensive and costly method.

The main problem in the ABE fermentation is the product inhibition due to butanol toxicity to the culture. Various strategies have been studied to overcome this problem. The butanol product can be removed from the fermentation broth by gas stripping or extraction as it is produced (Davison & Thompson, 1993; Lodi et al., 2018; Outram et al., 2017; Pyrgakis et al., 2016), and the butanol concentration in the fermentation broth is maintained below inhibitory levels. The removal of toxic components by a separation method may help to improve the fermentation process and reduce energy consumption (Mariano et al., 2011).

The current researches focus on making the ABE fermentation more productive and more economically attractive. Some new technologies have been applied to solve the problems regarding the low product concentration during fermentation. The selection and utilization of novel substrates, the pretreatment of substrates pre-treatment, genetic engineering techniques, the design for better fermentor have been considered to improve the performance of fermentation process (Bharathiraja et al., 2017; Pang et al., 2016; Qureshi et al., 2010).

The ABE process is investigated not only on the upstream process but also on the downstream process. The butanol concentration in the fermentation broth is very low due to butanol toxicity to the culture. Hence, the recovery of low concentrated butanol from fermentation broth is one of the key steps of biobutanol production. In the biobutanol production industry, butanol was usually separated from the fermentation broth first by distillation columns to achieve the butanol and water azeotrope (55.5 wt% butanol). Then it was followed by decantation and distillation to remove the remaining water, which is energy intensive and costly (Luyben, 2008). Efforts have been made to develop various approaches to recover butanol from the fermentation broth. These separation techniques include adsorption (Lin et al., 2012; Oudshoorn et al., 2009a; Qureshi et al., 2005; Saravanan et al., 2010), gas stripping (Groot et al., 1989; Qureshi & Blaschek, 2001), membrane pervaporation (Liu et al., 2005; Qureshi & Blaschek, 2000), extraction and supercritical extraction (Davison & Thompson, 1993; Groot et al., 1990), and hybrid recovery technologies (Kraemer et al., 2011; Xue et al., 2014). The detailed methods and research progress have been introduced in the following section.

2.3 Methods for biobutanol recovery

The production and application of biobutanol are promising, but the economical production of butanol by fermentation is limited by that the product with low concentrations is achieved from

the fermentation broth. The conventional recovery of butanol by distillation consumes more energy than the product contains (Goerlitz et al., 2018). Thus, efforts have been made to develop various approaches to recover butanol from the fermentation broth. A number of technologies currently available for butanol separation and purification such as gas stripping, extraction, and adsorption-based techniques are discussed below.

2.3.1 Distillation

Conventionally, distillation is used to separate and purify bio-alcohols from the fermentation broth (Errico et al., 2013). In the biobutanol production industry, the total concentration of acetone, ethanol, and butanol in the fermentation broth is no more than 20 g/L due to inhibition caused by butanol (Bankar et al., 2013; Cai et al., 2016; Faisal et al., 2018; Ladisch, 1991; Qureshi et al., 2005; Thirmal & Dahman, 2012). Acetone and ethanol are coproduced, so these components also need to be separated from the product stream from the fermentation unit. Hence, the recovery of butanol involves two steps: removing acetone and ethanol from the fermentation product, and separating butanol from water (Mariano & Filho, 2012). In biobutanol facilities, a series of five distillation columns are involved to recovery butanol (Mariano & Filho, 2012; van der Merwe et al., 2013) because a heterogeneous azeotrope (with 79.9 wt.% butanol in upper phase, 7.7 wt.% butanol in lower phase) of butanol and water (approx. 55.5 wt.% butanol) forms during the distillation (Mariano & Filho, 2012). Thus, the two distillation columns combined with a decanter are responsible for the separation of the butanol-water system (Friedl, 2016; Mariano & Filho, 2012). This leads to high energy consumption to break the butanol and water azeotrope (Xu et al., 2015). The separation scheme of distillation in the purification of biobutanol has some serious shortcomings such as the requirement of high energy and high operating costs due to the need for

multiple distillation units. It consumes the most energy of a bio-alcohol manufacturing process (Ladisich & Dyck, 1979).

2.3.2 Gas stripping

Gas stripping is studied for separation based on different volatilities. As an in-situ technology, it can be performed within the fermentor. Gas stripping is attractive, because it is simple and does not require expensive apparatus. During this process, the volatile butanol in the fermentation broth is captured by the stripping gas. The gas containing solvents will be condensed so that the enriched condensate is collected. In this process, volatile butanol can be condensed and recovered from the condenser (Qureshi & Blaschek, 2001). Gas stripping also does not harm the culture, and it helps to reduce the inhibition (Lodi et al., 2018; Qureshi & Blaschek, 2001).

Sometimes gas stripping is combined with pervaporation used for energy-saving product recovery (Xue et al., 2014). The use of hybrid techniques can increase the final product concentration (Outram et al., 2017). The high operation cost and low selectivity are the main drawbacks of this method.

2.3.3 Extraction

Butanol can be separated from water or other impurities by extraction due to their differences in the distribution coefficients or solubility in the extractant. Extraction used for butanol recovery is in situ method, butanol is extracted from its aqueous environment and concentrated in a solvent phase (Staggs & Nielsen, 2015). The nontoxic immiscible solvent, oleyl alcohol, is widely used to extract the majority of the butanol from the aqueous broth (Davison & Thompson, 1993; Groot et al., 1990). The solvent was added directly to the fermenting columnar reactor and removed directly

from it. The solvent had a distribution coefficient of near 3 for butanol (Davison & Thompson, 1993).

Some extractants are toxic and the emulsion problem is accompanied by this method. Besides, the extraction process is usually coupled with a second separation process to ultimately recover and purify butanol (Staggs & Nielsen, 2015). The solvent needs to be regenerated in the extraction-based separation system. The hybrid extraction–distillation process used for dehydration of bioethanol and separation of butanol from acetone–butanol–ethanol fermentation were studied (Avilés Martínez et al., 2012; Kraemer et al., 2011).

2.3.4 Membrane pervaporation

Pervaporation is an alternative for butanol recovery since it has low energy consumption, continuous operation, and easy process design (Smitha et al., 2004). Membrane permeation can combine with gas stripping or distillation to produce highly purified alcohols from ABE fermentation. The membrane is expected to selectively allow the desired component to permeate through it. Dense and phase-pure zeolite LTA membranes were studied for the recovery of isobutanol from water (Huang et al., 2014).

Many types of membranes, such as polyanion and polysalt membranes, hybrid poly(vinyl alcohol)/inorganic membranes, and poly (ether-block-amide) (PEBA)/ceramic hollow fiber (HF) composite membranes are developed and tested for the recovery of butanol from the fermentation broth or separation of butanol from dilute aqueous solutions (Bolto et al., 2011; Li et al., 2016; Liu et al., 2005; Wu et al., 2015).

Membrane permeation is useful for the removal of a minor component of a solution. The high operation cost and the low durability of the membranes also limit its industrial applications. It has been used with gas stripping as the new integrated process for energy-saving product recovery

from acetone–butanol–ethanol (Cai et al., 2016). A hybrid process including two-stage gas stripping and multi-stage pervaporation has been developed to improve butanol production (Xue et al., 2014).

2.3.5 Adsorption

Adsorption is a physical or chemical process involving the mass transport of adsorbates from the solution phase (i.e., bulk solution, film, and intraparticle transportation) to the interior surface of the porous adsorbent where the adsorption occurs. It can be considered as a process that enriches chemical species from a fluid phase on the surface of a solid material. Currently, adsorption is known as an effective method for separation and purification due to its low cost, high efficiency, and easy operation as compared to conventional separation methods (Grande, 2012). It is widely used for gas separation and a variety of drying operations. For example, separation of ethanol-water azeotrope by adsorption has been applied to replace the azeotropic distillation in the industry to save energy (Vane, 2008).

Adsorption has also been used for butanol recovery from aqueous solution in some lab scale studies (Lin et al., 2012; Oudshoorn et al., 2009a; Qureshi et al., 2005; Saravanan et al., 2010). Many adsorbents such as zeolite, molecular sieves, and polymeric resins have been used to purify bio-alcohols (Carmo & Gubulin, 1997; Lin et al., 2012; Oudshoorn et al., 2009a; Qureshi et al., 2005; Saravanan et al., 2010). It was proposed that the recovery of butanol by adsorption is a promising energy-efficient technique (Goerlitz et al., 2018). The energy requirement for butanol recovery by sorption-desorption processes has been calculated to be 1,948 kcal/kg butanol as compared to 5,789 kcal/kg butanol by steam stripping distillation. Other techniques such as gas stripping and pervaporation require 5,220 and 3,295 kcal/kg butanol, respectively (Qureshi et al., 2005). The comparison of the energy requirement of the different butanol separation techniques

shows that the distillation has much higher energy requirement than gas stripping, pervaporation, liquid-liquid extraction, and adsorption (Goerlitz et al., 2018). However, the composition of ABE fermentation broth is complex, the adsorption of butanol directly from fermentation broth is challenged by impurities in the fermentation broth.

Adsorption was studied for ethanol dehydration from azeotropic solution to produce anhydrous ethanol (Al-Asheh et al., 2004; Chopade et al., 2015; Pruksathorn & Vitidsant, 2009). Adsorption was also studied for butanol dehydration (Jayaprakash et al., 2017). However, butanol dehydration by adsorption is less developed, and limited research is done on separating water from the azeotrope of butanol and water.

In summary, among various alternative approaches for butanol recovery and dehydration, adsorption-based technologies have received considerable attention owing to their features including low cost, low energy consumption, economic feasibility, and easy operation (Grande, 2012; Lin et al., 2012; Oudshoorn et al., 2009b; Saravanan et al., 2010). Thus, it is feasible to use an adsorption based method to purify butanol to reduce energy consumption.

However, the composition of ABE fermentation broth is complex, and the concentration of butanol is low. Various hybrid downstream processes involving different separation techniques have been proposed to bring down the cost of separation of butanol from fermentation (Kraemer et al., 2011). These separation techniques include distillation combined with liquid-liquid extraction (Avilés Martínez et al., 2012), pervaporation combined with distillation (Van Hecke et al., 2018), distillation combined with adsorption (Qureshi et al., 2005), two-stage gas stripping (Xue et al., 2013), a combination of pervaporation and gas stripping (Setlhaku et al., 2013), etc. Thus, it may be suitable to combine adsorption with other technologies to produce pure butanol from fermentation broth.

As discussed in the early part of this chapter, use of a number of decantation and distillation cycles to break the butanol water azeotrope to achieve anhydrous butanol in the biobutanol industry is very energy-intensive. It was recently reported that using adsorption to break the butanol and water azeotrope required less energy than that required in the method of combination of decantation and distillation cycles (Xu et al., 2015). Thus, it is feasible to propose a hybrid downstream process involving preliminary distillation to achieving butanol water azeotrope from fermentation broth and then an adsorption process to breaking the azeotrope to obtain anhydrous butanol. In other words, in this hybrid process, adsorption is applied to replace the decantation and distillation cycles to separate the azeotrope of butanol and water generated from distillation. That led to the formation of this thesis project which is to develop an alternative technology of adsorption to remove water directly from the azeotrope of 55.5 wt.% butanol water vapor generated from the preliminary distillation in a hope to reduce or replace the downstream decantation and distillation cycles in biobutanol industry. The following sections further present the information relevant to using adsorption technology in bio-alcohols dehydration process.

2.4 Adsorption for alcohols dehydration

Currently, adsorption has been popularly applied in the bioethanol industry to break the ethanol-water azeotrope and dehydrate ethanol to achieve fuel-grade ethanol (Al-Asheh et al., 2004; Chopade et al., 2015; Pruksathorn & Vitidsant, 2009). Sorption was also studied for butanol dehydration in the laboratory scale (Jayaprakash et al., 2017). In general, the dehydration processes are carried out in column systems packed with adsorbents by swinging pressure from high (dehydration) to low (regeneration). Some processes swing temperature during dehydration and regeneration. The details are discussed below.

2.4.1 Pressure swing adsorption in a packed column

Packed columns have been commonly used in adsorption processes. Particularly, they are popular in dehydration (drying) of bioalcohols or organic vapors. In the dehydration process, it is possible to adsorb large quantities of moisture at the higher pressure, and then release that moisture at the low pressure during the regeneration process by swinging the pressure from high to low. Some materials such as zeolites, activated carbon, molecular sieves, and biosorbents are used as adsorbents to adsorb the target gas species at high pressure. Such a pressure swing process is called pressure swing adsorption (PSA) which is a widely used technology for purification of gases using solid adsorbents. It is based on that under different pressure the adsorbate's affinity for an adsorbent material is different (Ruthven et al., 1993). The PSA technology differs significantly from cryogenic distillation and extraction techniques. It's a good method for gas separation and purification for its low-cost operation, high product recovery, and operational simplicity (Errico et al., 2013). The PSA technology has been continuously improved, and its potential uses have been enlarged in other areas like bioethanol purification (Simo et al., 2009; Tajallipour et al., 2013; Jayaprakash et al., 2017).

For example, in a PSA drying system in a lab-scale, wet ethanol vapor feed stream entered into the column, then the water molecules contacted with the molecular sieves and transferred from the feed stream to the surface of the adsorbent at high or moderate pressure (Simo et al., 2009). Once the sorption process was done, inert gas (N_2) entered the column under vacuum from the bottom to regenerate the adsorbents. Temperature, pressure, feed concentration, feed flow rate, and particle size of adsorbents affected sorption performance (Chang et al., 2006a; Hu & Xie, 2006).

In real industrial application, dehydration has been done in a multi-column pressure swing adsorption process, by which water sorption (dehydration) could be operated in one column for around 10 mins and then switched to desorption (regeneration), and another column is operated for water adsorption. The PSA cycle can be divided into the adsorption stage and the desorption stage. In an ethanol drying process, the adsorption stage took about 10-15 mins (Pruksathorn & Vitidsant, 2009), and then the bed was depressurized, regenerated, and re-pressurized to the adsorption pressure. The optimal cycle time for the apparatus can be adjusted based on the cyclic capacity of the adsorbent. Temperature swing has been used together with pressure swing adsorption in some studies to enhance the desorption process (Jayaprakash et al., 2017; Tajallipour et al., 2013).

2.4.2 Inorganic adsorbents

Adsorption using inorganic adsorbents are widely applied in industry. The usage of inorganic adsorbents is around 30-50 million kg/yr (Yang, 1987). Activated alumina, silica gel, and molecular sieves were studied to adsorb water vapor (Zhou et al., 1998).

Alumina is a hydrated form of aluminum oxide (Al_2O_3). It produces an excellent dew point depression values as low as $-73\text{ }^\circ\text{C}$ but requires much more heat for regeneration. Alumina was used as a desiccant for water vapor adsorption or sorption, and drying of gases and liquids (Ouchi et al., 2014; Zhou et al., 1998). It has good resistance to liquids, but little resistance to disintegration due to mechanical agitation by the flowing gas.

Silica gels consist almost solely of silicon dioxide (SiO_2). It has a high affinity for water and other polar compounds. Silica gel is desirable for water removal. Alumina gels consist primarily of some hydrated form of Al_2O_3 . Silica alumina gels are a combination of silica and alumina gel. Gels can dehydrate gas to as low as 10 ppm and have the greatest ease of regeneration of all

desiccants. Silica gels can be used for their water sorption and methane hydrates dissociation (Aladko et al., 2004; Alcañiz-Monge et al., 2009). The surface of silica gels can be deposited and blocked easily by sulfur.

Molecular sieves can be used for gas dehydration. They are in crystalline forms of alkali metal (calcium or sodium) alumina-silicates, very similar to natural clays. They are highly porous, with a very narrow range of pore sizes, and very high surface area. They can remove water vapor from the mixed gas stream selectively. Commercial 3-A molecular sieve has been used in ethanol dehydration (Carmo & Gubulin, 1997; Chopade et al., 2015; Simo et al., 2009). However, molecular sieves are expensive adsorbents. The adsorption process accompanied by a high regeneration temperature and potential environmental problems.

2.4.3 Biosorbents

Various biobased adsorbents (Jayaprakash et al., 2017; Ladisch & Dyck, 1979; Quintero & Cardona, 2009; Ranjbar et al., 2013) have been reported to remove water from alcohols. Compared to conventional adsorbents such as zeolite, molecular sieves, and polymeric resins, biosorbents are ideal for dehydration of gaseous species for its high capability, low cost, environmental friendliness, and easy regeneration (Beery & Ladisch, 2001b; Benson & George, 2005; Crawshaw & Hills, 1990; Ladisch, 1997; Ladisch & Dyck, 1979). For example, they can be regenerated easily by heating at a lower temperature (105–110 °C) compared to conventional adsorbents such as molecular sieves, silica gels, calcium chloride, and so on (at least 175 °C, and up to around 300 °C) (Beery & Ladisch, 2001a; Fahmi et al., 1999). The energy cost of the dehydration of ethanol using CaO was reported to be 3669 kJ/kg ethanol, while the energy cost by the sorption using cellulose was 2873 kJ/kg ethanol (Boonfung & Rattanaphanee, 2010). More and more starch-based and

lignocellulosic enriched natural biomaterials were studied for alcohols drying operation (Benson & George, 2005; Crawshaw & Hills, 1990; Kim et al., 2011; Rebar et al., 1984).

The low-cost biosorbents sources include but not limited to natural materials, agricultural wastes/by-products and industrial wastes/by-products (Worch, 2012). The materials such as wood, chitin, clays, shells, and hulls from fruits and nuts, sawdust, straw, corncob waste, sunflower stalks, and so on are all possible to be used as adsorbents.

Every year abundant agricultural by-products including canola meal, oat hull, barley straw, wheat straw, and so on are generated and discarded. If these biomaterials can be used as adsorbents, it will not only provide green and low-cost adsorbents but also solve agricultural by-products disposal problem. Starch, starch-based materials, cellulose, and hemicellulose have an affinity for water (Al-Asheh et al., 2004). Composites of these materials are also able to adsorb or absorb water.

Rice straw and bagasse have been used as adsorbents for ethanol dehydration (ethanol feed concentration of 80–90%) (Rakshit et al., 1993). The final ethanol concentration above the azeotropic concentration was obtained. The energy analysis of the process indicated that this method is promising in reducing energy requirement for ethanol separation and in breaking the azeotrope. These bio-based materials required lower regenerated temperature.

Barley straw was investigated as adsorbent (Sun et al., 2007). The result demonstrated that it had higher water uptake compared to the wheat straw and crab shells. The barley straw was a potential biomaterial for removing water from ethanol-water mixtures (Sun et al., 2007).

The cassava, yellow dent corn, sugar cane bagasse, and upright elephant ear roots were selected as raw materials for water sorption (Quintero & Cardona, 2009). Water sorption capacity

ranges from 4 to 19 g/ 100 g were obtained of these materials. The tested materials showed an affinity with water. The results showed that biomass adsorbents are promising for water removal.

Dehydration of ethanol using biosorbents has been improved by appropriate design and the optimal selection of the adsorbents from starch-based and cellulose-based natural materials (Kim et al., 2011; Pruksathorn & Vitidsant, 2009). In comparison, butanol recovery and drying are less developed. Recently, dehydration of butanol using canola meal biosorbent provides a promising alternative way for bio-butanol production, which is more cost-efficient and more environmentally friendly compared with conventional distillation (Jayaprakash et al., 2017). Compared to starch-based adsorbents, lignocellulosic-based adsorbents might be a better choice for butanol dehydration due to better thermal stability and avoiding competing with food. Thus, it is necessary to study the sorption characteristics of potential lignocellulosic-based adsorbents and select the appropriate adsorbents for butanol drying.

Oat is an important cereal crop globally. The annual global production of oats is nearly 23 million tons (*World oats production holds steady*, 2018). Oat hull is the agricultural by-product of oat. It was produced from the milling process consisting of lemma and palea. The waste oat hulls have been used as fuel, packing material, and animal feed, but their output is higher than utilization (Banerjee et al., 2016). Thus, a significant amount of oat hull, the by-product of oat, are discarded. The waste oat hull needs to be utilized in a feasible and environmentally friendly way.

The price of oat hull from Schumitsch Seed Inc. is \$45 per ton in the year of 2018 (*Missouri Dairy Resource App*, n.d.). The price of molecular sieves used as a common desiccant is about \$1,000–\$4,000 per ton (*Molecular Sieve Price*, n.d.).

Oat hull, composed of cellulose, hemicellulose, and lignin, chemically composed of several metabolites such as phenols, ketones, aldehydes, and carboxylate (Paschoal et al., 2015), has

potential to remove water from butanol based on the conclusions from other studies that lignocellulosic materials can be a potential option for ethanol dehydration (Quintero & Cardona, 2009; Rakshit et al., 1993). There are other studies on oat hulls on dye removal (Banerjee et al., 2016); however, use of oat hull based materials for butanol dehydration has not been reported yet.

There are various adsorbent modification methods applied to increase the specific surface area, and make more sorption sites available for the sorption of water. Numerous modifying agents were used to enhance the dehydration capability of biosorbents. Modifying agents are such as sodium hydroxide (Anderson et al., 1996), hydrochloric acid (Lin et al., 2012; Sun et al., 2007), sulfuric acid, enzymes (Beery et al., 1998), and so on. Sodium hydroxide could disrupt the crystalline areas and make surface area more accessible; hydrochloric acid and sulfuric acid could increase pores in the surface; some enzymes can break down the protein matrix (Beery et al., 1998). Biosorbents were soaked in the agent solutions at a specified concentration for a certain period of time. After being soaked, the biosorbent was washed, rinsed and dried. In addition, a microwave-assisted alkali or acid pretreatment was used to improve the performance of the biosorbents (Agu et al., 2017; Yan & Niu, 2017).

However, the above-mentioned modification methods significantly increased the costs of adsorbents, and caused environmental issues because of using the chemical agents. Thus, it is necessary to develop a novel dehydration process using raw materials such as oat hulls and similar feedstocks without further chemical or physical treatment, which is environmentally friendly and cost-effective. If successful, it is preferable to use those similar low-cost adsorbents such as industrial wastes, natural materials, or agricultural by-products without requiring expensive additional pretreatment steps (Han et al., 2009).

The preliminary research results proved the feasibility of alcohols dehydration using agricultural by-products. However, there are limited studies in butanol dehydration by sorption using biosorbents. The sorption kinetics, equilibrium, and mechanisms are not well understood.

2.5 Adsorption equilibrium in alcohols dehydration

2.5.1 Isotherms and modeling

If an adsorbent and an adsorbate are contacted long enough, equilibrium is established between the amount of adsorbate adsorbed and the amount of adsorbate in solution. Adsorption equilibrium is one of the most fundamental properties of the adsorbate-adsorbent interaction. For a better understanding of this aspect, numerous theoretical and empirical models have been developed to describe reversible adsorption at thermodynamic equilibrium. The equilibrium relationship is described by isotherms. The equilibrium models help to analyze mass balances, momentum balance, reaction rate, and nonlinear multicomponent adsorption equilibrium isotherms. In the meantime, the adsorption theory is studied to describe the equilibrium and determine the sorption mechanisms. There are many theories in adsorption. Some of them are based on kinetic and thermodynamic approaches. However, sometimes the adsorption isotherm equations derived by these fundamental methods cannot describe the equilibrium data well because solid adsorbents are highly complex, and the assumptions made in these theories are far from reality. To address this challenge, a number of semi-empirical models have been developed to describe equilibrium data. They can be used to describe monolayer adsorption, multilayer adsorption and micro-pore filling.

Specifically, to analyze water sorption isotherms in the dehydration process, isotherm models were derived from kinetics and thermodynamics, semi-empirical, and empirical approaches. The

most popular models are such as Langmuir model, Freundlich model, Dubinin-Polanyi model, Brunner-Emmet-Teller (BET) model, Guggenheim, Anderson, and de Boer (GAB) model, Frenkel-Halsey-Hill (FHH) model, and so on (Al-Asheh et al., 2004; Chang et al., 2006a; Ouchi et al., 2014; Ranjbar et al., 2013; Tassist et al., 2010).

For example, in the study of water sorption on type 3A, type 4A molecular sieves, and bio-based sorbents from ethanol-water mixture in a packed column system, the equilibrium data under different inlet water contents were collected to study the isotherms (Al-Asheh et al., 2004). The Guggenheim, Anderson, and de Boer (GAB) model applicable to a wider range of partial pressure of adsorbate was used for data fitting. The parameters of the GAB model were regressed by software. The predicted data by the GAB model were compared with the experimental data using the sum square of residuals. The results showed the GAB model reasonably represented the water sorption data. The GAB parameters provide important information such as monolayer capacity and the difference of energies in the upper layers and in the monolayer. The GAB isotherm is a suitable isotherm for the characterization of water sorption on different materials.

The adsorption equilibrium and adsorption/desorption rate of water vapor in porous alumina film adsorbent were determined (Ouchi et al., 2014). The equilibrium data were analyzed by the BET equation for the infinite adsorption-layer. The parameters q_m (the sorbed amount by monomolecular coverage on the adsorbent surface) and C (a parameter on adsorption heat) can be determined from the slope and the intercept of the BET plot.

The Sircar's model and the potential theory were reported to have good performance in representing the isotherm data of water and ethanol adsorption on starch (Lee et al., 1991). The Dubinin-Polanyi models based on the adsorption potential theory of Polanyi were used to successfully describe equilibrium water sorption from ethanol-water and butanol-water systems to

natural materials such as corn meal, canola meal, and so on, which contain large pores (Chang et al., 2006a; Jayaprakash et al., 2017; Ranjbar et al., 2013). The parameters such as the limiting mass for sorption and the mean free energy were estimated by model fitting (Jayaprakash et al., 2017; Ranjbar et al., 2013). Polanyi adsorption potential theory assumes the adsorbed layer has a multilayer character, and it applies to the van der Waals equation (Dąbrowski, 2001). Polanyi potential theory assumes that the attracting potential field exists adjacent to the surface of the adsorbent and concentrate vapors there (Perry & Green, 2008). The strength of this field is the adsorption potential. The adsorption potential, which was defined by Polanyi, is equal to the work done to compress the solute from its partial pressure to its vapor pressure (Perry & Green, 2008). According to the potential theory, the equilibrium data at different temperatures can be described in a single characteristic adsorption curve by plotting equilibrium loading as a function of adsorption potential. The adsorption potential and the characteristic adsorption curve are basic concepts of the Polanyi theory. The Dubinin-Polanyi models for microporous and large pore materials have been recognized as a useful tool for the description of water adsorption equilibrium on heterogeneous surfaces such as biomaterials.

In addition, adsorption isotherms of ethanol and water vapors on different adsorbents were analyzed using Toth, Dubinin-Ashtakhov, Sips, hybrid Langmuir-Sips, and the excess surface work models (Gabruś & Downarowicz, 2016). Moreover, multicomponent adsorption model was developed for the adsorption process in biobutanol production (Jiao et al., 2015; Simo et al., 2006).

2.5.2 Site energy distribution analysis

The binding energy is defined as the energy associated with the adsorption of a target molecule on a specific type of adsorption site (Kumar et al., 2019). Different types of adsorption sites are located on the heterogeneous adsorbent surface. The site energy distribution analysis

provides information about the binding energy for the target molecule, the interactions between site and target molecule, the sites heterogeneity and the number density of the adsorbent sites, which are essential to study the heterogeneity of heterogeneous biosorbent. Using site energy distribution to analyze the adsorption data of heterogeneous materials is an effective method to study the system heterogeneity and the interaction between adsorbent and adsorbate.

The approximate energy distribution function is obtained using the Cerofolini approximation (condensation approximation) (Carter et al., 1995). In this way, the approximate distribution functions can be derived from isotherm equations, and the site energy distribution is written in terms of isotherm parameters. The sorption isotherms correspond to specific site energy distribution. The approximate site energy distribution provides a new way to analyze the equilibrium data. It relates the changes in isotherm parameters to changes in the energy characteristics of sorbent surfaces. In turn, site energy distribution changes may also indicate the specific mechanisms.

The approximate distribution is not normalized, and the area under the distribution curve can be interpreted as the maximum sorption capability (Carter et al., 1995; Shen et al., 2015). The mean of the site energy distribution can be used to depict the interaction forces between solute molecules and sorbents, and the width of the site energy distribution can be employed to describe the surface energy heterogeneity of the sorbents (Shen et al., 2015). The approximate energy distribution has been successfully used in data analysis in liquid phase and gas phase adsorption with Langmuir, Toth, Dubinin-Ashtakhov models, etc. as the overall isotherm (Carter et al., 1995; Kumar et al., 2011; Shen et al., 2015).

In the study of adsorption of hydrogen by pitch-based activated carbons, Kumar and co-workers (Kumar et al., 2011) used Toth isotherm and approximate site energy distribution method

to investigate the performance of adsorption of hydrogen on activated carbons containing heterogeneous surfaces. The site energy was analyzed and compared between different adsorbents. Shen and co-workers have applied approximate sorption site energy distributions to analyze the organic pollutants adsorption on carbonaceous based on the Dubinin-Ashtakhov isotherm modeling results (Shen et al., 2015). In addition, the average site energy and standard deviation of the site energy distribution were deduced and applied to analyze the sorption site heterogeneity and the interaction between sorbents and sorbates (Shen et al., 2015). Furthermore, site energy distribution analysis was successfully done for water sorption on the surface of biosorbent (Jayaprakash et al., 2017). The site energy analysis is effective for demonstrating the heterogeneous sorption site distribution of the sorbents.

2.6 Dynamics study in alcohols dehydration in packed columns

In the practical dehydration by adsorption in packed column systems, there are complex gas-solid interactions involving an unsteady-state process. Therefore, methods need to be developed to predict the dynamic performance and sorption characteristics using limited data. Mathematical models can be used to evaluate the sorption behaviour of fixed-bed columns and the effects of the design variables on the performance of the adsorption process.

Many mathematical models have been used to evaluate the effects of the design variables such as bed height, feed flow rate, temperature, initial adsorbate concentration, and pressure on the adsorption dynamic performance in fixed-bed columns (Chahbani & Tondeur, 2000; Chang et al., 2006b; Gorbach et al., 2004; Jiao et al., 2015; Serna-Guerrero & Sayari, 2010). Real adsorption in fixed bed columns is complex. Thus, it is very challenging to solve the models taking into account the equilibrium, axial dispersion, interactions between the adsorbates, mass transfer, and

sorption dynamics (Chu et al., 2011; Gutiérrez Ortiz et al., 2014). Reasonable simplification needs to be applied to determine the analytic solutions of the models.

Adsorption kinetics can be determined by analyzing adsorbate breakthrough curves. The Bohart-Adams model is widely used to describe the kinetics in a fixed bed in biosorption research (Chu, 2010; Faizal et al., 2014). It describes the sorbate-adsorbent interaction by the quasi-chemical rate expression (Bohart & Adams, 1920). This model is based on the assumption that the reaction rate is proportional to the sorbate concentration in the gas phase and the fraction of the sorbent capacity remaining (Karpowicz et al., 1995). This model assumes that the diffusion steps are very fast, and the rate is limited by surface interaction (adsorption) (Bohart & Adams, 1920; Gutiérrez Ortiz et al., 2014). After fitting it to breakthrough curves obtained from the experiments, the determined model parameters such as the Bohart-Adams rate constant and the saturated sorbate loading in sorbent are used for commercial adsorption column design (Thurgood & Cells, 2007). In addition, the Thomas model, which is similar to Bohart-Adams model, was successfully applied to study the dynamics for ethanol recovery by adsorption column (Gabruś & Downarowicz, 2016).

The general rate model (GRM) is a chromatographic model, which considers axial dispersion, pore diffusion resistance, film mass transfer, and nonlinear isothermal behaviors (Gu et al., 1990). A general rate model implementing a competitive isotherm and the convection/diffusion theory was used to study the sorption dynamics of acetone–butanol–ethanol (ABE) in a fixed-bed column at different operating conditions (Jiao et al., 2015). The model parameters such as external mass transfer coefficient, axial dispersion coefficient, and pore diffusion coefficient were calculated. Sorption of ethanol and water on crystalline molecular sieve and silicalite was measured, and intraparticle transport was described in terms of a pore diffusion model (Farhadpour & Bono, 1996).

The linear driving force (LDF) model is frequently used for describing the sorption kinetics in the packed column, because it is simple and easy to be solved (Sircar & Hufton, 2000). In the LDF model the pore diffusion and the film mass transfer are lumped into an effective mass transfer coefficient (Jiao et al., 2015). The analysis of mass transfer can be carried out using the model parameter mass transfer coefficient and the derived mass transfer resistance. An axially dispersed plug flow model based on the LDF approximation was used to predict the adsorption breakthrough curves of a biosorbent (Aguilera & Gutiérrez Ortiz, 2016). The LDF model was used to describe the adsorption kinetics of ethanol and butanol vapor in the packed column, and a plug flow model containing axial dispersion was used to predict the concentration profiles. (Claessens et al., 2019). An LDF based mass-transfer model, which was developed by Klinkenberg, was used to successfully simulate the breakthrough curves of ethanol dehydration in a biosorbent column (Chang et al., 2006b; Tajallipour et al., 2013), and the analysis of mass transfer was carried out using the model parameters. The breakthrough curves of water vapor adsorption on zeolite were simulated by a model based on linear driving force approximation (Gorbach et al., 2004).

Sorption based technologies using cellulosic biosorbents could be a promising method for bioalcohols purification (Jayaprakash et al., 2017). However, the dynamics of water sorption, mass transfer resistance, and controlling steps during water sorption on the cellulosic materials are not well understood. Dynamics study in dehydrating bioalcohols such as biobutanol and bioethanol was limited. Investigation in this area is essential to understand the fundamentals of water biosorption and for application in the industry (Fulazzaky et al., 2013).

2.7 Mechanisms of alcohols dehydration using biosorbents

Biosorption may base on a variety of mechanisms including absorption, adsorption, ion exchange, surface complexation, and precipitation (Fomina & Gadd, 2014). The polar attraction

between water molecules and polar groups of biosorbents is considered to be one of the major mechanisms for bio-alcohol dehydration using biosorbents (Chang et al., 2006a). The components of biosorbents contain polar groups such as hydroxyl groups and carboxyl groups (Lee & Rowell, 2004). The polar groups prefer to adsorb water molecules other than alcohols with lower polarity (Sun et al., 2007). The capillary condensation was also suggested to account for some of the sorbed water (Beery & Ladisch, 2001b). The amylopectin structures in the starch material physically trap water molecules in the matrix of chain branches (Rebar et al., 1984). When massive water molecules are present, water can penetrate into the sorbent cellulosic matrix by absorption.

The biosorbents may also work as molecule sieves which can separate water from alcohols due to that the size of a portion of their pores is smaller than that of alcohol molecules but bigger than that of water molecules (Sun et al., 2007).

Furthermore, the differences in the sorption rate can also lead to the selective removal of water from alcohol vapor in a sorption bed. For example, the sorption rate of ethanol was slower than that of water, which indicates that the ethanol dehydration by a biosorbent is likely a rate dependent process (Lee et al., 1991).

Overall speaking, bio-alcohols dehydration could be involved in any or the combination of the above mentioned multiple mechanisms based on a variety of mechanisms including absorption, adsorption, ion exchange, surface complexation, and precipitation. Considering the nature of biosorbents, water removal by biosorbents could be more reasonably considered to be sorption which may include adsorption and absorption. Sorption can be used to describe any system where a sorbent interacts with a sorbate (Fomina & Gadd, 2014). Sorption is the preferred term unless it is clear which process (absorption or adsorption) is operative (Fomina & Gadd, 2014). Thus, this

term “sorption” and its derived term “sorbate” are used where applicable in the chapters associated with the results and discussion of this thesis.

CHAPTER 3. MATERIALS AND METHODS

Contribution of this chapter to overall Ph.D. work

This chapter presents the materials, characterization methods, experiment equipment, and experimental procedures used in the overall study of this thesis.

3.1 Materials

The raw oat hull materials were obtained from Richardson Milling Ltd. (Saskatchewan, Canada). The raw oat hull material contains 37% cellulose, 35% hemicellulose, 7% lignin, 5% protein, 2% fat and 5% ash, according to the data provided by the oat hull supplier Richardson Milling. The oat hull based biosorbent with particle sizes ranging from 0.425 to 1.18 mm was used in sorption experiments. The pretreatment of the raw oat hull before it was used in the experiment can be seen in Chapter 4. Butanol used in the experiment is 1-butanol (ACS reagent grade 99.9%) purchased from Fisher Scientific (Ottawa, Ontario). All the water used in this study was distilled water. Butanol-water solutions were prepared at the required mass concentrations by mixing 1-butanol with distilled water.

3.2 Characterization methods used for oat hull based biosorbent

The biosorbent was characterized by various methods, such as surface area analysis, thermogravimetric analysis, *Fourier* transform infrared spectroscopy (FTIR), scanning electron microscopy (SEM), particle size distribution, and optical microscope imaging. The details of the measurements were given as follows.

The surface area and pore volume of the biosorbent were determined through N₂ adsorption-desorption isotherm at 77 K using the Brunner-Emmet-Teller (BET) theory by a surface area and

porosity analyzer (Micromeritics ASAP 2020). The tested samples (biosorbent based on oat hull) were degassed at 110 °C under the vacuum of 500 μ Hg for 12 h before measurement. The micropore and mesopore area were determined by the *t*-plot method and Barrett-Joyner-Halenda (BJH) method, respectively.

The particle size distribution of the biosorbent sieved to 0.425–1.18 mm was determined by Mastersizer 2000 (Malvern Instruments) particle size analyzer via a laser diffraction method. Samples were delivered by the compressed air passing through the measurement area. During measurement, sample particles were passed through the laser beam. The scattering intensity of particles was then measured by a photosensitive detector to calculate the particle size. The Mie theory of light scattering was used to calculate the size of the particles. The results were reported as the volume equivalent sphere diameter.

The thermal stability of the biosorbent (0.425–1.18 mm particle size) was estimated by the thermogravimetric analyzer (TA Instruments TGA Q500) in the range of 25 to 800 °C. The sample was weighed by the TGA instrument continuously as it was heated at the heating rate of 5 °C/min.

The functional groups of the biosorbent were determined by *Fourier* transform infrared spectroscopy (JASCO FT-IR 4100). The oat hull samples were finely ground to 0.125-0.250 mm before measurement. Each FTIR spectrum was measured from 500 to 4000 cm^{-1} at 4 cm^{-1} resolution with 64 scans.

The surface morphology of the biosorbent was investigated by JEOL JSM-6010LV scanning electron microscope. In this work, the measurements of biosorbent were carried on at 10 kV with magnification 1000 times.

Coomassie blue staining was conducted to study the water diffusion into the inner structure of the oat hull based biosorbent. Oat hull was stained with Coomassie staining solution (0.25% Coomassie brilliant blue, 50% methanol, 10% acetic acid, the rest is water) for 3 min at room

temperature on a shaker to ensure full contact staining. Then the sample was de-stained in a solution containing 50% methanol, 10% acetic acid, and 40% water for 30 min at room temperature. The stained sample was placed on a glass substrate and covered with a coverslip held in place by double-sided tape along one edge. Finally, imaging was performed using an Olympus BX51M optical microscope with a high-speed camera (Olympus K-TV0.63XC 7J19174) and a high-power illumination source (EXFO X-Cite series 120).

Water transport through oat hull was observed using the Olympus BX51M optical microscope with the high-power illumination source (EXFO X-Cite series 120). 5 μ L of blue dye solution (1 mL H₂O + 20 μ L of blue food dye (Assorted Food colors & egg dye, McCormick & Co., Inc, Hunt valley, MD)) was loaded to the edge of oat hull sample placed on the glass microscope slide. Optical microscopy imaging was performed after 40 min of adding the dye solution. Microscopy images were then analyzed using ImageJ (NIH) software.

The transport of the mixture of butanol and water through the oat hull biosorbent was also monitored using the Olympus BX51M optical microscope. Butanol-water solution was loaded to the edge of oat hull sample placed on the glass microscope slide. The optical microscopic images were taken in time intervals over several minutes following the initial addition of butanol-water solution. Microscopy images were then analyzed using ImageJ (NIH) software.

3.3 Experimental apparatuses

The experiments of butanol dehydration or sorption of water and/or butanol using the biosorbent based on oat hull was investigated in a continuous packed column system. The experimental setup is demonstrated in Figure 3.1. The stainless-steel column packed with the biosorbent was used as a fixed-bed dehydration apparatus. The internal diameter of the column is 4.75 cm (wall thickness 0.17 cm), and the length is 0.5 m. The column was loaded with 300 \pm 25 g

oat hull based biosorbent (0.425–1.18 mm particle size), and particle density is approximately 1440 kg/m³ (Agu et al., 2017). In this work, the volume median diameter of biosorbent particles (approximately 0.92 mm) was determined to present the diameter of the biosorbent particle size for dynamics analysis. The column is equipped with an oil heating jacket to maintain the temperature.

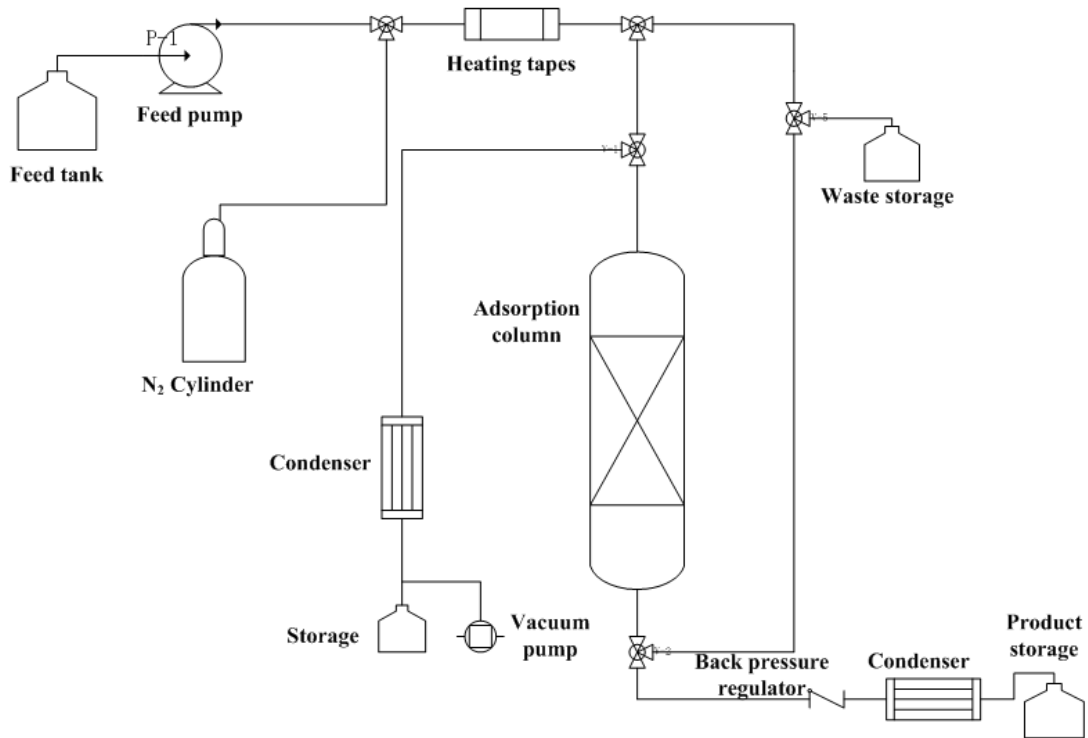


Figure 3.1 Schematic diagram of the experimental setup.

In addition to the column, the dehydration system is composed of a feed tank with stirring, a digital piston pump (Cole-Parmer, RK-74930-05), a gas flow controller to adjust the flow rate of the carrier gas, the pipeline equipped with the heating tape, two thermocouples (Omega K type, US) to monitor the temperature at the top and bottom of the packed column, a pressure transducer (Honeywell, US) to monitor the pressure in the column, a back pressure regulator connected to the

bottom of the column to maintain stable pressure, and a condenser connected to the outlet of the column to condense the effluent.

Water concentration in the feed and effluent was determined by Mettler Toledo Karl Fischer titrator (Mettler Toledo DL32). Butanol content in the feed and effluent samples was calculated by subtracting the mass of water from the total mass of the sample, and this method was cross-validated by a gas chromatograph (Jayaprakash et al., 2017).

3.4 Dehydration and sorption experiments

All experiments in regards to butanol dehydration or sorption of pure water or pure butanol were done by following the procedures described below.

First, the liquid butanol and/or water feed stored in a jacketed sealed tank with stirring was preheated to around 50 °C. In the meantime, the packed column system was set to the desired temperature. After the desired temperature was obtained, the feed pump was switched on and the liquid feed was pumped to the pipeline equipped with heating tapes to vaporize. The vaporized feed was carried by nitrogen at a flow rate of 680 mL/min. It is to point out that the use of vapor feed for dehydration makes it possible for the process developed in this work to apply in the real ABE industry to directly feed the butanol-water azeotrope vapor obtained from the preliminary distillation in the industry into the dehydration system. This can reduce the energy to be consumed by condensing the butanol-water azeotrope vapor. In addition, this method is to avoid the possible release of organic components of the biosorbent when it contacts the liquid solution.

In another note, the carrier gas (nitrogen) would not be used in the industrial dehydration process since it could add energy costs in the condensation step. The purpose of using it in this work is to study the fundamentals of water and butanol sorption. The sorption of non-polar gases

such as nitrogen, methane and carbon dioxide on the biosorbent was negligible (Ghanbari & Niu, 2018, 2019). Thus, nitrogen was used as carrier gas for this work.

Then the feed was led to bypass before it was fully vaporized. After the feed was fully vaporized, the feed stream was directed to the top of the column through a three-way valve. The pressure of the column was adjusted to the desired value by the back-pressure regulator. During the sorption process, the temperature and pressure at the top and the bottom of the column were monitored by thermocouples and pressure transducers. The effluent was condensed by a lab condenser with circulating cooling water maintained at 5 °C. Then the effluent was collected and weighed periodically. The bed was considered saturated (equilibrium) when the content of butanol and/or water in the effluent reached the same level in the feed. The feed pump and the feed line were then closed. The regeneration step started after each sorption run.

Then water or butanol breakthrough curves were generated by plotting water or butanol concentration in the effluent versus time. In order to obtain the amount of water and/or butanol sorbed on the biosorbent (called uptake, g/g dry biosorbent), the mass balance was done for both components. That being said, uptake at any time was calculated by subtracting the output mass of water or butanol from the input mass of water or butanol for the period of time and then divided by the total mass of the dry biosorbent packed in the column. Sorption capacity was calculated in a similar method but with all the data until the process reached equilibrium. Each experiment was run for two to three times. The results are presented as average value with standard deviation. The detailed experimental conditions used in the sorption of pure water or pure butanol and the dehydration in the butanol-water binary system are described as follows.

3.4.1 Sorption of pure water or butanol in the single component system

The pure water or butanol sorption on the biosorbent was investigated and compared in terms of the sorption isotherm and dynamics of these two components. In the experiments of the single component systems, similarly, pure water or pure butanol was vaporized and carried by N₂ (680 mL/min). The liquid feed flow rate ranges from 0.3 to 5 mL/min. The feed concentration was changed by adjusting the flow rate of liquid feed. 110 °C and 120 °C were chosen as operation temperatures to avoid condensation of the vapor feed in the column. The pressure of the system was set at 135 kPa to reduce energy consumption. The effluent was also condensed by a condenser with circulating cooling water maintained at 5 °C, and then collected and weighed periodically after the first drop was collected. Water or butanol sorption uptake was determined by the mass balance, i.e. the water/butanol input minus the water/butanol output per gram of biosorbent in the column.

3.4.2 Dehydration in the butanol-water binary system

The dehydration of low-grade butanol-water feed was carried out in the above mentioned packed column system. The mixtures of butanol and water vapor with different concentrations (56-92 wt% butanol) were used as feed. In another word, the butanol concentration of the feed in this study was close to or higher than that of the azeotrope of butanol and water, which is generated from distillation in the biobutanol production industry. The flow rate of liquid feed was 3 mL/min, which was vaporized and carried by nitrogen gas at a flow rate of 680 mL/min. The gas flow rate used in this work was based on the following considerations: 1) Ensured the butanol-water vapor had sufficient residence time within the column in order for water to be effectively sorbed by the packed biosorbent, and avoid high pressure drop across the column; 2) Let the column be saturated within a reasonable time period for sample collection.

The boiling point of the mixture of water and butanol is different from that of pure water or pure butanol. Thus, 110, 115, and 120 °C were chosen as the sorption temperature of the system to avoid condensation of the butanol-water mixture in the column. The pressure of the system was set at 135 kPa to reduce energy consumption. A higher pressure of 170 kPa was also tested to study the effect of pressure on the performance of the biosorbent.

3.5 Desorption

Desorption (regeneration) of the biosorbent was performed under vacuum in the same bed after the dehydration or sorption was done. Once the biosorbent packed in the column was saturated, the feed pump was switched off, and the valve of the feed line was closed at the same time. During the regeneration, hot nitrogen steam 850 mL/min was purged to the column from the bottom to flash out the adsorbate for 4 h under the pressure of 33 kPa at 105 °C. This regeneration temperature is much lower than that used for commercial adsorbents such as molecular sieves, silica gel, and alumina (at least 175 °C, and up to around 300 °C) (Beery & Ladisch, 2001a; Fahmi et al., 1999). It has been reported that the biomass-derived adsorbents are more beneficial as compared to other types of adsorbents due to lower energy demand (Boonfung & Rattanaphanee, 2010). For example, the energy cost of the dehydration of ethanol using CaO was reported to be 3,669 kJ/kg ethanol, while the energy cost by the adsorption using cellulose was 2,873 kJ/kg ethanol (Boonfung & Rattanaphanee, 2010). The conditions used for the desorption procedure were confirmed to be adequate not only to regenerate the column, but also to preserve the properties and stability of the biosorbent. The properties and stability of the biosorbent before and after sorption-desorption cycles are discussed in Chapter 9.

CHAPTER 4. PREPARATION AND CHARACTERIZATION OF AN OAT HULL BASED BIOSORBENT

Contribution of this chapter to overall Ph.D. work

This chapter presents the development and characterization results of the oat hull based biosorbent. They are important to develop the butanol dehydration or selective water sorption process and understand the characteristics and mechanisms.

4.1 Preparation of oat hull based biosorbent

The biosorbent used in this study was derived from a cellulosic material oat hull. The raw material was ground, air dried, and sieved by Canadian Standard Sieves Series (Combustion Engineering Canada Inc.) to sizes of 0.425–1.18 mm. Then, the oat hull particles were dried in an oven at 105 °C for 48 h and kept in desiccators. They were used as biosorbent without further treatment.

The dehydration of butanol by sorption using the oat hull based biosorbent is an environmentally friendly and cost-effective process. Further chemical and physical treatment of the raw oat hull will increase the cost. Also, the FTIR results of the raw oat hull sample in this study (data shown in Fig.4.3 of this chapter) were compared to that of the oat hull sample in another study (Banerjee et al., 2016), where the oat hull sample was washed liberally with distilled water for several times. The FTIR spectra of the two samples are consistent. In addition, the FTIR spectrum of the biosorbent in this study is largely consistent with the FTIR spectra of cellulose, hemicellulose, and lignin, three main components of oat hull (Yang et al., 2007). These results confirm that the raw oat hull material used in this study can reasonably represent the pure oat hull.

Thus, in this study, the raw oat hull material after the above mentioned simple treatment was used for experiments.

4.2 Characterization results of the biosorbent

4.2.1 Surface properties and particle size distribution

The specific surface area, pore volume and porosity of the biosorbent were determined by N₂ adsorption-desorption measurements. The BET surface area analysis revealed that the biosorbent had the specific surface area of 1.5 ± 0.3 m²/g. The *Barrett–Joyner–Halenda* (BJH) pore size distribution suggests that 32% of the pores fall in the macroporous category (>50 nm), and 65% of the pores belonged to mesopores (2–50 nm). The average pore diameter and pore volume were 8.1 nm and 0.003 cm³/g, respectively.

The particle size distribution of the biosorbent sieved to 0.425–1.18 mm was determined by the particle size analyzer described in Chapter 3. The volume-based particle size distribution of the biosorbent is shown in Figure 4.1. It can be seen from the results that the size of 60% of the biosorbent particles falls in the range of 0.41–1.19 mm. About 34% of them are bigger than 1.19 mm, and 6% of them are smaller than 0.41 mm. The volume median diameter of the particles $D(v, 0.5)$ is approximately 0.92 mm. It indicates that 50 % of the particles are bigger than 0.92 mm, and 50% of them are smaller than 0.92 mm. It was also used to present the diameter of the biosorbent for the kinetics analysis in Chapter 7 of this thesis.

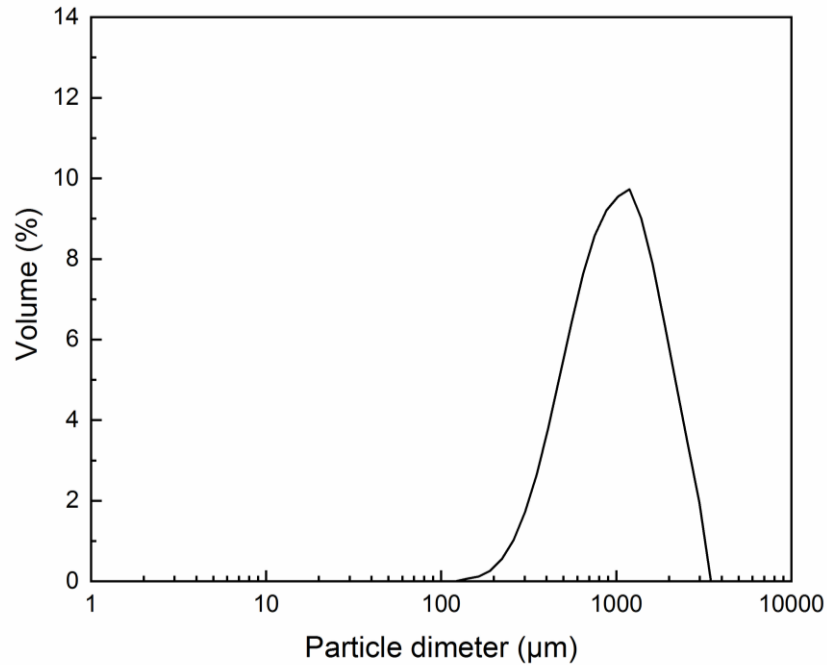


Figure 4.1 Particle size distribution of the biosorbent.

4.2.2 Thermal stability

Figure 4.2 shows the results of the thermogravimetric analysis (TGA). The oat hull based biosorbent (0.425–1.18 mm particle size) has high thermal stability up to 220 °C, which is higher than the chosen dehydration (sorption) temperature (≤ 120 °C) and desorption temperature of 105 °C in this research. There was a considerable weight loss at 220–315 °C, which corresponds to the decomposition of hemicellulose. The weight loss at 315–400 °C relates to the pyrolysis of cellulose (Yang et al., 2007). The pyrolysis of cellulose and hemicellulose mostly occurred within the above-mentioned temperature range, while the decomposition temperature range of lignin was wide, from 160 to 900 °C (Yang et al., 2007), so there was no characteristic weight loss observed for lignin in Figure 4.2.

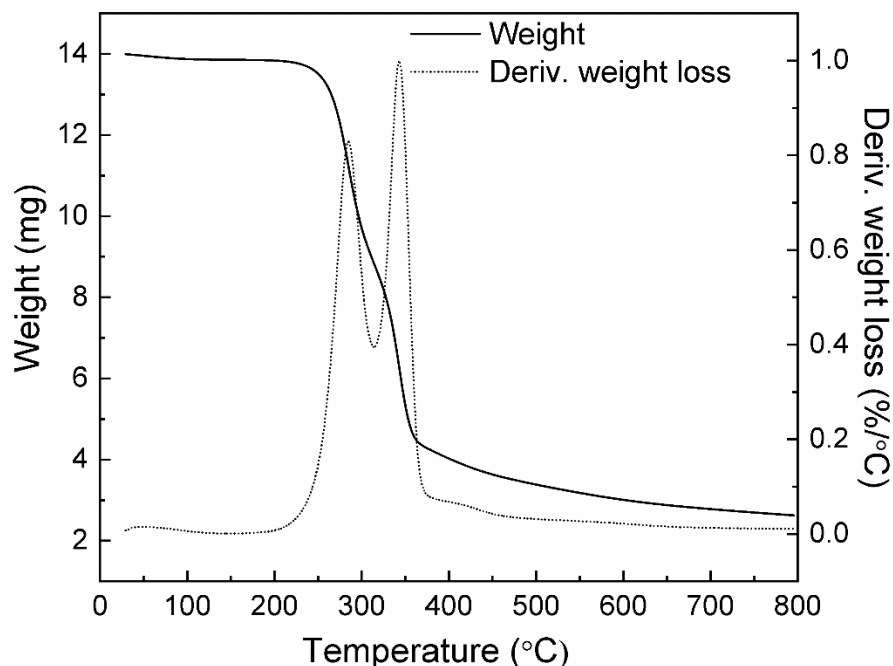


Figure 4.2 Thermogravimetric curves of the oat hull based biosorbent (0.425–1.18 mm particle size).

4.2.3 FTIR spectra

The functional groups in the biosorbent are observed in Figure 4.3(a). The O-H stretching was found at a broad peak at 3323 cm^{-1} . The existence of OH groups could indicate the occurrence of H-bonding which could play an important role in butanol dehydration.

The absorption band at 2921 cm^{-1} was attributed to C–H_n stretching; peaks at 1512 and 1726 were attributed to C=O stretching; the peak at 1633 cm^{-1} may indicate the existence of C=C of the aromatic ring in the lignin; the band at 1232 cm^{-1} may indicate the C–O stretching; absorption band at 1022 and 1149 cm^{-1} was due to C–O–C stretching vibration. The FTIR spectra of the biosorbent (oat hull) was largely consistent with the FTIR spectra of cellulose, hemicellulose, and lignin (Yang et al., 2007), the three main components of oat hull.

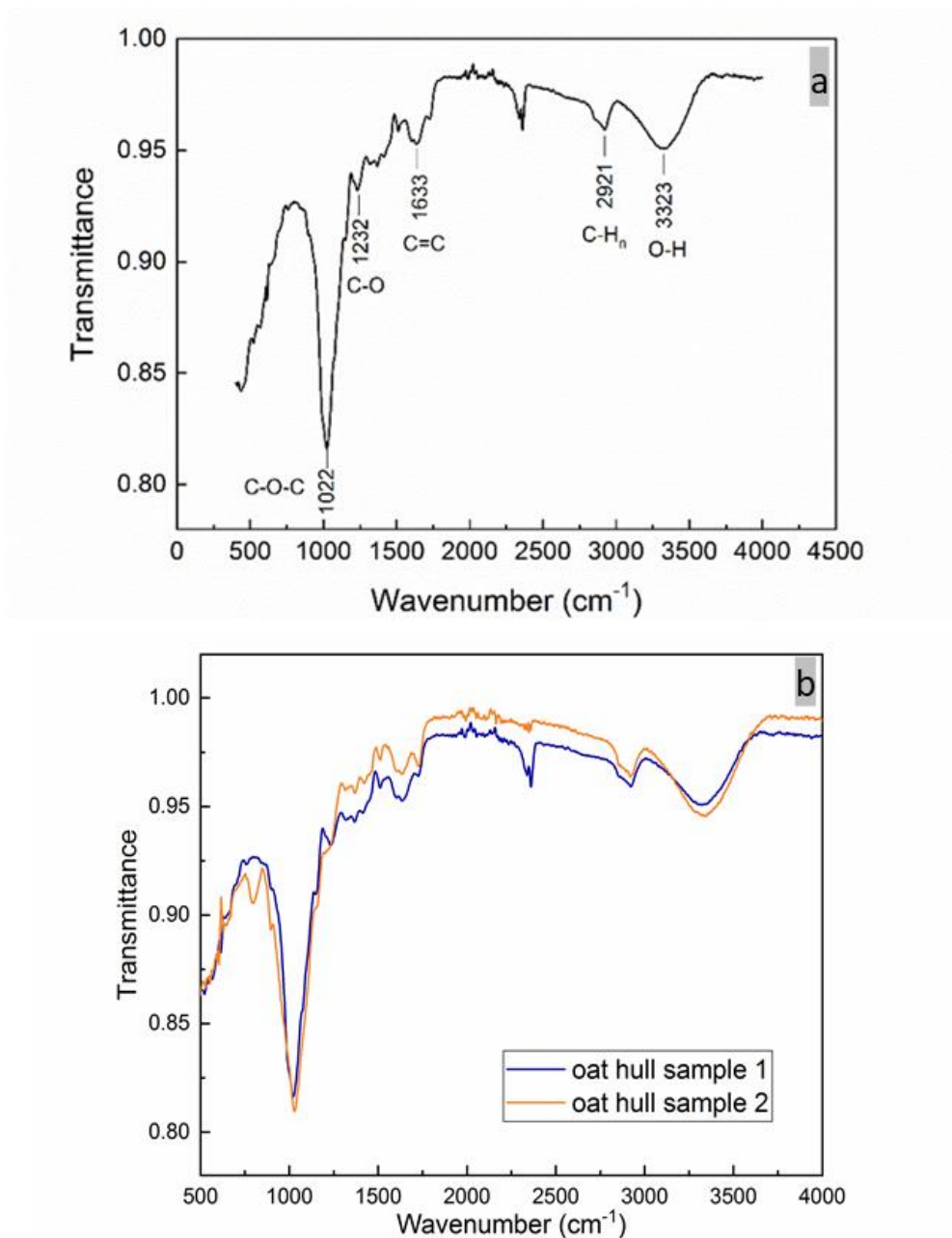


Figure 4.3 (a) FTIR spectra of oat hull based biosorbent; (b) FTIR spectra of two different batch oat hull based biosorbent.

Figure 4.3(b) shows the FTIR spectra of two different batch oat hull based biosorbent. The sample one is the batch of oat hull obtained in the year 2014, and sample 2 was the batch obtained in the year 2018. The two curves are overlapped, and almost all peaks sites are similar considering the error of analysis. The two batches of oat hull based biosorbent are similar according to the

FTIR results. The dehydration performances of the two batches of oat hull need to be investigated, and the results are shown in Chapter 5.

4.2.4 SEM analysis

The SEM images of the oat hull based biosorbents before and after butanol dehydration are shown in Figure 4.4. Figure 4.4(a) shows the texture and pore feature of the original biosorbent. There were deep holes and bundle-holes widely distributing on it. Fibered networks were also clearly visible. The deep pores and complicated reticular fiber structure probably play important roles in binding water molecules. The micrograph of the biosorbent after butanol dehydration and desorption shown in Figure 4.4(b) was captured to compare with that of the original biosorbent. The structure of fiber network and pores of the biosorbent before and after butanol dehydration are similar. The well-developed pores and bunched fiber were also clear and distinct on the biosorbent after butanol dehydration, which indicates the structure of oat hull based biosorbent was relatively stable during the butanol dehydration and desorption.

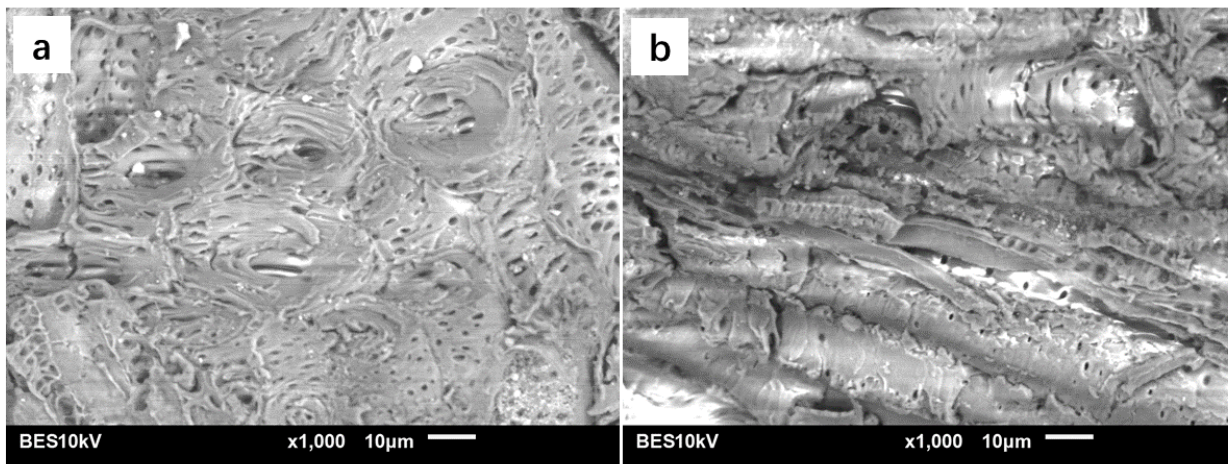


Figure 4.4 SEM images of oat hull based biosorbent (a) before sorption; (b) after sorption and regeneration.

4.2.5 Coomassie blue staining and optical microscopy imaging

The structure of the oat hull based biosorbent and water transport through it were observed by the optical microscope. Coomassie blue staining was conducted to study the water diffusion into the inner structure of the biosorbent. The detailed materials and methods are described in Chapter 3. Figure 4.5 shows the images of the biosorbent after contacting with Coomassie brilliant blue solution, which demonstrated that water diffused into the inner part of the oat hull. In certain areas, blue dots and lines were visualized. Oat hull contains cellulose, hemicellulose, lignin, and low content of protein. According to the literature (Sapan et al., 1999), Coomassie blue can bind to protein structures through ionic interactions between dye sulfonic acid groups and positive protein amine groups as well as Van der Waals.

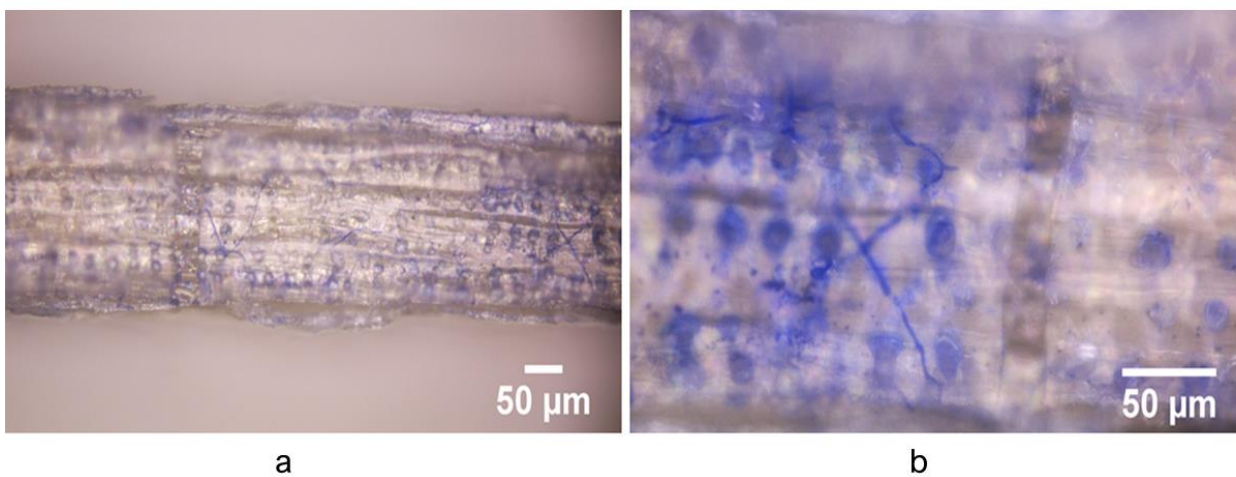


Figure 4.5 Coomassie blue stained oat hull (a) imaged using a 20x objective; (b) imaged using a 100x objective (Scale bars, 50 μ m).

In addition, Coomassie blue may also attach to cellulose, hemicellulose and lignin structures in oat hull according to lots of studies (Agnihotri & Giles, 1972; Annadurai et al., 2002; Menkiti et al., 2018; Sun et al., 2015; Zhang et al., 2016). The results indicated that water molecules

together with the dye molecules may reach the sorption sites of the cellulose, hemicellulose, and lignin in the biosorbent. The detailed investigation in regards could form an area of future research.

Figure 4.6 further shows that water diffused into individual oat hull particles, and the sorption occurred mainly along the longitudinal walls of the biosorbent.

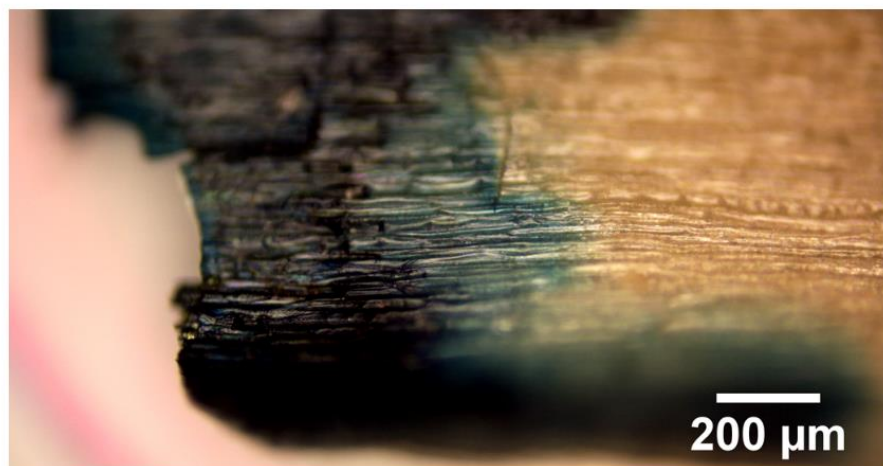


Figure 4.6 Optical microscopy image of oat hull particles after water-dye solution sorption.

In addition, the optical microscopy imaging provides information on the dynamic butanol-water solution transport through the biosorbent particles. Specifically, after addition, the butanol-water solution diffused into individual oat hull particles. As it travelled through the hull's structure with time, empty sorption sites were replaced by filled sites, with a reduction of gas bubbles in a non-uniform manner as can be seen in Figure 4.7. The optical microscopy assists to monitor the progress of how the adsorbates (water and/or butanol) sorbed on the sorption sites of oat hull. However, the competitive and dynamic sorption of water and butanol molecules need to be further studied.

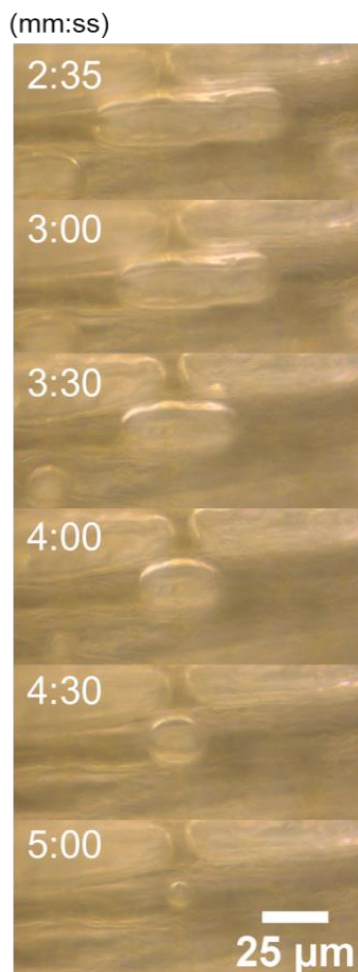


Figure 4.7 Time lapse images of an oat hull particle upon the addition of the solution using a 50x objective (Scale bar, 50 μm).

4.3 Chapter summary

In this chapter, the oat hull based biosorbent was characterized by various methods. Basic properties such as the specific surface area and particle size distribution were determined. The thermogravimetric analysis was carried out to study the thermal stability of this biosorbent. The high thermal stability of the biosorbent was shown at up to 220 °C, which indicated that the biosorbent is expected to be thermally stable when used in butanol dehydration and regeneration at 105–120 °C in this research. The functional groups in the biosorbent were analyzed by FTIR.

The FTIR spectra of this biosorbent was largely consistent with the FTIR spectra of oat hull reported in other studies. SEM analysis provides the texture and pore features of the biosorbent. The micrographs of the biosorbent before and after dehydration (sorption) and desorption were compared to confirm that the structure of oat hull based biosorbent was relatively stable during dehydration and desorption. Coomassie blue staining and the optical microscopy assists to visualize water diffusion into the inner structure of the oat hull based biosorbent.

CHAPTER 5. PRODUCTION OF ANHYDROUS BIOBUTANOL USING THE OAT HULL BASED BIOSORBENT

Contribution of this chapter to overall Ph.D. work

Sorption could be a promising method for removing water from butanol efficiently. However, there are limited studies in butanol dehydration using biosorbents. This chapter aims to investigate whether the oat hull based biosorbent can be applied for butanol dehydration. Thus, the performance of the oat hull biosorbent for pure water or pure butanol sorption was first investigated. Then the experiments of the butanol-water binary system were carried out to obtain the information on butanol dehydration, water selectivity over butanol, competitive sorption, and influence of different operating conditions. Finally, butanol dehydration performances of oat hull materials of different batches were evaluated.

5.1 Performance of oat hull biosorbent for pure water or pure butanol sorption

Pure water and pure butanol vapor sorption on the oat hull based biosorbent were first determined in the single component system in the packed column. The detailed description of the experimental procedure can be found in Chapter 3.

The water sorption breakthrough curves were plotted by the ratio of the mass of water (sorbate) in the effluent to that in feed versus time. The breakthrough curves also provide the information of the breakthrough time, equilibrium time, effluent concentration profile, and sorption of sorbate along with time. The shape of the breakthrough curve can estimate the utilization of the sorption bed and the rate of mass transfer.

The breakthrough curves of water and butanol sorption on the oat hull biosorbent were depicted in Figures 5.1 and 5.2 respectively. It can be seen that the time for the first drop of the

effluent changes with different feed concentrations. The higher the feed concentration, the shorter the time for the first drop to occur. When the sorbates with higher concentration passed into the column, it took less time to reach equilibrium. The breakthrough curves presented in Figures 5.1 and 5.2 indicate faster sorption speed occurred in the first half of the curves which became slower when the process approached equilibrium. At the beginning of sorption, the slope of the breakthrough curve is steep, since there is a high concentration gradient between the biosorbent and the feed. The shape of the breakthrough curves and the equilibrium time suggest that the feed concentration of adsorbates affects the sorption rate in this system. The higher the feed concentration, the higher the mass transfer rate.

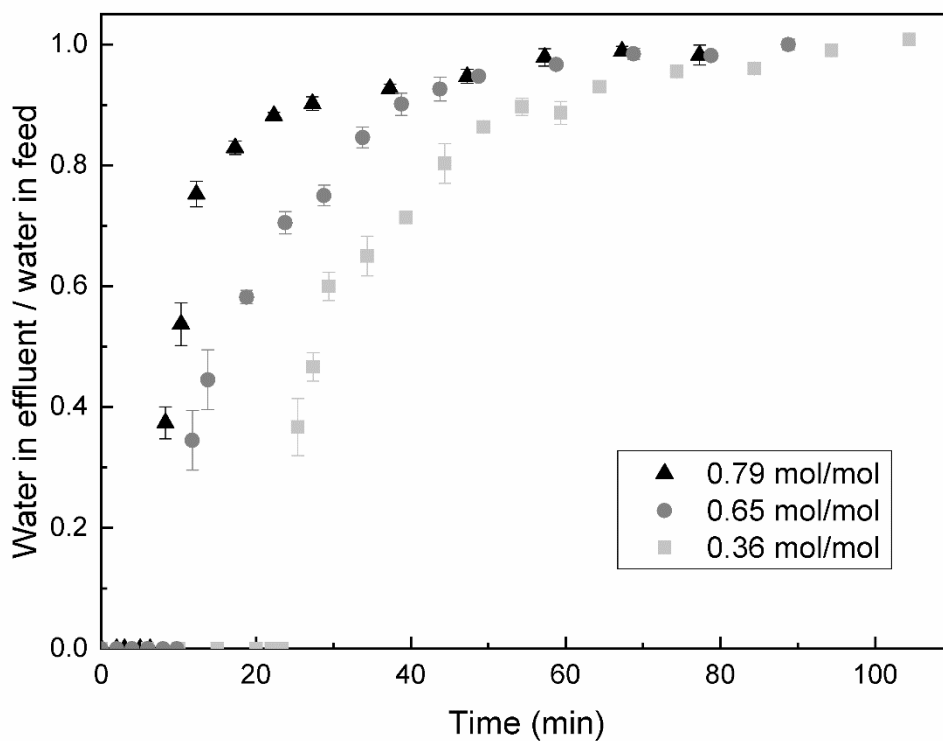


Figure 5.1 The breakthrough curves of water sorption on the biosorbent at 120 °C, 135 kPa at different feed concentrations. Error bars represent standard deviations.

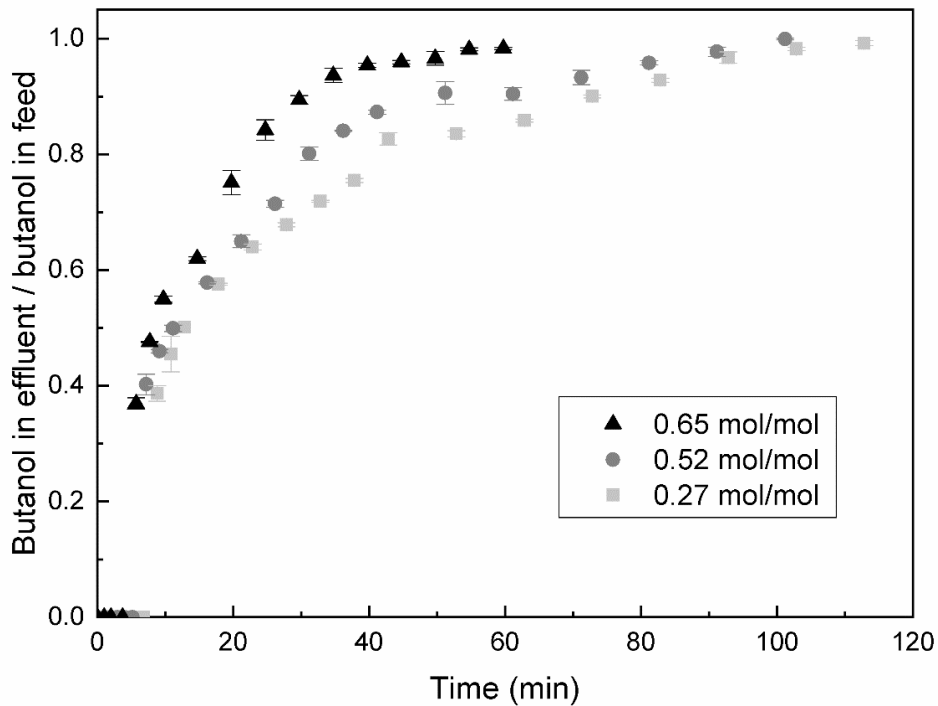


Figure 5.2 The breakthrough curves of butanol sorption on the biosorbent at 120 °C, 135 kPa at different feed concentrations.

To compare the capability of the oat hull based biosorbent for water and butanol sorption, the capacity of sorbed pure water and pure butanol was calculated based on the data of the respective breakthrough curves after the process reached equilibrium. Specifically, it was calculated by the total input amount of water or butanol in feed minus that in effluent at equilibrium which was then divided by the total mass of the dry biosorbent packed in the column. The sorption capacity of pure water and pure butanol vapor at the same experimental conditions are depicted in Figure 5.3. The results show the increase in sorption with the increase of mole fraction of sorbate. Importantly, the water sorption capacity of the biosorbent is much higher than the butanol sorption capacity. Besides, the affinity of water for the biosorbent is stronger than that of butanol. The results suggest that the oat hull based biosorbent has a great potential for butanol dehydration in the butanol-water

binary system, and selective water sorption over butanol on oat hull could be achieved in a butanol-water binary system when feed concentration is properly chosen.

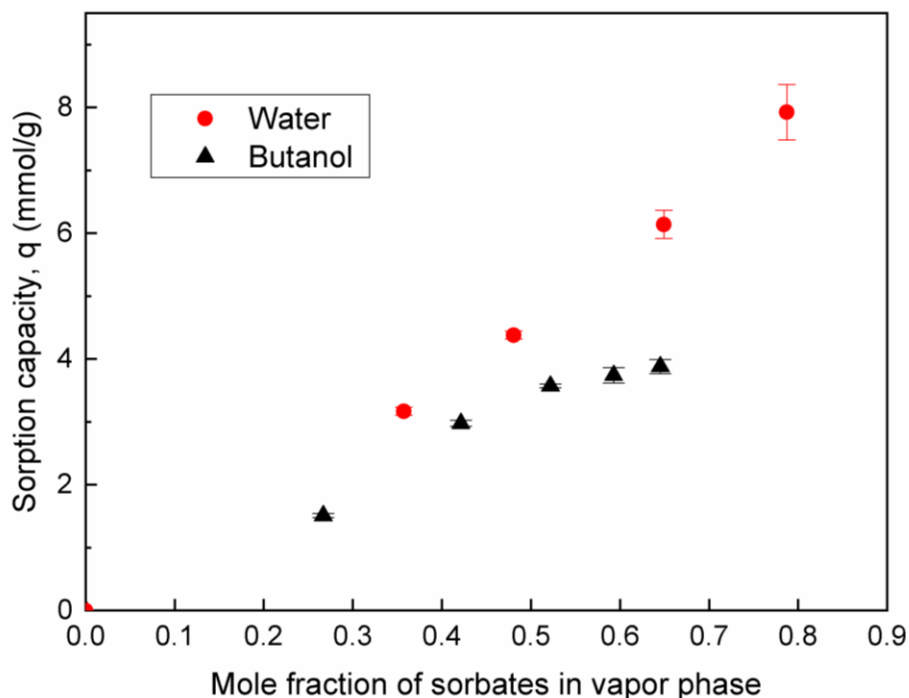


Figure 5.3 The equilibrium sorption capacity of water and butanol on the biosorbent at 120 °C, 135 kPa.

5.2 Performance of oat hull biosorbent for butanol dehydration

This work aims to develop an alternative technology of sorption to remove water directly from the azeotrope of butanol and water vapor generated from distillation to enrich butanol in a hope to reduce or replace the downstream decantation and distillation cycles in the bio-butanol industry. Thus, the experiments of the butanol-water binary system were carried out to obtain information such as water selectivity over butanol, competitive sorption, and the influence of different operating conditions.

For the binary system study, the butanol concentrations of the feed are close to or higher than that of the binary azeotrope of butanol and water (56-92 wt% butanol). The detailed experimental procedure can be found in Chapter 3.

The water separation factor was calculated from Eq. 5.1. X_w and Y_w are the mass concentration of water in the biosorbent and vapor phases, respectively. X_b and Y_b are the mass concentration of butanol in the biosorbent and vapor phases, respectively. The higher water separation factors indicate that water sorption is more favorable.

$$\alpha = \frac{X_w / Y_w}{X_b / Y_b} \quad (5.1)$$

Some of the results with corresponding conditions were listed in Table 5.1. The separation factor of water over butanol is higher than 1, which indicates water has a higher sorption affinity on the biosorbent. More water was sorbed by the biosorbent, so the butanol solution was enriched. The results describe the competitive sorption of water and butanol. At the same temperature, the separation factors increased with the decrease of butanol concentration in the feed. With the increase of butanol content in the feed, the sorption of water dropped sharply, while the sorption of butanol raised when the other conditions were the same, because more butanol molecules competed with water molecules for the sorption sites.

Table 5.1 Sorption capacities of water and butanol on oat hull and separation factors (135 kPa, 110 °C, 0.425–1.18 mm).

Temperature (°C)	Butanol concentration in the feed (wt%)	Water sorption capacity (mg/g)	Butanol sorption capacity (mg/g)	Separation factor
110	56.6±0.7	138±9	58±5	2.94±0.13
110	69.1±0.3	89±3	90±4	2.28±0.05
110	79.7±0.6	67±1	181±9	1.50±0.03
110	90.3±0.7	34±5	300±6	1.06±0.07

Note: Uncertainty was determined by the standard deviation.

The comparison of water sorption capacity of different biosorbents was displayed in Table 5.2. The comparison shows that the oat hull based biosorbent has a comparable water sorption capacity, and it is promising for butanol dehydration. The optimization of conditions for this process using the oat hull based biosorbent is worth being pursued further.

Table 5.2 Comparison of water sorption capacity of different biosorbents at similar conditions.

Adsorbent	Adsorbate	Alcohol concentration in feed (wt%)	Water sorption capacity (mg/g)	Max alcohol concentration achieved (wt%)
Oat hull (this work)	Butanol-water	56.6±0.7	138±9	95.3
Canola meal (Jayaprakash et al., 2017)	Butanol-water	55.0	160	96.7
Oat hull (this work)	Butanol-water	90.3±0.7	34±5	99.0
Canola meal (Ranjbar et al., 2013)	Ethanol-water	95.0	16	99.0

The breakthrough curves of butanol at 110 °C and various feed concentrations are presented as a function of time in Figure 5.4. The concentration of effluent changed significantly within 60 min and then changed slowly when approaching equilibrium. It shows that the oat hull based biosorbent was able to concentrate the lower grade butanol and water mixture to butanol products of high purity. The highest butanol concentrations of effluent obtained from the feed of various butanol contents (56.6%, 69.1%, 79.7%, and 90.3%) are 95.3%, 97.1%, 98.1%, and 99.0%, respectively. The highest water sorption capacity is 138 mg/g obtained at 110 °C, when the butanol concentration in the feed is 56.6 wt.%. The results demonstrate that the oat hull based biosorbent is able to dehydrate the butanol water mixtures at the azeotrope (≈ 56 wt.%), and with higher butanol concentration.

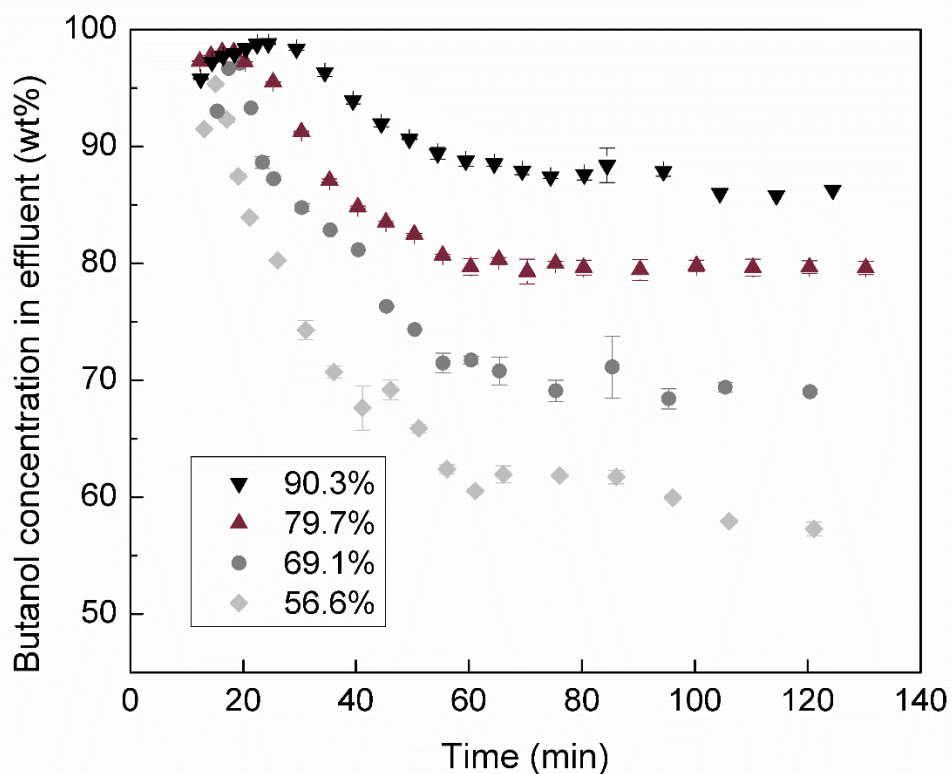


Figure 5.4 Butanol product concentration profiles during dehydration at 110 °C, 135 kPa, and 3 mL/min liquid feed rate with different feeding concentrations.

During the dynamic process of water sorption before equilibrium, the water separation from butanol is effective because the water molecules are smaller, and they have higher polarity than butanol molecules to interact with the polar groups in the biosorbent. As a result, they were sorbed faster than butanol molecules. Particularly, water separation was more effective at the initial stage of sorption, as shown through the breakthrough curves in Figure 5.4. Thus, the product butanol concentration was high at the initial stage of sorption, then gradually decreased as more butanol molecules were sorbed with time till equilibrium. In a regular pressure swing adsorption process for drying applications in industry, the adsorption process is usually operated for a few minutes (Sircar, 2002), which is much earlier before equilibrium is reached. Thus, the results achieved in this work demonstrated that the oat hull based biosorbent has a promising potential for industrial application of drying butanol in a pressure swing adsorption process.

5.3 Effects of the operation parameters of the butanol-water binary system

5.3.1 Effect of temperature

The effect of temperature on sorption of water and butanol from the binary vapor system onto the oat hull based biosorbent was studied at 110, 115, and 120 °C with other conditions set as the same. The results are shown in Table 5.3. The water and butanol uptake capacity decreased as the temperature increased, indicating either water or butanol sorption was exothermic.

Table 5.3 Sorption capacities of water and butanol on oat hull at different temperatures (135 kPa, 0.425–1.18 mm).

Temperature (°C)	Butanol concentration in the feed (wt%)	Water sorption capacity (mg/g)	Butanol sorption capacity (mg/g)	Separation factor
110	56.6±0.7	138±9	58±5	2.9±0.1
120	56.5±0.1	61±1	26±1	3.09±0.07
110	79.7±0.6	67±1	181±9	1.50±0.03
115	79.8±0.6	47±2	150±4	1.2±0.1

The butanol production profiles at two different temperatures (110 and 120 °C) are shown in Figure 5.5. The curve of 110 °C is over that of 120 °C, which shows the product concentrations obtained at a lower temperature are higher than those at the higher temperature. The highest product concentration obtained at 110 °C temperature is higher than that at 120 °C. Compared with 110 °C, the effluent concentration decreased faster at 120 °C, and the slope of the breakthrough curve is steeper. The steeper slope may imply a higher rate of mass transfer, which was caused by a higher rate of diffusion of sorbate molecules into the biosorbent. The results in this section

indicate that the sorption temperature has a significant effect on the performance of butanol dehydration on the oat hull based biosorbent. More detailed work on the effect of temperature on the dynamics can be seen in Chapter 8.

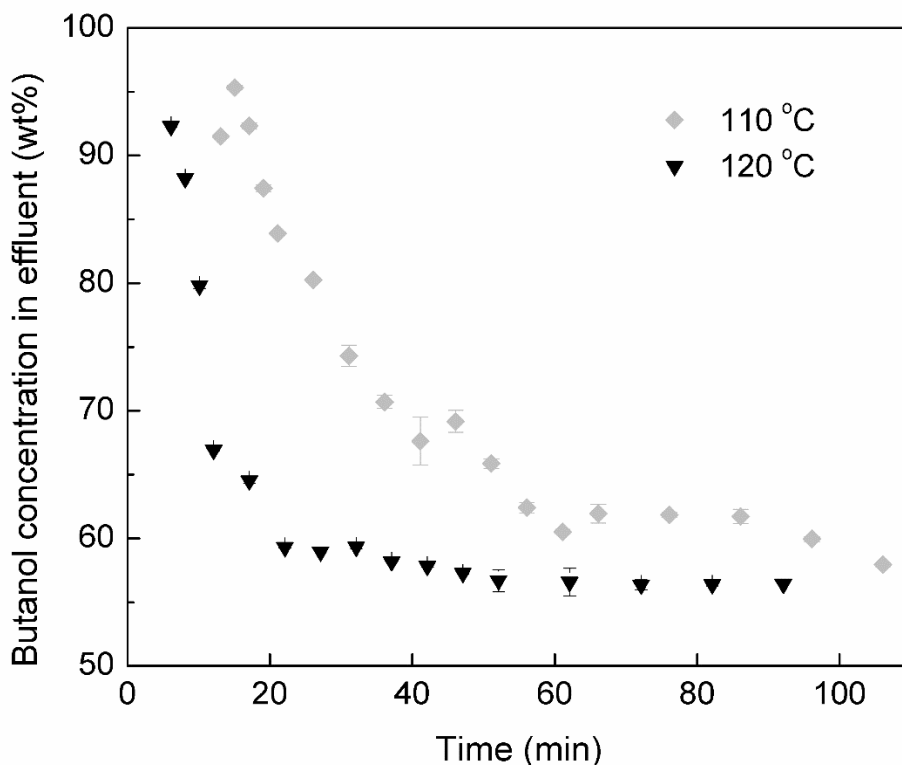


Figure 5.5 Butanol product concentration profiles at different sorption temperatures (135 kPa, 56 wt.% butanol in feeding concentration, 0.425–1.18 mm particle size).

5.3.2 Effect of pressure

To study the effect of total pressure on the sorption performance, the butanol dehydration experiments were carried out at 135 and 200 kPa, while other conditions were kept as same. Table 5.4 summarizes the results. It can be seen that at the tested pressure range, the sorption capacity of water did not change significantly while that of butanol slightly increased probably because of a slight increase of driving force for butanol sorption. Thus, the equilibrium separation factor of water over butanol decreased.

Table 5.4 Sorption capacities and separation factor of water and butanol on oat hull at different pressure (110 °C, 0.425–1.18 mm particle size).

Pressure (kPa)	Butanol concentration in the feed (wt%)	Water sorption capacity (mg/g)	Butanol sorption capacity (mg/g)	Separation factor
135	56.6±0.7	138±9	58±5	2.9±0.1
200	56.8±0.6	144±5	71±4	2.7±0.1

The butanol product profiles presented in Figure 5.6 also show that the profiles are almost overlapped with each other at the tested pressure range. The achieved highest product concentration slightly decreased from 95 wt.% to 93 wt.% as pressure was increased from 135 kPa to 200 kPa. Also, the equilibrium was reached slightly earlier, which may imply a slightly higher mass transfer rate at 200 kPa. The lower pressure of 135 kPa used in this work was close to the atmospheric pressure. Considering that the effect of pressure at the tested range did not significantly affect the dehydration performance, the low pressure of 135 kPa was used in the rest investigation to reduce energy consumption when this technology is applied in the ABE industry.

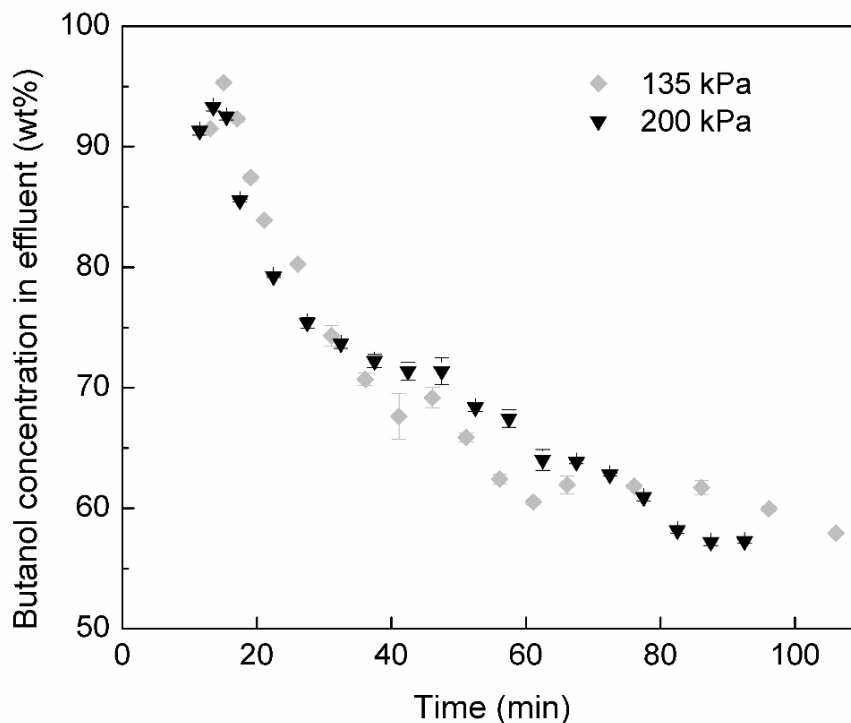


Figure 5.6 Butanol product concentration profiles at different pressure (110 °C, 56 wt.% butanol in feeding concentration, 0.425–1.18 mm particle size).

5.3.3 Effect of feed concentration

The effect of feed concentration on sorption performance was investigated by varying the butanol concentration in the feed stream, keeping other conditions the same. The results obtained at different feed concentrations at 110 °C and 135 kPa are shown in Table 5.1. The results demonstrated the competitive sorption of water and butanol. At the same temperature, either water or butanol sorption capacity increased as its feed concentration was increased. This is because sorption can be driven by the concentration gradient. When the concentration of a sorbate (water or butanol) in the vapor feed is higher, the force driving the sorbate molecules to move from the higher concentration region in the bulk vapor phase to the lower concentration region of the biosorbent is higher. Thus, the respective sorption capacity is higher. In the case of the separation factor of water over butanol, it increased with the decrease of butanol concentration. At the lower

butanol feed concentration, the driving force of the butanol concentration gradient could be lower, and fewer butanol molecules competed with water molecules for the sorption sites. Thus, the separation factor increased.

Butanol production profiles obtained at different feed concentrations are shown in Figure 5.4. As demonstrated in this figure, higher purity of butanol product (95–99%) was achieved with lower butanol concentration in the feed stream (56.6%–90.3%). But in general, a lower butanol feed concentration led to a lower butanol product concentration profile with time and a steeper slope of the profile. The same trends were also found for the runs at other sorption temperatures. The effect of feed concentration on dynamics can be seen in Chapter 8.

5.3.4 Effect of particle size

Experiments using the biosorbent with particle sizes 0.425–1.18 and 1.18–3.25 mm were carried out to study the effect of particle size on butanol dehydration. The experiments were performed by holding the sorption temperature at 110 °C, pressure at 135 kPa, and the feed butanol concentration at around 56 wt.%. The sorption results of biosorbent with different particle sizes are displayed in Table 5.5. It can be seen that the sorption capacity did not change significantly, when using these two different size biosorbent particles considering the experimental errors. The selectivity of water sorption over butanol sorption did not have significant change as the particle size decreased. The results are expected.

Table 5.5 Sorption capacities of water and butanol on oat hull at different particle sizes (110 °C, 135 kPa).

Particle size (mm)	Butanol concentration in the feed (wt%)	Water sorption capacity (mg/g)	Butanol sorption capacity (mg/g)	Separation factor
0.425–1.18	56.6±0.7	138±9	58±5	2.94±0.13
1.18–3.25	56.5±0.8	124±6	55±4	2.91±0.16

Butanol production profiles of the biosorbents with different particle sizes are shown in Figure 5.7. As can be seen, the slope of the curve is slightly steeper when the sizes of biosorbent particles are smaller. The slightly steeper slope may indicate a slightly higher mass transfer rate. The smaller the particle size, the higher the surface area available for mass transfer. Thus, the mass transport rate is higher. However, the effect of different particle sizes on dehydration performance is insignificant. A similar phenomenon was observed for butanol dehydration using canola meal particles in the sizes of 0.425–1.18 mm and 4.7 mm pellets (Jayaprakash, 2016).

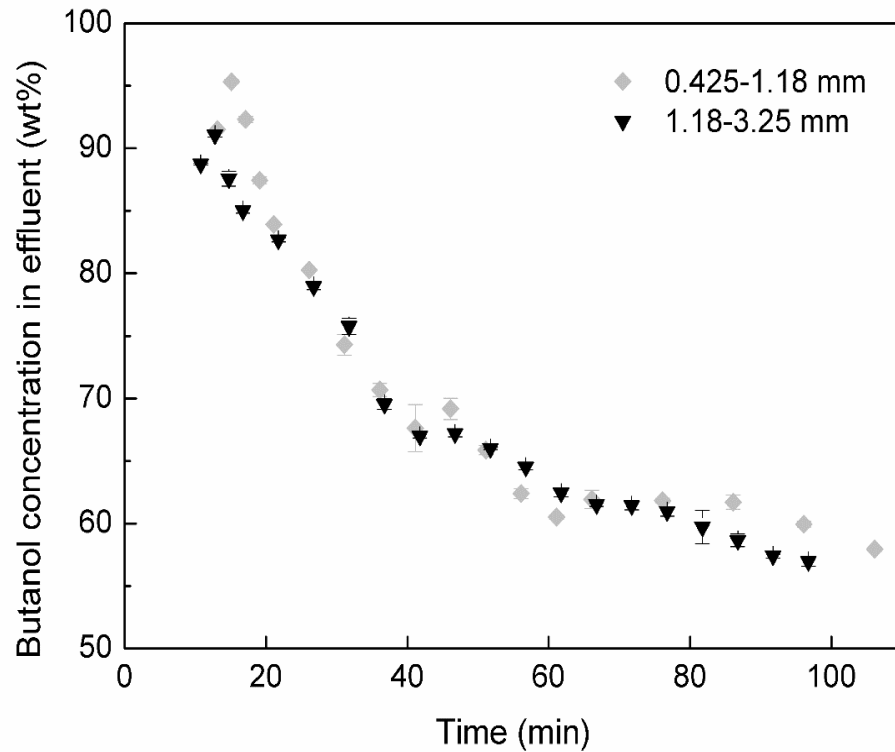


Figure 5.7 Butanol product concentration profiles using different particle sizes (110 °C, 135 kPa, 56 wt.% butanol in feeding concentration).

5.3.5 Effect of different batches of oat hulls

Most of the experiments in this thesis were done using the oat hull material obtained in the year 2014. To determine whether there are differences between different batch oat hull materials, the oat hulls obtained in the year 2018 were used to compare its butanol dehydration performance with that of the 2014 batch. The results can be seen in Table 5.6. Water sorption capacity, butanol sorption capacity, and water separation factors of the two batches are similar by considering the experimental errors though the average values of the sorption capacity of the 2018 batch look slightly higher.

In addition, the FTIR spectra of the two different batches oat hull based biosorbents presented in Figure 4.3(b) of Chapter 4 shows that the two batches biosorbents are similar in terms of the functional group and the main composition.

Table 5.6 Sorption capacities of water and butanol on the biosorbent with different batches (110 °C, 135 kPa, 0.425–1.18 mm particle size).

Batch	Butanol concentration in the feed (wt%)	Water sorption capacity (mg/g)	Butanol sorption capacity (mg/g)	Separation factor
2014	56.6±0.7	138±9	58±5	2.9±0.3
2018	56±1	146±8	66±4	2.88±0.08

The butanol product concentration profiles using the oat hull biosorbents of the two batches are shown in Figure 5.8. In general, the two curves are overlapped. Based on the tested results, the batch of 2014 year and 2018 year oat hulls did not demonstrate a significant difference in butanol dehydration.

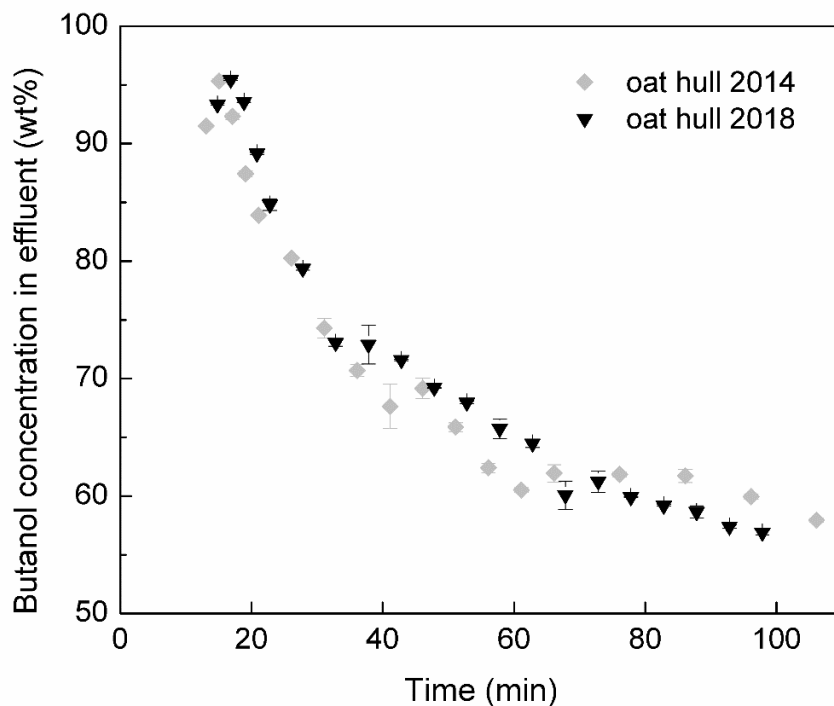


Figure 5.8 Butanol product concentration profiles on the biosorbent with different batch (110 °C, 135 kPa, 56.6 wt.% butanol in feeding concentration, 0.425–1.18 mm particle size).

5.4 Chapter summary

It is concluded from pure water and pure butanol sorption performance that the affinity of water for the oat hull based biosorbent is stronger than that of butanol, and the water sorption capacity of the biosorbent is also higher than butanol sorption capacity. Through the dehydration process develop in this work, high purity butanol products (95.3%, 97.1%, 98.1%, and 99.0%) were achieved from low-grade butanol-water mixtures (56.6%, 69.1%, 79.7%, and 90.3%), respectively. This demonstrated the oat hull based biosorbent was able to successfully dehydrate butanol and water mixtures at the water/butanol azeotrope and higher butanol concentration. The values of the separation factor of water over butanol are higher than 1, which indicates that the oat hull based biosorbent was able to effectively remove water from butanol. The effects of different parameters were studied. The higher temperature leads to a higher rate of mass transfer but lower

sorption capacity. The pressure at the tested range did not significantly affect dehydration performance. Increasing water content in the feed led to steeper slopes of the breakthrough curves, implying the higher rate of the mass transfer due to the higher driving force. The higher butanol concentration in the feed led to a lower separation factor, and lower water sorption capacity. The effect of different particle sizes on dehydration performance is insignificant at the tested ranges. The oat hull obtained in 2014 and 2018 did not demonstrate a significant difference in the performance of butanol dehydration.

The effects of pressure and particle size of the biosorbent at the tested ranges are insignificant. Thus, further investigation of the sorption equilibrium and dynamics are focused at various temperature and/or feed concentration in the following chapters.

CHAPTER 6. EQUILIBRIUM AND MODELING STUDY OF WATER AND BUTANOL SORPTION

Contribution of this chapter to overall Ph.D. work

This work aims to develop an alternative technology of sorption to remove water directly from the azeotrope of butanol and water vapor generated from the distillation in biobutanol industry in a hope to reduce or replace the downstream decantation and distillation cycles in the bio-butanol industry and contribute to science and engineering of sorption. For that, it is essential to understand the fundamentals of water and butanol sorption equilibrium. In this chapter, the sorption equilibrium isotherms of water and butanol in the single component system and the butanol-water binary system were studied experimentally, which were analyzed by the Dubinin-Polanyi model. Besides, the approximate sorption site energy distribution was calculated, and thermodynamic parameters were determined based on the modeling results.

6.1 Equilibrium and modeling study of water sorption

The Dubinin-Polanyi models are based on the adsorption potential theory of Polanyi, which assumes the adsorbed layer has a multilayer character, and it applies to the van der Waals equation (Dąbrowski, 2001). The adsorption potential is the work done to transfer molecules from gas to the adsorption phase. According to the potential theory, the equilibrium data at different temperatures can be described in a single characteristic adsorption curve by plotting equilibrium loading as a function of adsorption potential. The equilibrium data obtained at different temperatures can be represented in a single curve rather than in multiple curves by the Dubinin-Polanyi model.

The large pore Dubinin-Polanyi model was used to successfully describe equilibrium water sorption from binary ethanol-water, and butanol-water systems into natural materials such as corn meal, canola meal, and so on, which mainly contain large pores (Chang et al., 2006a; Jayaprakash et al., 2017; Ranjbar et al., 2013). The biosorbent used in this work is based on the raw oat hull material, and the results of SEM and pore size distribution show the material mainly contains mesopores and macropores, basically large pores. Thus, in this work, the large pore Dubinin-Polanyi model was chosen in comparison with the micropore Dubinin-Polanyi model to investigate their capability to simulate the equilibrium sorption of water and butanol from the single component system, and binary butanol-water system.

The following Eq. 6.1 and Eq. 6.2 are Dubinin-Polanyi models for micropore and large pore materials respectively.

$$\ln q = \ln q_0 - \frac{\kappa_1}{\beta} [RT \ln(p^s/p_i)]^2 \quad (6.1)$$

$$\ln q = \ln q_0 - \frac{\kappa_2}{\beta} [RT \ln(p^s/p_i)] \quad (6.2)$$

$$\varepsilon = RT \ln \left(\frac{P^s}{P_i} \right) \quad (6.3)$$

where q is equilibrium loading of the adsorbate with the unit g adsorbed adsorbate/g adsorbent; q_0 is limiting mass for sorption (g adsorbate/g adsorbent); and β is affinity coefficient. P_i is the partial pressure of the adsorbate at sorption temperature (kPa); and P^s is the saturated vapor pressure of the adsorbate at the same temperature (kPa). Adsorption potential can be calculated by Eq. 6.3. The parameters in large pore Dubinin-Polanyi model and micropore Dubinin-Polanyi are different. κ_1 is pore constant for micropore materials, and κ_2 is pore constant for large pore materials. κ_1 and κ_2 are related to the distribution of pore volume (Chang et al., 2006a).

6.1.1 Equilibrium study of pure water sorption

The water sorption isotherm in the pure water sorption system at 120 °C was shown in Figure 6.1(a). The isotherm is similar in shape to Type-II isotherm. The middle section of the isotherm is almost linear. The equilibrium uptake increased with the increase of pressure ratios without a saturation limit as did in Type I isotherm. Type-II isotherms suggest the multi-layer sorption formed at high relative pressures after monolayer coverage on the sorbent, and the sorbents are porous or have pore diameters larger than micropores (Lowell & Shields, 1984). The shape of the water sorption isotherm suggests that the biosorbent used in this work is more likely to be a large pore material, and the multi-layer sorption might occur on the biosorbent.

The aforementioned Dubinin-Polanyi models were used to describe the water equilibrium data in the pure water sorption system. Figures 6.1(b) and 6.2 demonstrate the experimental isotherm data for water sorption in the pure water sorption system and the fitting results of the Dubinin-Polanyi models. The fitting results and isotherm parameters obtained from model fitting are listed in Table 6.1.

The value of the correlation coefficient ($R^2=0.96$) for the large pore model is higher than that of the micropore Dubinin-Polanyi model ($R^2=0.85$), and the residual sum of squares ($RSS=0.006$) is smaller than that of micropore Dubinin-Polanyi model ($RSS=0.022$). This indicates that the large pore Dubinin-Polanyi model is better to describe the equilibrium data for pure water sorption, compared with the micropore Dubinin-Polanyi model. This is consistent with the fact that the biosorbent mainly contains mesopores and macropores. The value of the limiting mass for sorption q_0 was estimated by model fitting as well.

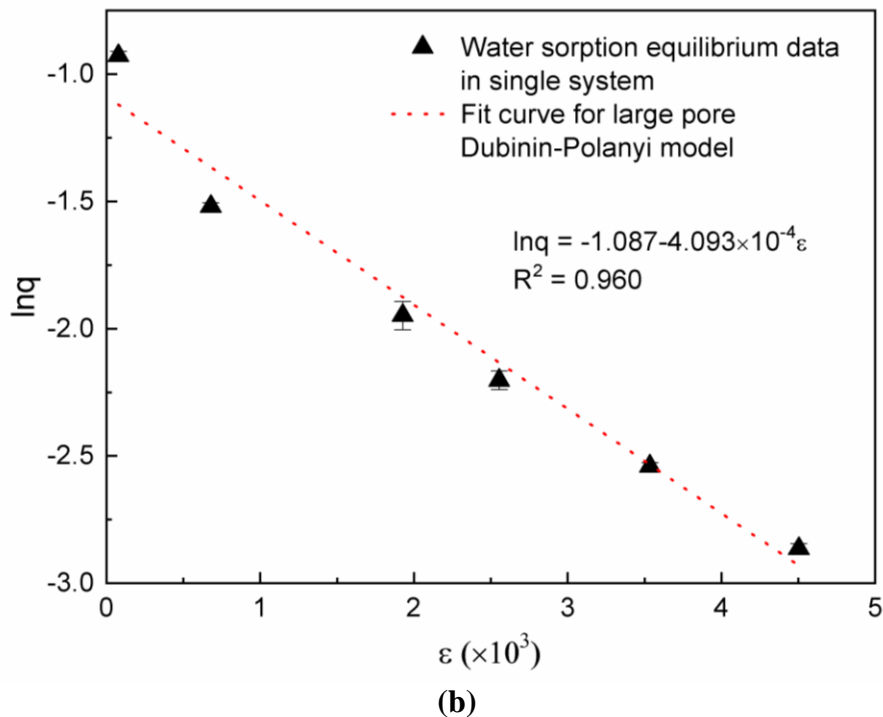
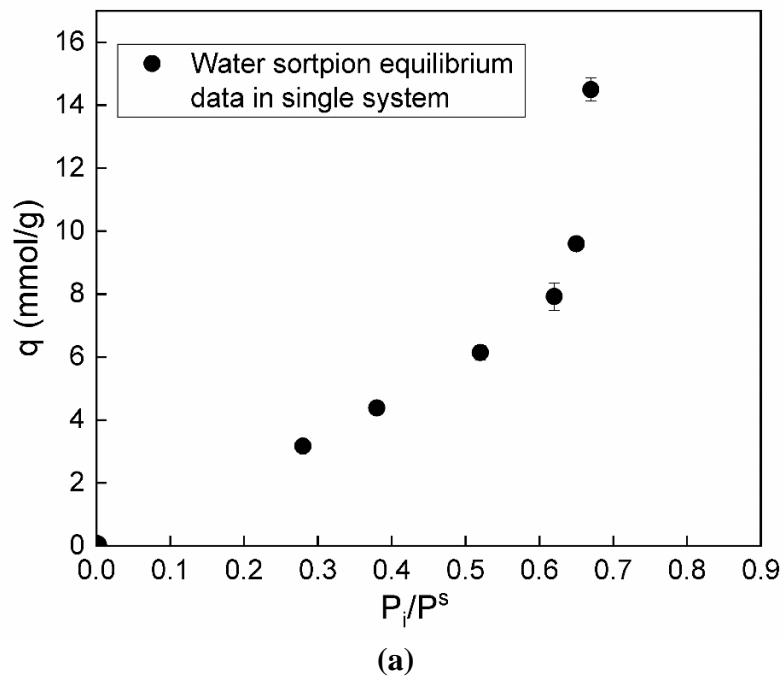


Figure 6.1 (a) Water sorption isotherm in the pure water system, (b) Equilibrium water sorption data in the pure water system and fitting results of the large pore Dubinin-Polanyi model. Pressure of 135 kPa, temperature of 120 °C, carrier gas flow rate 680 mL/min.

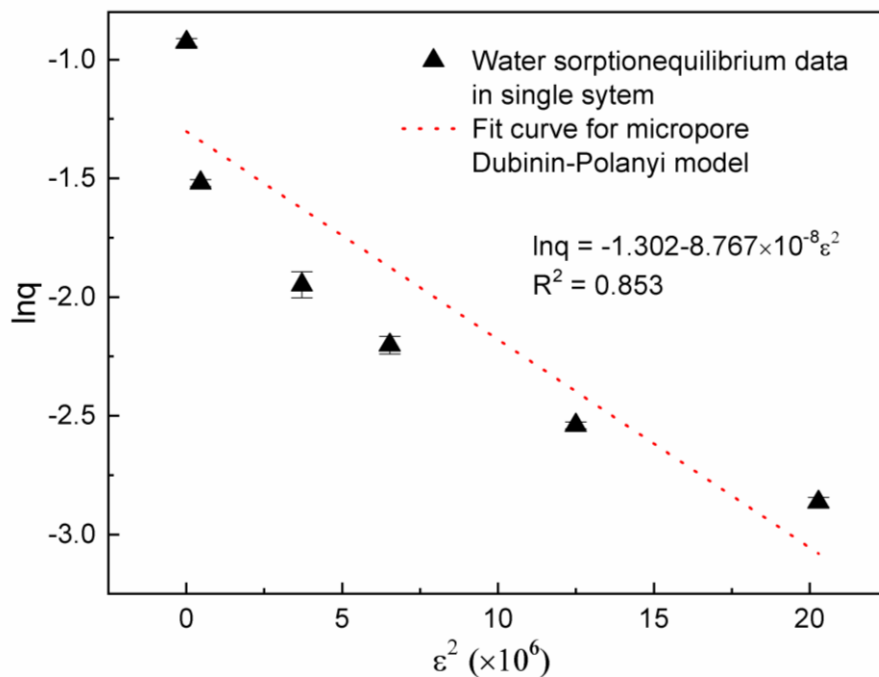


Figure 6.2 Equilibrium water sorption data in the pure water system and fitting results of the micropore Dubinin-Polanyi model (pressure of 135 kPa, temperature of 120 °C, carrier gas flow rate 680 mL/min).

Table 6.1 Fitting results of the Dubinin-Polanyi models of pure water sorption.

<i>Single water sorption system</i>	q_0 (mmol/g)	κ/β	R^2	RSS	P value
Large pore Dubinin-Polanyi model	18.7±1.7	(4.09±0.17)E-4	0.96	0.006	3.8E-4
Micropore Dubinin-Polanyi model	15.1±1.9	(8.77±0.16)E-8	0.85	0.022	5.4E-4

Degrees of freedom: 4.

6.1.2 Water sorption equilibrium study in binary mixture system

The Dubinin-Polanyi models were also used to describe the water equilibrium data in the binary system. The characteristic curve of Polanyi adsorption potential theory was demonstrated in Figure 6.3. In this figure, the quantity of water loading on the biosorbent q versus sorption

potential ε is plotted. It can be seen from Figure 6.3 that nearly all the data points tend to compose one curve. This discovery indicates that the Polanyi adsorption potential theory has the potential to be successfully applied in this case.

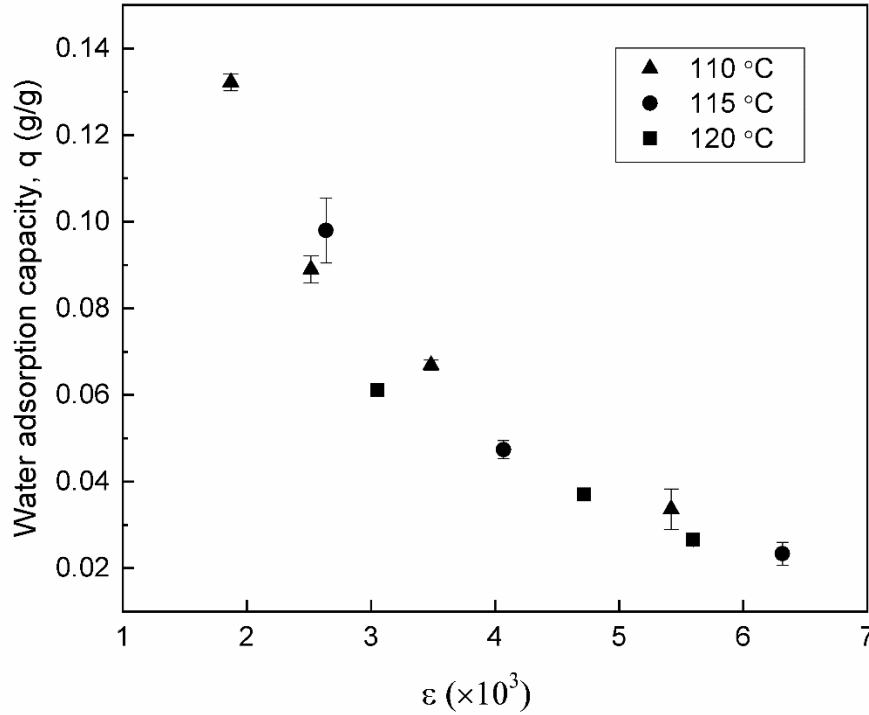


Figure 6.3 Water sorption characteristic curve based on the Polanyi adsorption potential theory (pressure of 135 kPa, temperature of 110–120 °C, carrier gas flow rate 680 mL/min).

The fitting curves of the Dubinin-Polanyi models are presented in Figures 6.4 and 6.5. The fitting curves generated by the large pore Dubinin-Polanyi model are closed to almost all the experiment data points within the range of conditions applied in this study. Again, the large pore Dubinin-Polanyi model provided a satisfactory fitting to water sorption on the oat hull based biosorbent. The fitting results are listed in Table 6.2. The P value of the large pore Dubinin-Polanyi model is far less than 0.05, which indicates that this model described the equilibrium data well. Again, the results show that the large pore model is superior to the micropore model in representing

the experimental water sorption data in the binary butanol-water system due to the higher correlation coefficient (R^2) value and the lower residual sum of squares (RSS).

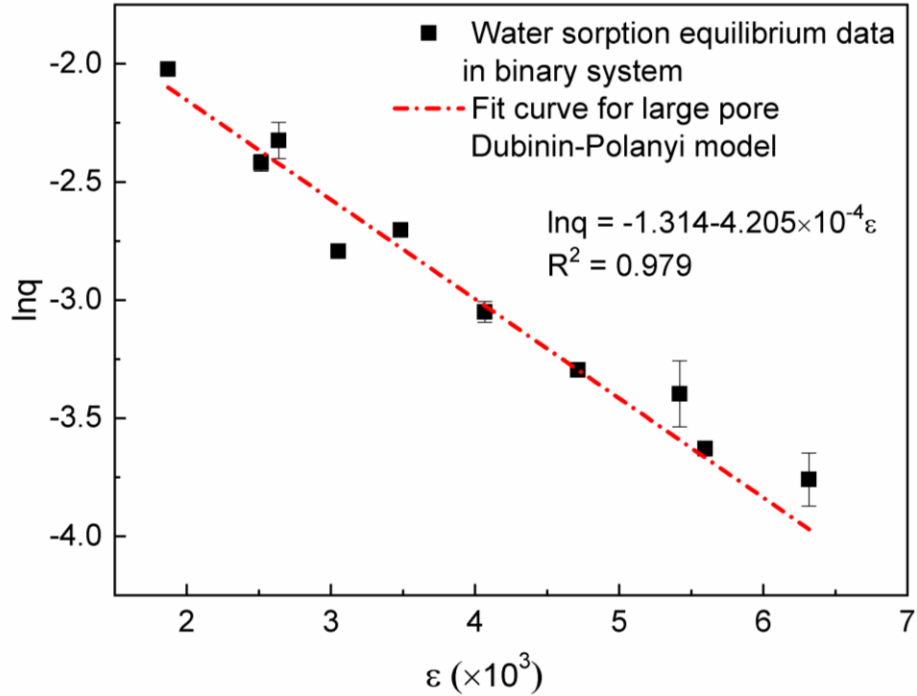


Figure 6.4 Equilibrium water sorption data in the binary butanol-water system and fitted curve of large pore Dubinin-Polanyi model (pressure of 135 kPa, temperature of 110–120 °C, carrier gas flow rate 680 mL/min).

This result is consistent with the results of water sorption from Ranjbar’s study on water sorption from the ethanol-water system (Ranjbar et al., 2013) and Jayaprakash’s study of the butanol-water system (Jayaprakash et al., 2017). The R^2 value of large pore Dubinin-Polanyi model in Ranjbar’s study and Jayaprakash’s study were 0.97 and 0.96, respectively, which are higher than that of the micropore Dubinin-Polanyi model. The results of these studies similarly indicate that the large pore model is better than the micropore Dubinin-Polanyi model to present the water sorption in water-alcohol systems.

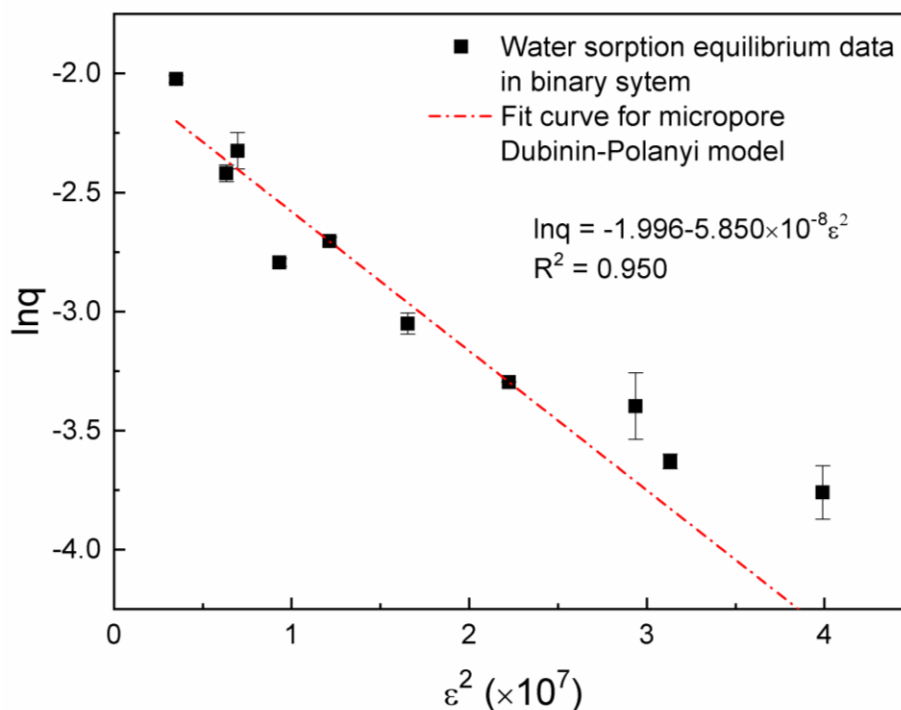


Figure 6.5 Equilibrium water sorption data in the binary butanol-water system and fitted curve of micropore Dubinin-Polanyi model (pressure of 135 kPa, temperature of 110–120 °C, carrier gas flow rate 680 mL/min).

Thus, the water sorption data in the single water system and binary butanol-water system were both well described by the large pore Dubinin-Polanyi model. The better fitting results of the large pore Dubinin-Polanyi model indicate that water sorption in this system is based on large pores, which are consistent with the results of pore size distribution that the oat hull material mainly contains large pores (mesopores and macropores). It is also noted that though the Dubinin-Polanyi model based on the Polanyi adsorption potential theory well described the experimental data, the actual water uptake in this system could be sorption considering the nature of the biosorbent.

Table 6.2 Fitting results of the Dubinin-Polanyi models of water sorption in binary system.

<i>Binary butanol-water system</i>	q_0 (mmol/g)	κ/β	R^2	RSS	P value
Large pore Dubinin-Polanyi model	14.9±1.1	(4.20±0.21)E-4	0.98	0.0005	3.5E-8
Micropore Dubinin-Polanyi model	7.6±0.4	(5.85±0.44)E-8	0.95	0.0011	1.1E-6

Degrees of freedom: 8.

The model parameters obtained from model fitting are listed in Tables 6.1. and 6.2. The modelling results of the large pore Dubinin-Polanyi model demonstrated that q_0 , limiting mass for sorption (mmol adsorbate/g adsorbent) decreased about 20% from 18.7 of the single water system to 14.9 of the binary butanol-water system. This indicated that butanol molecules may compete with water molecules for a minor portion of the sorption sites on the biosorbent. The values of κ/β obtained from large pore Dubinin-Polanyi model in this work are similar to those, which were reported in other studies (Chang et al., 2006a; Ranjbar et al., 2013) (around 3×10^{-4}) in the ethanol-water binary vapor system using biosorbent.

6.2 Site energy distribution analysis of the biosorbent for water sorption

There are a lot of theories developed to describe the sorption process. It's important to select a proper isotherm according to the nature of adsorbent to analyze the experimental data. The bio-based sorbents have a complex structure and heterogeneous surface. Hence, the energy distribution theory is applicable to investigate the heterogeneity of adsorbents. From this analysis method, more information such as the parameters effects and the interaction between sorbent and sorbate will be obtained. The site energy distribution has great advantages to deal with the sorption data of the bio-based materials.

Analysis of site energy distribution is an effective method to describe the surface energy characteristics of the adsorbent for a targeted adsorbate. Site energy distribution of adsorbent is associated with sorption isotherm. Equation (6.4) defines the total sorption capacity (q_e) on a heterogeneous surface as the integral of an energetically homogeneous local isotherm (q_h) multiplied by a site energy frequency distribution ($F(E)$) over a range of energies. However, in most cases, the local isotherm is not clear, and neither is the overall isotherm. It is difficult to obtain the exact distribution. The approximate site energy distribution proposed by Cerofolini (Cerofolini, 1974) provides a widely-accepted solution. Based on the Cerofolini approximation the equilibrium pressure can be represented as a function of the site energy as can be seen in Eq. 6.5.

$$q_e(p) = \int_0^{\infty} q_h(E, p) F(E) dE \quad (6.4)$$

$$p = p^s \exp\left(-\frac{E^*}{RT}\right) \quad (6.5)$$

By plugging Eq. 6.5 into isotherm expression Eq. 6.2, $q(p)$ can be represented as $q(E^*)$. E^* is the difference of sorption energies between the sorbate and solvent based on the reference point E_s ($E^* = E - E_s$). E_s is the reference state of E , and it represents the lowest physically realizable sorption energy (Carter et al., 1995). The site energy distribution can be obtained by differentiating theoretical isotherm expression with respect to E^* based on Eq. 6.6.

$$F(E^*) = -\frac{dq(E^*)}{dE^*} \quad (6.6)$$

In this way, the approximate distribution function can be written in terms of parameters from an isotherm. In this work, the large pore Dubinin-Polanyi model for water sorption was used because it provided better fitting to the equilibrium data. The site energy distribution function based on the large pore Dubinin-Polanyi isotherm model (Eq. 6.2) is derived and presented in Eq. 6.7.

$$F(E^*) = \frac{\kappa_2}{\beta} \times \frac{q_0}{\exp\left(\frac{\kappa_2 E^*}{\beta}\right)} \quad (6.7)$$

Figure 6.6 presents the approximate site energy distribution curves of oat hull biosorbent for water sorption in the single water system, and butanol-water binary system calculated by Eq. 6.7. The distribution curves are plotted by the sorption capacity per unit of site energy versus site energy. They are not normalized, showing the heterogeneity of the biosorbent and water sorption characteristics. Besides, the area under the site energy distribution curve can be interpreted as the maximum water sorption capability. Generally, over 98% of the water sorption in either the single or the binary system took place on the site with energy lower than 10,000 J/mol, confirming water sorption by the biosorbent is physical sorption, because the energy of chemical sorption is usually 50,000–400,000 J/mol (Jain, 2016).

By comparison and analysis, it was found that the water sorption capacity per unit of site energy in the binary system was slightly lower than that in the single water system throughout the entire range of site energy. This difference describes the minor effect of butanol on water sorption.

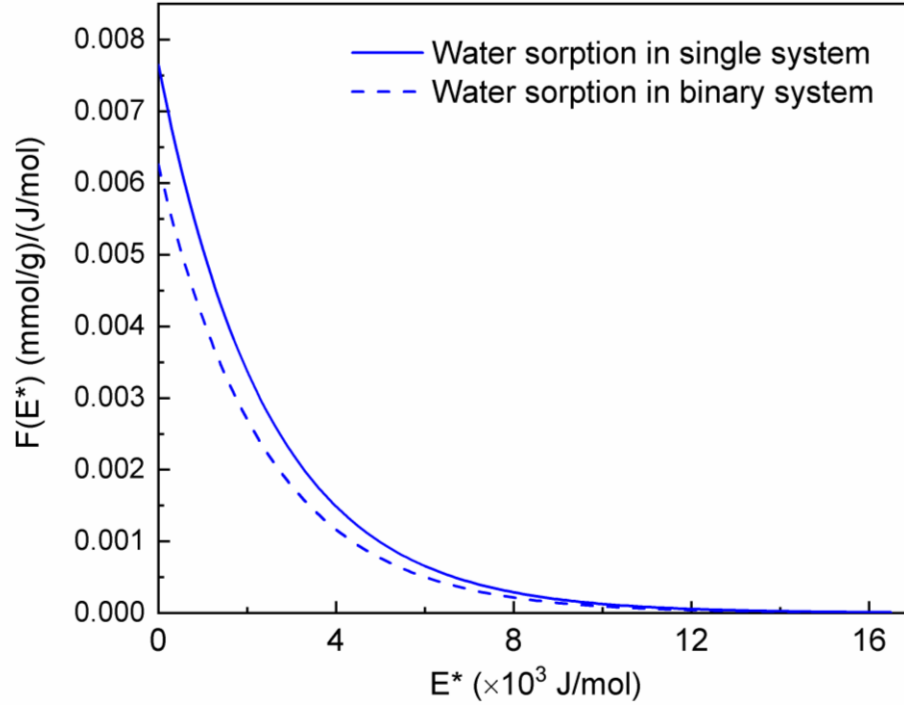


Figure 6.6 Site energy distribution of oat hull biosorbent for water sorption according to the large pore Dubinin-Polanyi model.

The weighted mean site energy (E_m) was also determined for water sorption in this study. It is an indicator of the affinity of the adsorbate for the adsorbent surface, which can be calculated by the Eq. 6.8 below.

$$E_m = \frac{\int_0^{+\infty} E^* \times F(E^*) dE^*}{\int_0^{+\infty} F(E^*) dE^*} \quad (6.8)$$

Plugging Eq. 6.7 in Eq. 6.8 and integrating led to Eqs. 6.9 and 6.10.

$$E_m = \frac{\int_0^{+\infty} \frac{\kappa_2}{\beta} q_0 E^* \exp\left(-\frac{\kappa_2 E^*}{\beta}\right) dE^*}{\int_0^{+\infty} \frac{\kappa_2}{\beta} q_0 \exp\left(-\frac{\kappa_2 E^*}{\beta}\right) dE^*} \quad (6.9)$$

$$E_m = \frac{\beta}{\kappa_2} \quad (6.10)$$

In this work, the weighted mean site energy for water sorption in the pure water system and in the butanol-water binary system are 2443 ± 102 J/mol and 2378 ± 119 J/mol, which were calculated based on the Dubinin-Polanyi model for large pores. The slightly higher weighted mean site energy means higher sorption affinity. It indicated that the affinity between water and the biosorbent in the single water system is a little higher than that in the butanol-water binary system. It may be because in the binary system the butanol molecules may interact with water molecules for a portion of the sites. However, such an impact is not significant. Therefore the weighted mean site energy of water sorption in the single water system and the butanol-water binary system are close. The site energy distribution of water sorption on canola meal biosorbent reported similar results with this work. The weighted mean site energy is reported to be 3330 J/mol, and the range of site energy is within 14,000 J/mol (Jayaprakash et al., 2017). The site energy distribution provides an approach to analyze the equilibrium data. It relates the changes in isotherm parameters to changes in the energy characteristics of sorbent surfaces.

In this work, the large pore Dubinin-Polanyi model, which assumes the multilayer sorption and applies well to systems involving van der Waals force, is able to describe water sorption on the biosorbent. This suggests the van der Waals forces may be one of the dominant mechanisms in water sorption on the biosorbent, and the sorption may have the multilayer character. The site energy distribution analysis provides evidence that water sorption on the biosorbent is physisorption. The binding force is weak compared with the chemisorption, which confirms the van der Waals forces may be dominant in water sorption. The dipole-dipole attraction, one kind of van der Waals forces, may suggest the mechanism of water molecules sorption on the biosorbent since water molecules have high polarity, and there are many polar groups such as hydroxyl and carboxyl on the biosorbent. The hydrogen bond formed by water and the hydroxyl groups on the

surface of the biosorbent may be also involved in the sorption process (Anderson et al., 1996; Beery et al., 1998).

6.3 Equilibrium and modeling study of butanol sorption

The sorption properties of the oat hull based biosorbent could be different for different adsorbates. Thus, analysis of butanol sorption equilibrium is also necessary to better understand the whole dehydration process. As such, butanol sorption isotherms in both pure butanol system and butanol-water binary system were analyzed in this section.

6.3.1 Equilibrium study of pure butanol sorption

The Dubinin-Polanyi models were also used to describe the butanol equilibrium data in the pure butanol sorption system. Figures 6.7 and 6.8 demonstrate the butanol sorption equilibrium data and the fitting results of the Dubinin-Polanyi model. It can be seen from these two figures, both of the large pore and the micropore Dubinin-Polanyi model are able to describe the experimental data. The fitting results and isotherm parameters obtained from model fitting are listed in Table 6.3.

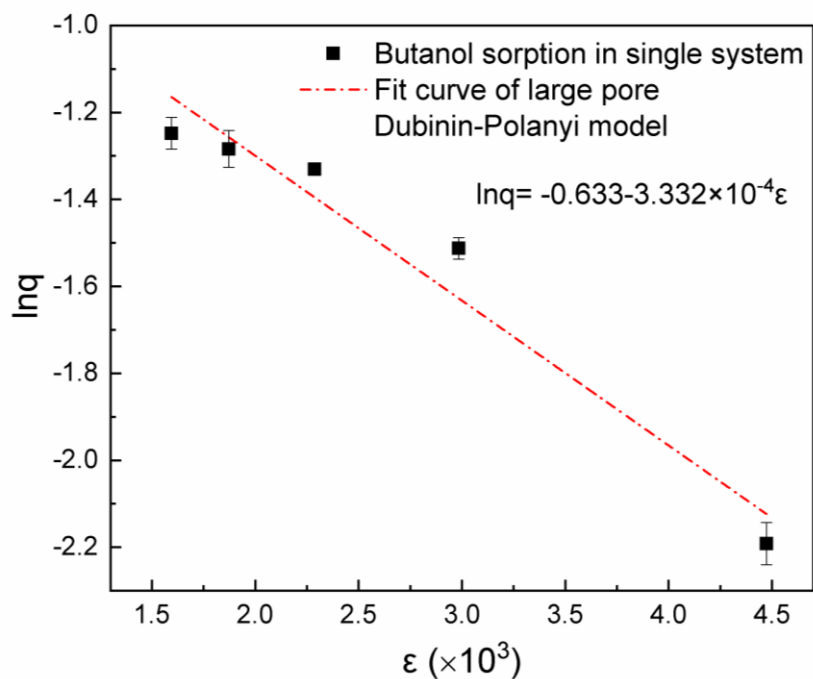


Figure 6.7 Butanol sorption data in the single system and fitting curve of the large pore Dubinin-Polanyi model (pressure of 135 kPa, temperature of 120 °C, carrier gas flow rate 680 mL/min).

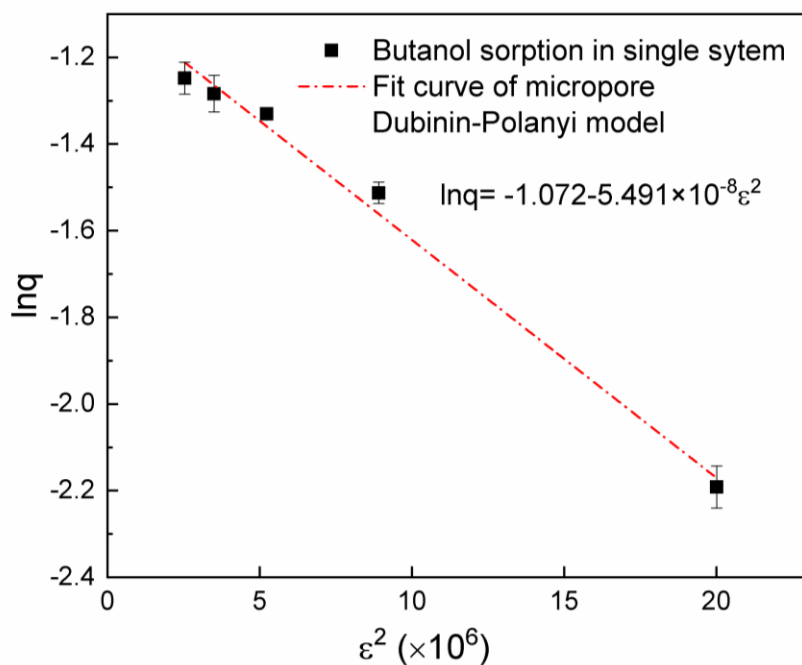


Figure 6.8 Butanol sorption data in the single system and fitting curve of the micropore Dubinin-Polanyi model (pressure of 135 kPa, temperature of 120 °C, carrier gas flow rate 680 mL/min).

Both of the large pore and micropore Dubinin-Polanyi models provided satisfactory simulation results for pure butanol sorption. The values of the correlation coefficient for the large pore Dubinin-Polanyi model and micropore Dubinin-Polanyi model are 0.96 and 0.98, respectively. The P values of both models are far less than 0.05. The values of the parameters were estimated by model fitting. The estimated values of q_0 , (limiting mass for sorption) for butanol sorption are lower than those for water sorption in the single system, which again implies water has higher sorption capacity on the oat hull based biosorbent.

Table 6.3 Fitting results of the Dubinin-Polanyi models of pure butanol sorption.

<i>Single butanol sorption system</i>	q_0 (mmol/g)	κ/β	R^2	RSS	P value
Large pore Dubinin-Polanyi model	7.2±1.3	(3.33±0.43)E-4	0.96	0.0016	4.6E-3
Micropore Dubinin-Polanyi model	4.6±0.1	(5.49±0.29)E-8	0.98	0.0003	3.4E-4

Degrees of freedom: 3.

6.3.2 Butanol sorption equilibrium study in binary mixture system

In the previous section, the large pore and micropore Dubinin-Polanyi models were used to describe pure butanol sorption on the oat hull based biosorbent in the single component system. In this section, the two models were also used to investigate their capability to describe the butanol sorption from the binary butanol-water system. The results were compared with those in the single butanol system.

Figures 6.9 and 6.10 demonstrate the experimental data of butanol sorption in the binary system and the fitting results of the Dubinin-Polanyi models. The fitting results and isotherm parameters obtained from model fitting are listed in Table 6.4. The P values of both models are far

less than 0.05, which indicates that these two models described the equilibrium data well. Both of the models provided similar performance to describe the butanol sorption equilibrium data in the binary system. The true sorption mechanism needs to be further investigated.

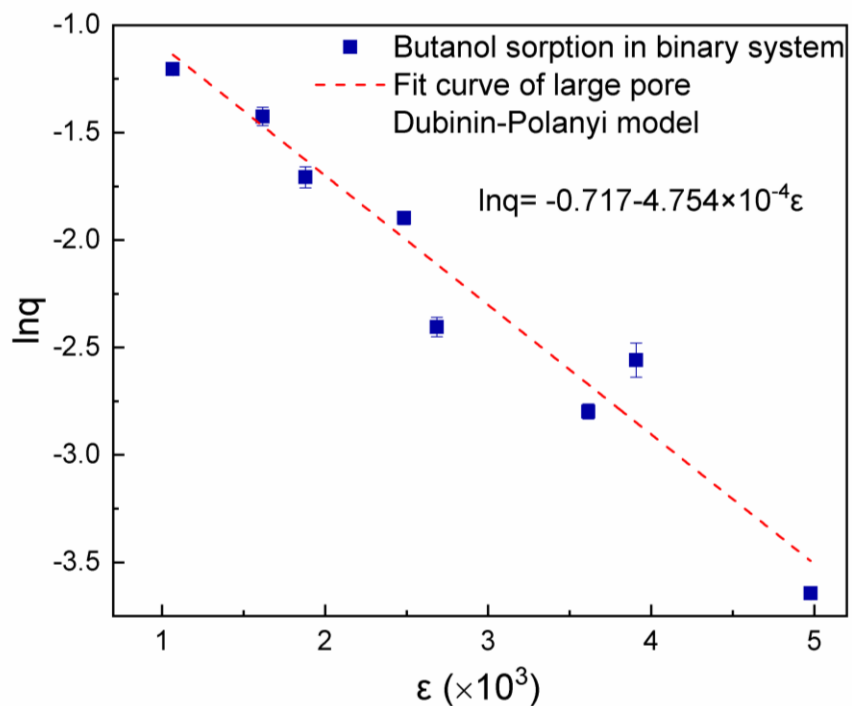


Figure 6.9 Butanol sorption data in the butanol-water binary system and fitting curve of the large pore Dubinin-Polanyi model (pressure of 135 kPa, temperature of 110–120 °C, carrier gas flow rate 680 mL/min).

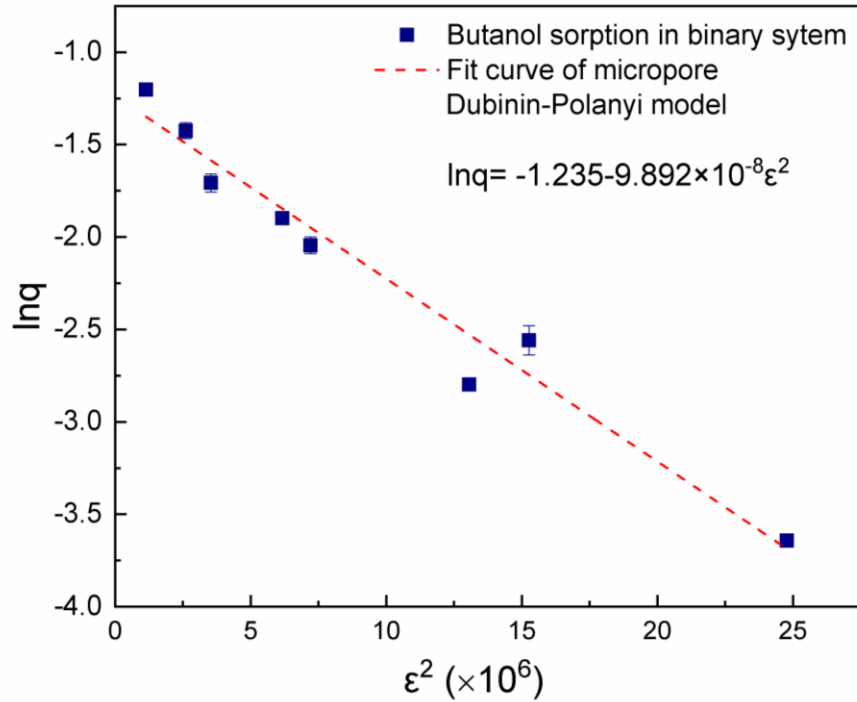


Figure 6.10 Butanol sorption data in the butanol-water binary system and fitting curve of the micropore Dubinin-Polanyi model (pressure of 135 kPa, temperature of 110–120 °C, carrier gas flow rate 680 mL/min).

Table 6.4 Fitting results of the Dubinin-Polanyi models of butanol sorption in the binary system.

<i>Binary butanol-water system</i>	q_0 (mmol/g)	κ/β	R^2	RSS	P value
Large pore Dubinin-Polanyi model	6.6±0.7	(4.75±0.31)E-4	0.97	0.001	6.3E-5
Micropore Dubinin-Polanyi model	3.9±0.3	(9.89±0.83)E-8	0.95	0.003	7.4E-5

Degrees of freedom: 6.

In summary, butanol sorption data in the pure butanol system and binary butanol-water system were both satisfactorily described by the large pore and micropore Dubinin-Polanyi models. Also, according to the fitting results, the values of q_0 (limiting mass for sorption) obtained from single butanol sorption system are 4.2–7.2 (mmol/g), slightly higher than those in butanol-water

system 3.9–6.6 (mmol/g). This indicated that competitive sorption occurred between butanol and water for sorption sites on the biosorbent when water was present in the system.

The results of water sorption and butanol sorption were compared. The estimated values of q_0 for butanol sorption are lower than those for water sorption in the butanol-water binary system, which implies the oat hull based biosorbent has higher water sorption capacity. Though both the large pore and micropore models provided satisfactory simulation results, the real butanol sorption mechanism needs to be further investigated.

6.4 Site energy distribution analysis of the biosorbent for butanol sorption

Site energy distribution in butanol sorption was determined based on the large pore Dubinin-Polanyi modeling results, using Equation (6.7) in a similar approach to that in the case of water sorption. This was done to compare the results with water sorption.

Figure 6.11 presents the approximate site energy distribution curves of oat hull based biosorbent for butanol sorption in the single butanol system and butanol-water binary system. To compare the cases of butanol and water, the site energy distribution of water sorption in the binary system was also shown in this figure.

It can be seen from Figure 6.11 that over 99% of the butanol sorption took place on the site with energy lower than 10,000 J/mol, similar to that of water sorption. This again indicates the butanol sorption is also physical. Besides, the site energy distribution of butanol sorption in the single and binary systems are different. Within the lower energy range, 0–2,000 J/mol, butanol sorption capacity per unit of site energy in the single system is higher than that in the binary system. That means more butanol molecules were able to be sorbed on the lower energy sites in the pure butanol single system. When there is water present in the system, fewer butanol molecules were sorbed because of the competition of water molecules. This can be supported by the site energy

distribution of water sorption in the binary system which shows much higher water sorption capacity throughout all the energy range shown in this figure. Again, the results demonstrated that the biosorbent has a higher water sorption affinity. In the higher energy range, 2,000–9,000 J/mol, butanol sorption capacity per unit of site energy is slightly higher in the binary system, however, the difference is insignificant. Dubinin-Polanyi model, which assumes the multilayer sorption and applies to the van der Waals equation, is able to describe butanol sorption on the biosorbent. This suggests the van der Waals forces may be one of the dominant mechanisms in butanol sorption on the biosorbent. The site energy distribution analysis provides the evidence that butanol sorption on the biosorbent is physisorption, and the binding force is weak compared with the chemisorption, which confirms the van der Waals forces may be one of the dominant mechanisms in butanol sorption. The dipole-dipole attraction, one kind of van der Waals forces, may suggest the mechanism of butanol molecules sorption on the biosorbent since there are many polar groups such as hydroxyl and carboxyl on the biosorbent. The hydrogen bonding formed between sorbates and the above mentioned polar groups may be also involved in the sorption process. Butanol molecules have lower polarity compared to water, and the polar groups prefer to adsorb water molecules other than alcohols with lower polarity (Sun et al., 2007). This is consistent with the result shown in Figure 6.11, that water sorption capacity is higher than that of butanol. This mechanism is also supported by that the decreasing polarity of the alcohol reduces the alcohol sorption competition between the water and the alcohol on the starch (Carmo et al., 2004).

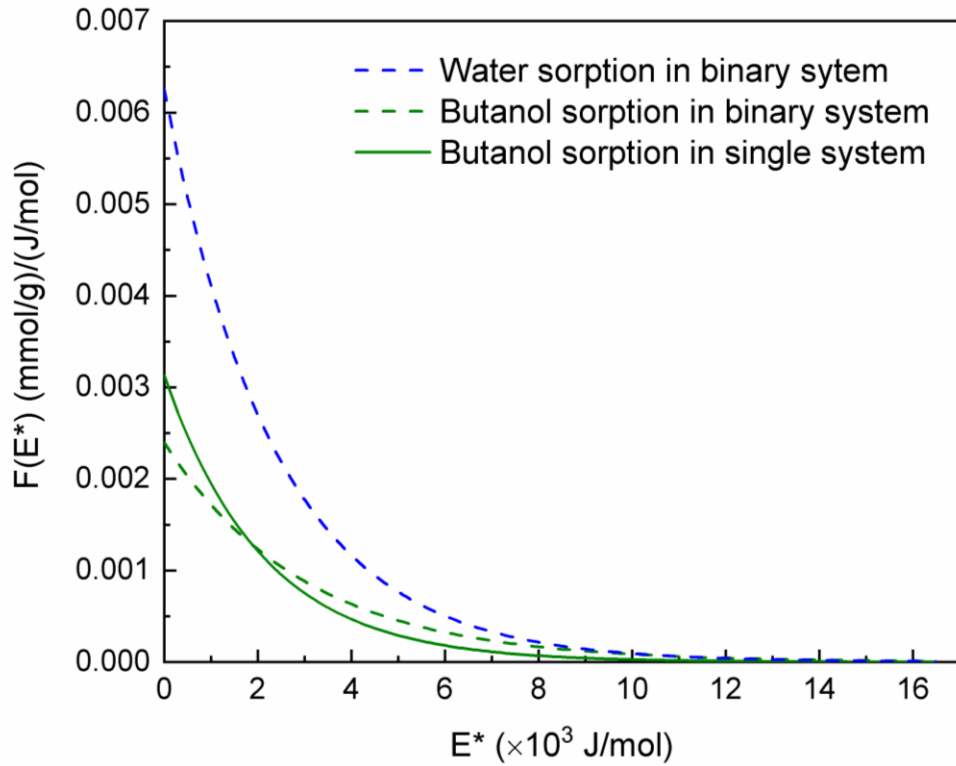


Figure 6.11 Site energy distribution of oat hulls for butanol sorption according to the large pore Dubinin-Polanyi model.

The weighted mean site energy (E_m) was also determined for butanol sorption in this study. It is an indicator of the affinity of the adsorbate for the adsorbent surface, which was calculated by Eq. 6.8. In this work, the weighted mean site energy for butanol sorption in the single system and the butanol-water binary system are 3003 ± 372 J/mol and 2105 ± 137 J/mol, respectively. The higher weighted mean site energy indicates higher sorption affinity. It indicated that the affinity between butanol and the biosorbent in the single butanol system is higher than that in the butanol-water binary system. It may be because in the binary system the butanol molecules may interact with water molecules sorption. In addition, the weighted mean site energy for water sorption in the butanol-water binary system is 2378 ± 119 J/mol, which is higher than that of butanol (2105 ± 137 J/mol), again showing higher affinity. Thus, water sorption is more competitive than butanol in the butanol-water binary system.

Moreover, the area under the site energy distribution curve can represent the maximum sorption capability. By observation, the maximum water sorption capacity is much higher than that of butanol in either single or binary system.

In summary, the analysis of energy characteristics of sorption demonstrated that the surface of the biosorbent was heterogeneous; and it has higher affinity for water and higher water sorption capacity than butanol. Besides, either the higher water sorption or lower butanol sorption is physical.

6.5 Thermodynamic study

The thermodynamic investigation provides the information of the inherent energetic changes involved in the sorption process and the feasibility of the sorption process, through the estimated values of the thermodynamic parameters, such as the standard free energy change (ΔG^o), the standard enthalpy change (ΔH^o), and the standard entropy change (ΔS^o). In this work, ΔH^o and ΔS^o were estimated by the linear form of the van't Hoff equation given as (Chang, 2000):

$$\ln K_0 = \frac{\Delta S^o}{R} - \frac{\Delta H^o}{RT} \quad (6.11)$$

$$\Delta G^o = \Delta H^o - T\Delta S^o \quad (6.12)$$

R is the universal gas constant (8.314 J/(mol·K)); T is the temperature (K); K_0 is the thermodynamic distribution coefficient. $\ln(1/K_0)$ can be determined by plotting $\ln(P/q)$ versus q and extrapolating to zero q (Barrer & Davies, 1970; Kumar et al., 2019). The value of ΔH^o and ΔS^o were calculated from the slope and intercept of $\ln K_0$ versus $1/T$.

The estimated thermodynamic parameters for water and butanol sorption on the biosorbent are shown in Table 6.5. The values of ΔG^o are negative at the tested temperatures, which indicates the thermodynamic feasibility and spontaneous nature of the sorption process. The absolute value

of ΔG° decreased at the higher temperature, which indicates the lower temperature favors the sorption process. The estimated ΔH° of water sorption is -15.4 kJ/mol, and that of butanol sorption is -7.6 kJ/mol. This result again confirmed the physical and exothermic nature of the sorption process. This is consistent with the experimental results reported in Chapter 5 that the water and butanol uptake capacity decreased as the temperature was increased. The value of ΔH° of water sorption is similar to those (-35.8 to -43.23 kJ/mol) reported in ethanol dehydration systems using canola meal and molecule sieves (Carmo & Gubulin, 1997; Ranjbar et al., 2013). The values of ΔS° are negative, which suggests the decreased randomness during the process of sorption, due to the freedom of movement of sorbate molecules get restricted during sorption (Jain, 2016). As a result, the entropy of sorbate decreases, and the entropy change of sorption is negative.

Table 6.5 Thermodynamic parameters for water and butanol sorption on the biosorbent.

	ΔG° (kJ/mol)		ΔH° (kJ/mol)	ΔS° (kJ/mol/K)
	110 °C	120 °C		
Water sorption	-5.5	-5.2	-15.4	-0.026
Butanol sorption	-3.4	-3.3	-7.6	-0.011

6.6 Chapter summary

Compared with the micropore Dubinin-Polanyi model, the Dubinin-Polanyi model for large pore materials is better for simulating the experimental water sorption equilibrium data in both pure water sorption system and butanol-water binary system. The results indicate that water sorption in this system is based on large pores, which are consistent with the fact that the oat hulls material mainly contains large pores (mesopores and macropores). The difference in limiting

sorption mass of water sorption in pure water and butanol-water binary system proves the competitive sorption between water and butanol. The analysis of site energy distribution shows that 98% of water sorption took place on the sites having energy lower than 10,000 J/mol, confirming the water sorption is physical. The calculated values of weighted mean site energy for water sorption are 2443 ± 102 J/mol and 2378 ± 119 J/mol in the single water sorption system and butanol-water binary system; thus, the affinity between water and the biosorbent in the single water system is higher than that in the butanol-water binary system.

The large pore and micropore Dubinin-Polanyi models were both able to describe butanol sorption equilibrium data in either pure butanol sorption system or butanol-water binary system. The value of limiting mass for sorption (q_0) obtained from pure butanol or binary system is lower than those for water sorption in the butanol-water binary system, which implies water has higher sorption performance on the oat hull based biosorbent. The site energy distribution analysis provides evidence that butanol sorption on the biosorbent is physisorption. The area under the site energy distribution curves shows the maximum water sorption capacity is much higher than that of butanol in either single or binary system. The weighted mean site energy for water sorption in the butanol-water binary system is 2378 ± 119 J/mol, which is higher than that of butanol (2105 ± 137 J/mol), showing a higher affinity of water to the biosorbent. Thus, water sorption is more competitive than butanol in the butanol-water binary system. The dipole-dipole attraction, one kind of van der Waals forces, may suggest one of the major mechanisms of water and butanol molecules sorption on the biosorbent.

The thermodynamic study provided evidence of the spontaneity and exothermic nature of the sorption process.

CHAPTER 7. DYNAMIC AND MODELING STUDY OF PURE WATER AND PURE BUTANOL SORPTION

Contribution of this chapter to overall Ph.D. work

In this chapter, pure water and pure butanol sorption on the biosorbent was studied to investigate and compare the sorption dynamics of these two components. An in-depth analysis of the mass transfer of water and butanol sorption process has been carried out through experimental work and theoretical modeling. The mass transfer coefficients and mass transfer resistances were determined for pure water and pure butanol sorption on the biosorbent. The rate-controlling step of water and butanol sorption on the oat hull in the fixed-bed column has been investigated based on the model fitting results.

7.1 Dynamic study and models considered in this chapter

This chapter studies the mass transfer of pure water and pure butanol sorption on the biosorbent in the single component sorption system. In this chapter, “pure” or “single” were used to distinguish this system with butanol-water binary system. In this system, nitrogen was used as carrier gas. The sorption nitrogen on the biosorbent was negligible. It is essential to understand the fundamentals of pure water and pure butanol sorption dynamic behavior on the oat hull based biosorbent. To extract more information about the mass transfer, a dynamic model was applied to simulate the breakthrough curves and determine the mass transfer resistance.

In this chapter, the Klinkenberg model was considered. The Klinkenberg model is based on linear sorption equilibrium isotherm and linear driving force (LDF) approximation for sorption kinetics. It assumes the internal and external mass transfer processes are the rate controlling step. The overall mass transfer resistance can be determined by model fitting.

The LDF model is as follows:

$$\frac{\partial \bar{q}}{\partial t} = k_{LDF}(q^* - \bar{q}) \quad (7.1)$$

where k_{LDF} is overall mass transfer coefficient, and q^* is adsorbate loading in adsorbent in equilibrium with the adsorbate concentration in the bulk fluid. \bar{q} is the average loading of adsorbate on adsorbent.

Linear isotherm (Chang et al., 2006b; Ruthven, 1984) is used to correlate the loading of sorbate on the biosorbent to sorbate concentration in the fluid phase, as shown in Eq. 7.2:

$$(q^* - \bar{q}) = K(c - c^*) \quad (7.2)$$

where c is the adsorbate concentration in fluid phase; c^* is the adsorbate concentration at equilibrium; K is the equilibrium constant in the linear sorption isotherm. q and c are expressed in moles of adsorbate per unit volume of the adsorbent and moles of adsorbate per unit volume of the fluid phase, respectively (Ruthven, 1984).

If the LDF approximation (Eq. 7.1) and the linear equilibrium equation (Eq. 7.2) are plugged in the mass balance equation of adsorbate (Eq. 7.3) derived for the adsorption column, the adsorbate concentration in the fluid phase at time t and position z can be determined.

$$\frac{\partial c}{\partial t} + u \frac{\partial c}{\partial z} + \frac{(1 - \varepsilon_b)}{\varepsilon_b} \frac{\partial \bar{q}}{\partial t} - D_L \frac{\partial^2 c}{\partial z^2} = 0 \quad (7.3)$$

$$c(0, z) = q(0, z) = 0 \quad (t = 0) \quad (7.3.1)$$

$$c(t, 0) = c_0, c(t, Z) = c_{ef} \quad (t > 0) \quad (7.3.2)$$

where t is time; z is the distance from the bed entrance; ε_b is the void fraction of bed, which is calculated by the difference between the bed volume and packed biosorbent volume divided by the bed volume; and u is the interstitial velocity which equals superficial velocity divided by the

void fraction of bed. The superficial velocity is the velocity of the fluid flowing through the empty column. It is calculated as the volumetric flow rate of that fluid divided by the cross-sectional area of the column. D_L is the axial dispersion coefficient; c_0 is sorbate concentration in feed; c_{ef} is the concentration of the sorbate in the effluent; and Z is the length of the column.

In Eq. 7.3, the first term accounts for the accumulation rate of the sorbate; the second term represents axial variation in fluid velocity; the third term is the sorption rate based on \bar{q} ; the fourth term is axial dispersion. When axial dispersion is negligible, the boundary condition at Z is not needed.

With the assumptions that axial dispersion is negligible and the process is isothermal, an approximate analytical solution was discussed by Klinkenberg and summarized by Ruthven as shown in Eq. 7.4 (Klinkenberg, 1954; Klinkenberg, 1948; Ruthven, 1984). In this work, the temperature of the bed was controlled by the jacket of the column, and the isothermal assumption was made.

$$\frac{c}{c_0} \approx \frac{1}{2} \left[1 + \operatorname{erf} \left(\sqrt{\tau} - \sqrt{\xi} + \frac{1}{8\sqrt{\tau}} + \frac{1}{8\sqrt{\xi}} \right) \right] \quad (7.4)$$

$$\operatorname{erf}(x) = \frac{2}{\sqrt{\pi}} \int_0^x e^{-\eta^2} d\eta \quad (7.5)$$

$$\xi = \frac{k_{LDF} K Z}{u} \left(\frac{1 - \varepsilon_b}{\varepsilon_b} \right) \quad (7.6)$$

$$\tau = k_{LDF} \left(t - \frac{Z}{u} \right) \quad (7.7)$$

ξ is dimensionless distance; τ is dimensionless time. $\operatorname{erf}(x)$ is the error function, which is represented by Eq. 7.5. The mass transfer coefficient (k_{LDF}) can be determined by fitting the experimental breakthrough curves to the equation 7.4. The mass transfer coefficient is related to

mass transfer resistance. The relationship of the overall mass transfer resistance with external and internal mass transfer resistances is expressed as shown in Eq. 7.8 (Gorbach et al., 2004; Gutiérrez Ortiz et al., 2014; Malek & Farooq, 1997):

$$\frac{1}{k_{LDF}} = \frac{R_p K}{3k_c} + \frac{R_p^2 K}{15D_e} \quad (7.8)$$

$$Sh = \frac{D_p k_c}{D_i} \quad (7.9)$$

$$Sh = 2 + 1.1Re^{0.6}Sc^{1/3} \quad (7.10)$$

$$Re = \frac{D_p \rho u}{\mu} \quad (7.11)$$

$$Sc = \frac{\mu}{\rho D_i} \quad (7.12)$$

In Eq. 7.8, R_p is the radius of the adsorbent particles; k_c is the external mass transfer coefficient; D_e is effective diffusivity. The overall mass transfer resistance can be represented by the first term ($1/k_{LDF}$) in Eq. 7.8 (Chang et al., 2006b; Gorbach et al., 2004; Gutiérrez Ortiz et al., 2014). The external mass transfer resistance can be calculated according to the second term ($R_p K/3k_c$) of Eq. 7.8. Then the internal mass transfer resistance ($R_p^2 K/15D_e$) can be obtained by subtracting the external mass transfer resistance from the overall mass transfer resistance.

The external mass transfer coefficient (k_c) can be estimated from Sherwood number (Sh), Reynolds number (Re), and Schmidt number (Sc) according to the correlation Eq. 7.9 and Eq. 7.10 (Wakao & Funazkri, 1978). In addition, external and internal mass transfer resistance can also be determined by Eq. 7.8 once k_{LDF} and k_c are obtained. The value of the external and internal mass transfer resistance can be compared to find the limitation step of this process.

In Eq. 7.11 and Eq. 7.12, D_i is molecular diffusivity. D_p is the average diameter of adsorbent particles, which is taken to be the equivalent of the volume median diameter of particles determined by particle size distribution in Chapter 4. μ and ρ are the viscosity of vapor and density of vapor, respectively.

The experiment conditions are as follows: absolute total pressure of 135 kPa, and sorption temperature at 110 and 120 °C. The bed void fraction was 0.76. The volume median diameter of particles (approximately 0.92 mm) was used to present the diameter of the biosorbent for kinetics analysis. The feed concentration was changed by adjusting the flow rate of liquid feed. Nitrogen (680 mL/min) was used as the carrier gas. A column with an inside diameter of 47.5 mm and length of 0.5 m was used as the sorption bed. More information about the sorption apparatus and experiment procedure can be found in Chapter 3. The preparation of the oat hull based biosorbent and the characterization information of this material can be found in Chapter 4.

7.2 Sorption of water and butanol at different temperatures

Considering water and butanol sorption on the biosorbent is exothermic, and to avoid the condensation of vapor feed, 110 and 120 °C were chosen as initial bed temperatures. During the sorption process, the bed temperature had a little fluctuation due to sorption heat generation in the column, and the bed temperature was gradually controlled with time by the fluid in the jacket of the column. Figure 7.1 shows the breakthrough curves of water sorption on oat hull biosorbent in the single water sorption system at the two different temperatures. The slope of the water breakthrough curve at 120 °C is steeper than that at 110 °C, and the breakthrough time of 120 °C is shorter than that of 110 °C. Figure 7.1 also shows the simulation of the Klinkenberg model (Eq.7.4) to experimental data at different experiment temperatures. The simulated curve generated by the Klinkenberg model fits data points generally. The fitting results can be seen in Table 7.1.

The values of the correlation coefficient (R^2) are high, the values of residual sum of squares (RSS) are low, and the modeling curves well describe almost all the data points. Thus, the model gave a satisfactory fit to the water sorption breakthrough curves.

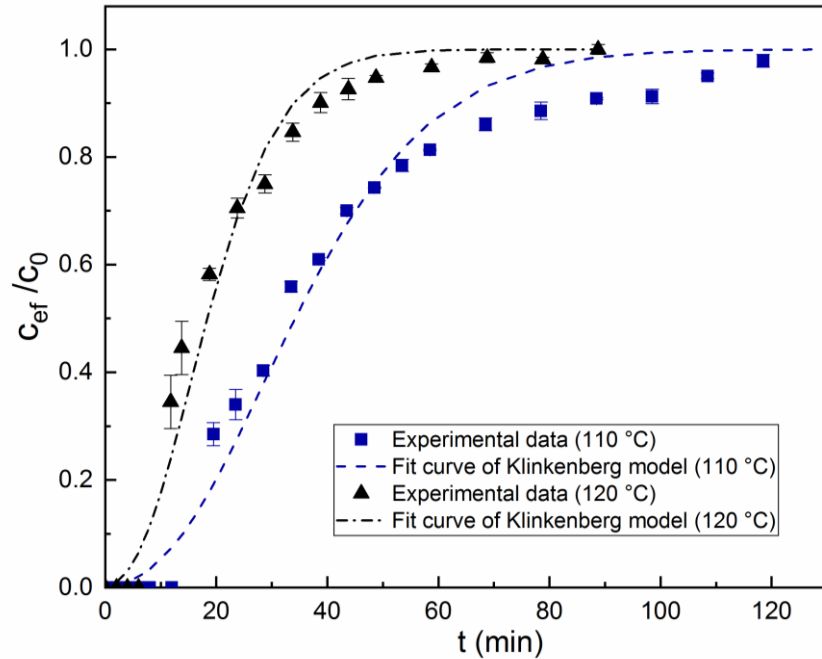


Figure 7.1 Breakthrough curves of water sorption on the biosorbent at different temperatures and the simulation curves of the Klinkenberg model (feed water concentration of 0.65 mol/mol, 135 kPa).

The butanol breakthrough curves of the single butanol sorption system at different temperatures are presented in Figure 7.2. The shape of the butanol breakthrough curves shows the same trend as that in the pure water sorption system. The simulation results of the Klinkenberg model are depicted in Figure 7.2 as well. The simulated curves generated by the Klinkenberg model are consistent with the experimental data, too.

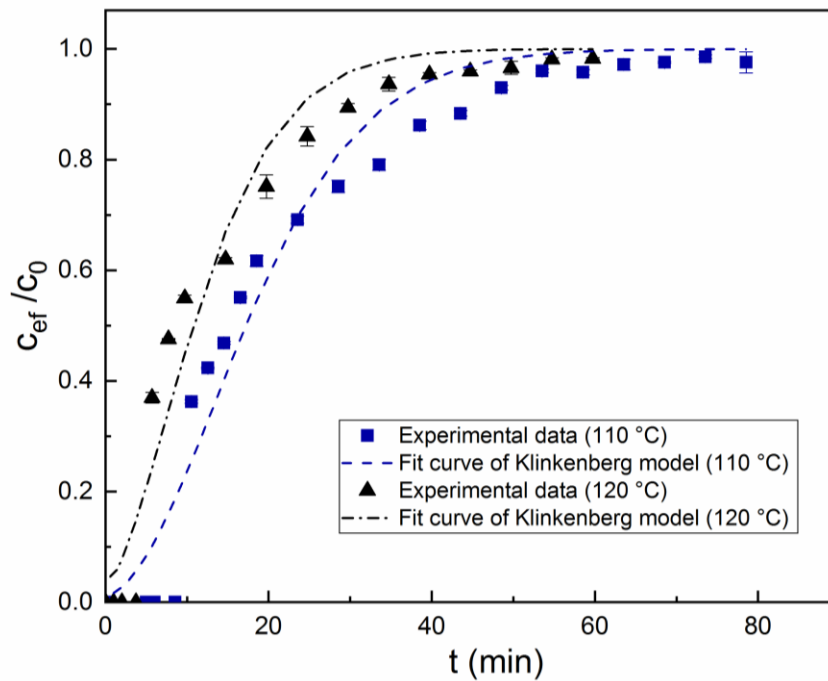


Figure 7.2 Breakthrough curves of butanol sorption on the biosorbent at different temperatures and the simulation curves of the Klinkenberg model (feed concentration of 0.65 mol/mol, 135 kPa).

Thus, the Klinkenberg model satisfactorily described the water and butanol breakthrough curves of pure water and pure butanol sorption systems by the biosorbent. The parameters in the Klinkenberg model were estimated by model fitting, and the results are listed in Table 7.1. The parameters in the Klinkenberg model were used to study the sorption mass transfer. The estimated values of mass transfer resistances using Eqs. (7.8-7.12) for water sorption and butanol sorption are shown in Table 7.1. In general, for both water and butanol sorption on oat hull biosorbent, the internal mass transfer resistances are higher than the external mass transfer resistances. This result may suggest the sorption rate is controlled by pore diffusion. This is consistent with the structure of oat hulls, which are porous, as observed through the SEM images (Banerjee et al., 2016; Huang et al., 2019).

Table 7.1 Fitting results of the Klinkenberg model at different temperatures.

T (°C)	K	k_{LDF} (s ⁻¹)	k_c (m/s)	$1/k_{LDF}$ (s)	$R_p K/3k_c$ (s)	$R_p^2 K/15D_e$ (s)	R^2	RSS	DF
Water									
110	358	0.0043	0.063	232.6	0.9	231.7	0.97	0.12	19
120	195	0.0059	0.064	169.5	0.5	169.0	0.97	0.09	15
Butanol									
110	189	0.0042	0.051	238.1	0.6	237.5	0.96	0.12	20
120	123	0.0046	0.052	217.4	0.4	217.0	0.96	0.09	15

DF: degrees of freedom.

In both Figures 7.1 and 7.2, the slope of the breakthrough curve of 120 °C is steeper than that of 110 °C. In addition, the fitting results showed that the values of mass transfer coefficients k_{LDF} (s⁻¹) increased as the temperature increased. The comparison of the results at two different temperatures suggests that the increase in temperature caused the increase in the rate of mass transfer. The results also show that the mass transfer resistances decreased as the temperature increased. This conclusion is consistent with those in previous studies (Carmo et al., 2004; Chang et al., 2006b). The results such as the mass transfer coefficient and mass transfer resistance obtained in the single component sorption system will be compared with those in the binary system, which will be discussed in Chapter 8.

In addition, Table 7.1 shows the values of fitted mass transfer coefficient k_{LDF} of water sorption are higher than those of butanol sorption at the same operating conditions in the pure water and pure butanol systems. The higher mass transfer coefficient k_{LDF} suggests a higher mass transfer rate. Thus, the rate of pure water sorption on the oat hull biosorbent was faster than that

of pure butanol sorption. Besides, the butanol sorption affinity (K value) is lower than that of water, which can also be seen in the isotherms of water and butanol in the single system. The values of overall mass transfer resistance of water sorption are lower than that of butanol at the same conditions. This result suggests that water has more favorable sorption performance compared with butanol. This conclusion will be further discussed with the results in the butanol-water binary system in Chapter 8 to explain the basis of the separation of the butanol-water mixture by the oat hull biosorbent.

The estimated mass transfer coefficient of water sorption by a canola meal based biosorbent in the ethanol-water binary system was reported to be 0.0040 in another study (Tajallipour et al., 2013). This value is a little bit lower than the mass transfer coefficient value of water sorption at similar conditions in this study. It may be because of the fact that in single component system water sorption has less mass transfer resistance without the competitions of other components. The values of D_e were calculated from the internal mass transfer resistance. The values of D_e of water at different temperatures are estimated to vary from 1.62×10^{-8} to $2.16 \times 10^{-8} \text{ m}^2\text{s}^{-1}$. The values of D_e are consistent with those of other studies where the effective moisture diffusivity varied from 0.35×10^{-9} to $2.14 \times 10^{-8} \text{ m}^2\text{s}^{-1}$ (Angelopoulos et al., 2016; Vagenas & Karathanos, 1991). The values of D_e of butanol are estimated to vary from 7.94×10^{-9} to $1.11 \times 10^{-8} \text{ m}^2\text{s}^{-1}$, which are lower than those of water.

In summary, the Klinkenberg model was able to simulate both of water sorption and butanol sorption breakthrough curves at the tested two temperatures with satisfaction. The estimated model parameters were further used to evaluate the mass transfer resistances, and the values suggested the pure water or butanol sorption on the oat hull based biosorbent was controlled by mass transfer.

Comparing with butanol, water has more favorable sorption performance on the oat hull biosorbent due to a higher affinity to the biosorbent and higher sorption speed.

7.3 Sorption of water and butanol at different feed concentrations

Figure 7.3 shows the experimental breakthrough curves and simulated curves of water sorption in a pure water sorption system at different initial concentrations. These breakthrough curves of different feed concentrations indicate that the feed concentration affected the sorption rate. After the breakthrough, the increase in the effluent concentration of higher feed concentration is more significant than that of lower feed concentration. The shape of the breakthrough curves suggests that a higher driving force leads to a higher sorption rate.

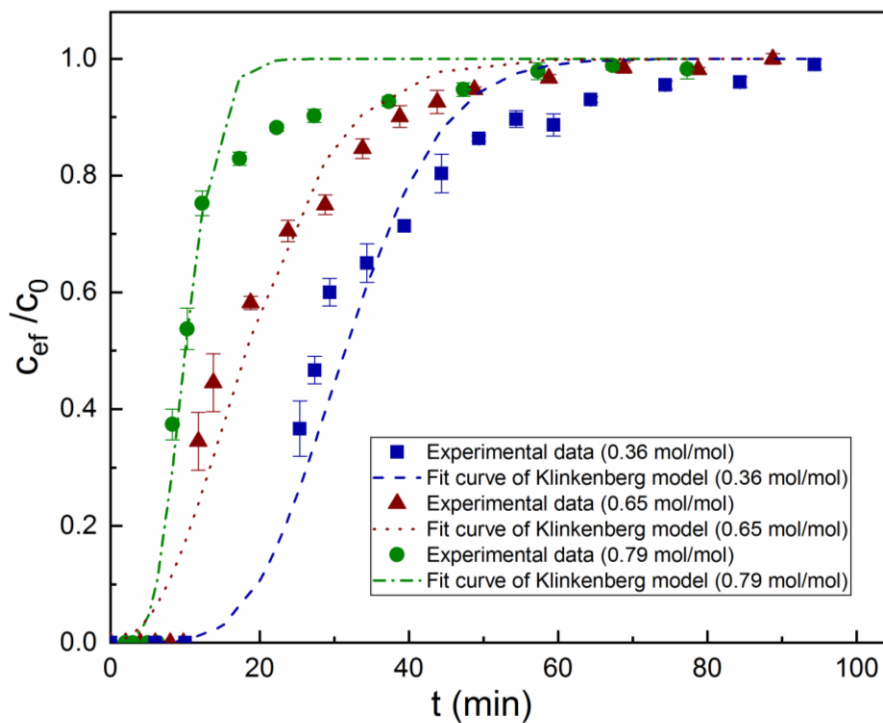


Figure 7.3 Breakthrough curves of water sorption on the biosorbent at different feed concentrations and the simulation curves of the Klinkenberg model (120 °C, 135 kPa).

The simulated curves of the Klinkenberg model (Eq. 7.4) can be seen in Figure 7.3. The simulated water breakthrough curves are able to describe almost all the data points in the feed concentration range of this study. The values of parameters estimated by model fitting and the estimated mass transfer resistance are listed in Table 2. The fitting results show that the process at higher feed concentration has a larger mass transfer coefficient and lower mass transfer resistance, which is consistent with the trend of slope changes in the breakthrough curves in Figure 7.3. The mass transfer resistances obtained at different initial concentrations lead to the same conclusion as in section 7.2 that the estimated values of internal mass transfer resistance are higher than those of external mass transfer resistance.

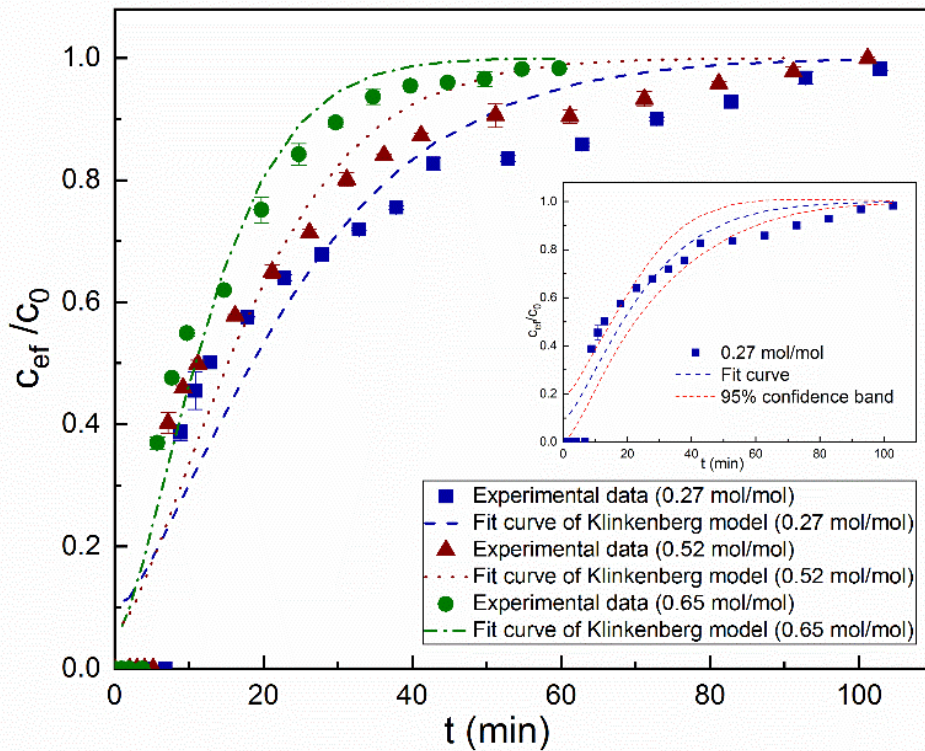


Figure 7.4 Breakthrough curves of butanol sorption on the biosorbent at different feed concentrations and the simulation curves of the Klinkenberg model (120 °C, 135 kPa).

The breakthrough curves of butanol sorption at different feed concentrations were also simulated by the Klinkenberg model. The results are presented in Figure 7.4. The parameters and

mass transfer resistances are shown in Table 7.2. As can be seen from Figure 7.4 and Table 7.2, the simulated curves are able to describe the trend of experimental points at different feed concentrations. The fitting result for 0.27 mol/mol feed concentration is not as good as those at other conditions. However, most data points of 0.27 mol/mol feed concentration fall in or close to the 95% confidence interval area, which can be observed in the inset of Figure 7.4. The fitting result is acceptable. The comparison between the pure butanol sorption experiments with different feed concentrations gives a similar conclusion as in the pure water sorption system that the butanol mass transfer rate increased with the increase in feed concentration, and the sorption process is controlled by internal diffusion. D_e were calculated from the internal mass transfer resistance. The values of D_e of water at different feed concentrations are estimated to vary from 1.53×10^{-8} to $4.01 \times 10^{-8} \text{ m}^2\text{s}^{-1}$. The range of values of D_e is similar to that at different temperatures shown in section 7.2. The values of D_e of butanol at different feed concentrations are estimated to vary from 3.45×10^{-9} to $7.94 \times 10^{-9} \text{ m}^2\text{s}^{-1}$, which are lower than those of water.

Table 7.2 Fitting results of the Klinkenberg model at different feed concentrations.

Concentration in feed (mol/mol)	k_{LDF} (s^{-1})	k_c (m/s)	$1/k_{LDF}$ (s)	$R_p K/3k_c$ (s)	$R_p^2 K/15D_e$ (s)	R^2	RSS	DF
Water								
0.79	0.0146	0.074	68.5	0.4	68.1	0.97	0.07	13
0.65	0.0059	0.064	169.5	0.5	169.0	0.97	0.09	15
0.36	0.0056	0.058	178.6	0.5	178.1	0.95	0.17	16
Butanol								
0.65	0.0046	0.052	217.4	0.4	217.0	0.96	0.09	15
0.52	0.0031	0.049	322.6	0.4	322.2	0.94	0.17	18
0.27	0.0020	0.044	500.0	0.4	499.6	0.92	0.18	17

DF: degrees of freedom.

In this work, the Klinkenberg model gives a satisfactory fit of the data at different conditions. However, some breakthrough curves simulated by the Klinkenberg model seem to show overprediction of sorption. It may be because that the Klinkenberg model assumes linear isotherm, which may have divergence with some data points of the real isotherms. In addition, the overprediction could be due to the fact that the temperature of the column has a little fluctuation because of sorption heat generated in the column. In practice, particularly under adiabatic conditions, where the sorption heat cannot be removed instantly, consideration should be made to decrease the divergence between model and experimental data, for an example, considering a combined wave front model (Ladisich et al., 1984).

7.4 Chapter summary

In this chapter, the dynamics of pure water sorption and pure butanol sorption on the oat hull biosorbent in the single component sorption system were studied respectively. The Klinkenberg model simulated the breakthrough curves of water and butanol sorption on the oat hull biosorbent in the single component sorption system at different temperatures and feed concentrations with satisfaction.

The overall, external, and internal mass transfer resistances were estimated by the parameters obtained from model fitting. The rate of pure water or butanol sorption on the oat hull based biosorbent was controlled by mass transfer resistance. It was concluded that for both pure water sorption and pure butanol sorption on the biosorbent, the mass transfer coefficients increased with the increase of temperature and feed concentration. The mass transfer behavior for pure water and pure butanol sorption on the oat hull based biosorbent will be compared with that in the binary system presented in Chapter 8.

The values of overall mass transfer resistance of pure water sorption are lower than those of butanol at the same conditions. This observation suggests that water has more favorable sorption performance compared with butanol, and it is possible that the kinetically driven competitive sorption occurred between water and butanol in the butanol-water binary system. This conclusion is discussed with the results in the butanol-water binary system to explain the basis of the separation of the butanol-water mixture by the oat hull biosorbent in Chapter 8.

CHAPTER 8. DYNAMICS OF WATER SORPTION FROM BUTANOL- WATER VAPOR

Contribution of this chapter to overall Ph.D. work

In this chapter, the dynamics of water sorption from butanol-water vapor was investigated by analyzing water breakthrough curves in the binary system in aid of the Bohart-Adams model and the Klinkenberg model. The suitability of the two models to study the sorption dynamics and mechanisms was evaluated based on the modeling results. The effects of different conditions, i.e., sorption temperature and feed concentrations were investigated. The fitting results of the Klinkenberg model were further processed to determine the overall, external, and internal mass transfer resistances and the rate-limited step in the binary system. Moreover, the kinetically driven competitive sorption of butanol and water was discussed to explain the basis of the separation of the butanol-water mixture by the oat hull biosorbent.

8.1 Dynamic models

Chapter 5 demonstrated that the oat hull based biosorbent was able to produce high purity butanol product from butanol and water mixture with a wide concentration range. This provides an alternative method to break the butanol-water azeotrope, and then to reduce or replace the multiple downstream decantation and distillation units following the preliminary distillation. However, the dynamics of water sorption from the butanol-water vapor and the mass transfer resistance of water sorption on cellulosic materials such as oat hulls are not well understood. Investigation in this area is essential to understand the fundamentals of water biosorption and for application in the industry (Fulazzaky et al., 2013).

This chapter aims to investigate the dynamics of water sorption from the water/butanol mixture using oat hull biosorbent in the packed column. The focuses are on the analysis of water breakthrough curves and mass transfer in aid of mathematical modeling. A simulation of breakthrough curves by dynamic models can provide valuable information and assist in evaluating rate-controlling steps. Many mathematical models have been used for this purpose, among which the Bohart-Adams model and the Klinkenberg model are widely used to simulate the water breakthrough curves (Chang et al., 2006b; Chu, 2010; Gutiérrez Ortiz et al., 2014; Han et al., 2009; Tajallipour et al., 2013). In this work, the two dynamic models were applied to simulate the water breakthrough curves and determine the mass transfer resistance. The Bohart-Adams model assumes that the diffusion steps are very fast, and the surface sorption is the rate-controlling step. The second one, the Klinkenberg model described in detail in Chapter 7, based on linear driving force (LDF) model and linear sorption isotherm, and assumes that mass transfer is the rate-controlling step when the surface sorption step is fast. The details of the models are described as follows.

In general, the practical sorption processes in a fixed bed are complex. It is very challenging to solve models taking into account the equilibrium, axial dispersion, and mass transfer for such processes. Reasonable simplification needs to be applied to provide a shortcut to an analytic expression of the models. The mass balance of sorbate in the fluid phase in the column is the same as that described in Chapter 7, and again presented in Eq. 8.1 here for clarity of presentation in this chapter:

$$\frac{\partial c}{\partial t} + u \frac{\partial c}{\partial z} + \frac{(1 - \varepsilon_b)}{\varepsilon_b} \frac{\partial \bar{q}}{\partial t} - D_L \frac{\partial^2 c}{\partial z^2} = 0 \quad (8.1)$$

The initial and boundary conditions are as follows:

$$c(0, z) = q(0, z) = 0 \quad (t = 0) \quad (8.2)$$

$$c(t, 0) = c_0, \quad c(t, Z) = c_{ef} \quad (t > 0) \quad (8.3)$$

where t is time; z is the distance from the bed entrance; c is the water concentration; c_0 is the water concentration in feed; c_{ef} is the concentration of the sorbate in the effluent; ε_b is the void fraction of bed; u is the interstitial velocity; \bar{q} is the average loading of adsorbate on adsorbent; D_L is the axial dispersion coefficient; and Z is the length of the column.

In Eq. 8.1, again the first term accounts for the accumulation rate of the adsorbate; the second term represents axial variation in fluid velocity; the third term represents the sorption rate based on \bar{q} ; the fourth term accounts for axial dispersion (Purnomo & Prasetya, 2007; Tajallipour et al., 2013). Similarly, the axial dispersion is assumed to be negligible in this work; thus, the boundary condition at Z is not needed. In this work, the temperature of the bed was controlled by the jacket of the column, and the isothermal assumption was made. The mass balance equation for the sorption column together with the initial and boundary conditions were used to simulate the dynamics of water sorption in the fixed bed. The term of the sorption rate expression in Eq. 8.1 was determined by the Bohart-Adams model and the Klinkenberg model.

8.1.1 Bohart-Adams model

The Bohart-Adams model is widely used to describe the breakthrough curves for biosorption research. After fitting it to breakthrough curves obtained from the experiments, the determined model parameters are used for commercial sorption column design. The Bohart-Adams model describes the sorbate-adsorbent interaction by the quasi-chemical rate expression (Bohart & Adams, 1920). This model assumes that the diffusion steps are very fast, and the rate is limited by

surface interaction (adsorption) (Bohart & Adams, 1920; Gutiérrez Ortiz et al., 2014). The rate expression is as follows:

$$\frac{\partial \bar{q}}{\partial t} = k_{BA}c(q_s - \bar{q}) \quad (8.4)$$

By replacing $\partial \bar{q} / \partial t$ in Eq. 8.1 using Eq. 8.4, the analytical solution of Eq. 8.1 was derived as shown in Eq. 8.5 below. This equation has been used in various adsorption processes (Chu, 2010; Karpowicz et al., 1995; Ruthven, 1984).

$$\ln \left(\frac{c_0}{c_{ef}} - 1 \right) = \frac{k_{BA}q_s Z}{u} \left(\frac{1 - \varepsilon_b}{\varepsilon_b} \right) - k_{BA}c_0 t \quad (8.5)$$

where k_{BA} is the Bohart-Adams rate constant; q_s is the saturated adsorbate loading in adsorbent; c_{ef} is sorbate concentration in the effluent; and Z is the length of the column. The parameters k_{BA} and q_s can be calculated from the slope and intercept by linear regression. This model was tested in this work to simulate water sorption breakthrough curves in comparison with the Klinkenberg model.

8.1.2 Klinkenberg model

The Bohart-Adams model, which is based on the premise that the process is controlled by the surface adsorption step, does not account for the external and internal diffusion limitations in the overall process (Gutiérrez Ortiz et al., 2014). The biosorbent is porous, so the Klinkenberg model considering mass transfer limitation by diffusion is also applied in this work. As described in Chapter 7, it is represented by the LDF approximation of mass transfer. The LDF model is a lumped model for sorption. In addition, the linear sorption isotherm is used to correlate the water uptake to water concentration. The sorption isotherm of water on the oat hull based biosorbent can be seen in Chapter 6. It is reasonable to use linear isotherm under the tested conditions of this study.

In this model, the surface sorption process is assumed to be much faster than both external and internal mass transfer. The overall mass transfer resistance is determined by model fitting. Then the internal and external mass transfer resistance can be calculated. Thus, this model can help to determine external and internal mass transfer resistances of the sorption process. The detailed description of the Klinkenberg model and the calculations of the total, external, and internal mass transfer resistances are presented in Chapter 7.

Specifically in this chapter, replacing $\partial\bar{q}/\partial t$ in Eq. 8.1 by the LDF equation (Eq. 7.1) and inputting the linear equilibrium isotherm (Eq. 7.2) obtained an approximate analytical solution the same as that in Chapter 7, as shown in Eq. 8.6 (Klinkenberg, 1954; Klinkenberg, 1948; Ruthven, 1984).

$$\frac{c}{c_0} \approx \frac{1}{2} \left[1 + \operatorname{erf} \left(\sqrt{\tau} - \sqrt{\xi} + \frac{1}{8\sqrt{\tau}} + \frac{1}{8\sqrt{\xi}} \right) \right] \quad (8.6)$$

$$\operatorname{erf}(x) = \frac{2}{\sqrt{\pi}} \int_0^x e^{-\eta^2} d\eta \quad (8.7)$$

$$\xi = \frac{k_{LDF} K Z}{u} \left(\frac{1 - \varepsilon_b}{\varepsilon_b} \right) \quad (8.8)$$

$$\tau = k_{LDF} \left(t - \frac{Z}{u} \right) \quad (8.9)$$

ξ is dimensionless distance; τ is dimensionless time. $\operatorname{erf}(x)$ is the error function. k_{LDF} is overall mass transfer coefficient; K is the equilibrium constant in linear sorption isotherm. The mass transfer coefficient (k_{LDF}) can be determined by fitting the experimental water breakthrough curves to the Klinkenberg model (Eq. 8.6). Then similarly, the overall, external, and internal mass transfer resistances were determined by Eqs. (7.8-7.12) (Chang et al., 2006b; Gorbach et al., 2004; Gutiérrez Ortiz et al., 2014).

8.2 Simulation of water breakthrough curves and comparisons

Considering the sorption was dominated by water, and the system was complex, this chapter focused on the dynamic water sorption and modeling. Thus, water breakthrough curves obtained from butanol-water vapor by varying the key parameters including temperature and feed concentration were simulated and discussed in this work. The fitting results for the two models were compared to study the sorption dynamics and mechanisms.

The breakthrough curves of water obtained at temperatures of 110 °C and 120 °C (feed concentration 56 wt% butanol, pressure 135 kPa, carrier gas flow rate 680 mL/min) are presented in Figs. 8.1 and 8.2. At a higher temperature, e.g. 120 °C, the slope of the breakthrough curve is steeper, indicating a higher mass transfer rate. In addition, at the beginning of sorption, the slopes of both breakthrough curves are steep, which indicates the possible higher mass transfer rate due to the higher water concentration gradient between biosorbent and vapor feed. When sorption approaches equilibrium, the slope flattens, indicating a slower mass transfer rate.

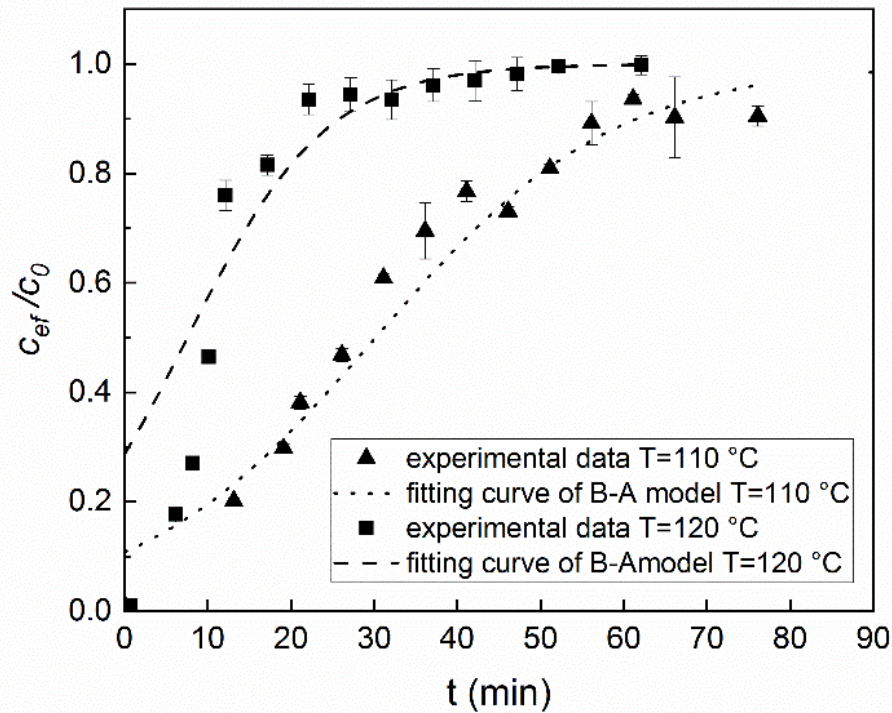


Figure 8.1 Breakthrough curves of water sorption on the biosorbent (pressure of 135 kPa, 44 wt% water and 56 wt% butanol in the feed, carrier gas flow rate 680 mL/min) at different temperatures, and simulation curves of the Bohart-Adams model.

Figures 8.1 and 8.2 also show the fitting results of the Bohart-Adams model and Klinkenberg model. Figure 8.1 shows that the Bohart-Adams model partially fitted the experimental data. However, it did not fit the data points at the beginning of the breakthrough curves satisfactorily. The values of the parameters k_{BA} and q_s were estimated by model fitting.

Figure 8.2 shows that the Klinkenberg model successfully fitted the data points. The curves generated by this model are more consistent with the experimental data than those generated by the Bohart-Adams model.

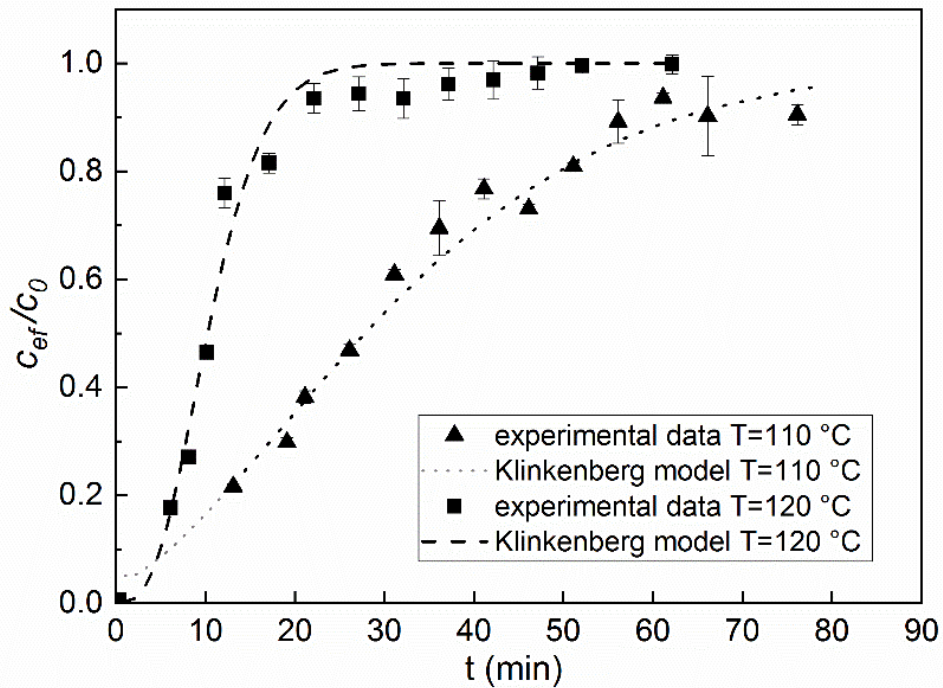


Figure 8.2 Breakthrough curves of water sorption on the biosorbent (pressure of 135 kPa, 44 wt% water and 56 wt% butanol in the feed, carrier gas flow rate 680 mL/min) at different temperatures, and simulation curves of the Klinkenberg model.

The values of the parameters of the Klinkenberg model were estimated by model fitting as well. The fitting results and the parameters obtained from model fitting are listed in Table 8.1. The model simulation was evaluated by the value of the correlation coefficient (R^2) and the residual sum of squares (RSS). The values of R^2 of the Klinkenberg model are higher than those of the Bohart-Adams model, and the values of RSS of the Klinkenberg model are smaller. A comparison of the fitting results shows that the Klinkenberg model is more suitable to simulate the water sorption from the butanol-water mixture than the Bohart-Adams model.

Table 8.1 Fitting results of water breakthrough curves by the Bohart-Adams model and the Klinkenberg model (135 kPa, 44 wt% water and 56 wt% butanol in the feed).

Bohart-Adams model					
T ($^{\circ}\text{C}$)	q_s (g/cm^3)	k_{BA} ($\text{cm}^3\text{g}^{-1}\text{min}^{-1}$)	R^2	RSS	Degrees of freedom
110	86.5	0.175	0.90	0.074	12
120	22.0	0.286	0.90	0.179	12
Klinkenberg model					
T ($^{\circ}\text{C}$)	K	k_{LDF} (s^{-1})	R^2	RSS	Degrees of freedom
110	316	0.0026	0.98	0.029	12
120	139	0.0091	0.98	0.033	12

The above results suggest that the water sorption mechanism and dynamics are more likely close to the Klinkenberg model's theory. The Bohart-Adams model assumes that the diffusion steps are very fast, and the overall sorption rate is limited by the surface adsorption step. On the other hand, the Klinkenberg model is based on the mass transfer limitation. The biosorbent is porous, and intrinsic water sorption on the biosorbent is physical and fast; thus it is reasonable to conclude that mass transfer is the rate-controlling step instead of surface sorption.

8.3 Interpretation of water sorption data obtained at different sorption temperatures

As discussed in the last section, the Klinkenberg model described the data of water sorption on the biosorbent more satisfactorily. Thus, mass transfer resistance was further analyzed in this section based on the Klinkenberg modeling results. This information is important as the mass transfer resistance and rate-limited steps are not clear for water sorption on the oat hull biosorbent. Similar to the pure water system as described in Chapter 7, the overall water mass transfer

resistance ($1/k_{LDF}$), external mass transfer resistance ($R_p K/3k_c$), and internal mass transfer resistance ($R_p^2 K/15D_e$) in the butanol-water mixture were estimated using the parameters obtained from the model fitting according to Eqs. (7.8-7.12). The water or butanol sorption process is exothermic as discussed in Chapter 6. The higher temperature results in the higher mass transfer rate, but it decreased the sorption capability. This conclusion is consistent with that in previous studies (Carmo et al., 2004; Chang et al., 2006b).

The results of water mass transfer resistances at various conditions are listed in Table 8.2. Overall, the values of internal mass transfer resistance are much higher than those of external mass transfer resistance. This finding successfully identified that the water sorption rate on the biosorbent was mainly controlled by internal mass transfer resistance. This is consistent with the texture of oat hull material, which is porous, as observed through the SEM images reported in Chapter 4. This result is similar to the study of ethanol dehydration using a canola meal based biosorbent, which found that the internal mass transfer resistance is higher than external mass transfer resistance (Tajallipour et al., 2013). However, compared with water vapor sorption on zeolites, which have significant amounts of micropores (Gorbach et al., 2004), the internal mass transfer resistance of water sorption on the biosorbent in this work is much lower than that using zeolites.

Table 8.2 Results of water mass transfer study for water sorption in the binary system at different sorption temperatures based on the Klinkenberg modeling results.

T ($^{\circ}C$)	Sh	k_c (m/s)	$1/k_{LDF}$ (s)	$R_p K/3k_c$ (s)	$R_p^2 K/15D_e$ (s)
110	3.17	0.064	384.6	0.8	383.8
120	3.14	0.065	109.9	0.3	109.6

The comparison of the mass transfer at different temperatures confirmed that the water sorption mass transfer rate increased with the increase in temperature. This could be due to the higher temperature accelerating the diffusion of water molecules. The adsorption equilibrium constant declined as sorption temperature increased, again supporting that the water sorption by the biosorbent in this work is exothermic. The effects of the sorption temperature on the sorption capacity for the oat hull based biosorbent were discussed in Chapter 5. The results obtained in this work are consistent with those of the previous work that the increase of temperature caused the increase in sorption rate, though it decreased the sorption capacity at equilibrium (Carmo et al., 2004). The value of D_e was calculated from the internal mass transfer resistance, which was determined by the model parameters. The values of D_e of different temperatures are varied from 1.15×10^{-8} to $1.77 \times 10^{-8} \text{ m}^2\text{s}^{-1}$. The values of D_e are consistent with those in other studies, where the effective moisture diffusivity varied from 0.35×10^{-9} to $2.14 \times 10^{-8} \text{ m}^2\text{s}^{-1}$ (Angelopoulos et al., 2016; Vagenas & Karathanos, 1991).

8.4 Simulation of water breakthrough curves at different feed concentrations

The breakthrough curves for water sorption in the binary system at different feed concentrations were further stimulated by the Klinkenberg model, as shown in Figure 8.3. The experimental data shows that the feed concentration of adsorbates affected the sorption rate. Especially at the beginning of sorption, the slope of the breakthrough curve obtained by higher water content in the feed is steeper than that of lower water content in the feed, indicating a higher mass transfer rate due to the higher mass transfer driving force. The modeling results and parameters obtained from model fitting are listed in Table 8.3.

The changes of the mass transfer coefficient of different feed concentrations indicate that the higher water content leads to a higher mass transfer rate due to the higher mass transfer driving

force. This was confirmed by the shape and slope of the breakthrough curves. The external and internal mass transfer resistances decreased when the water content in the feed stream was increased. The estimated values of internal mass transfer resistance are higher than those of external mass transfer resistance, which is consistent with the conclusion in the last section. The values of D_e of different feed concentrations are varied from 1.15×10^{-8} to $2.22 \times 10^{-8} \text{ m}^2\text{s}^{-1}$, which are similar to the values of different temperatures shown in section 8.3.

In addition, the Klinkenberg model was able to simulate the water breakthrough curves within the condition range of this study. However, the fitting results in cases of 70 and 80 wt.% of butanol concentration in the feed ($R^2=0.96, 0.94$) are not as good as the 56 wt.% of butanol concentration ($R^2=0.98$). This observation is because that the Klinkenberg model assumed that the water sorption isotherm is without the effect of butanol. When butanol concentration in the feed was higher, the sorption of butanol increased; thus, such an assumption caused the modeling results to deviate from the experimental data. In the tested range of this work, this model provides satisfactory results. To apply this model to an extended range of butanol concentration, it is necessary to consider the effect of butanol in a water sorption isotherm. However, determining an analytical solution for the model will prove challenging. This can form an area of future research.

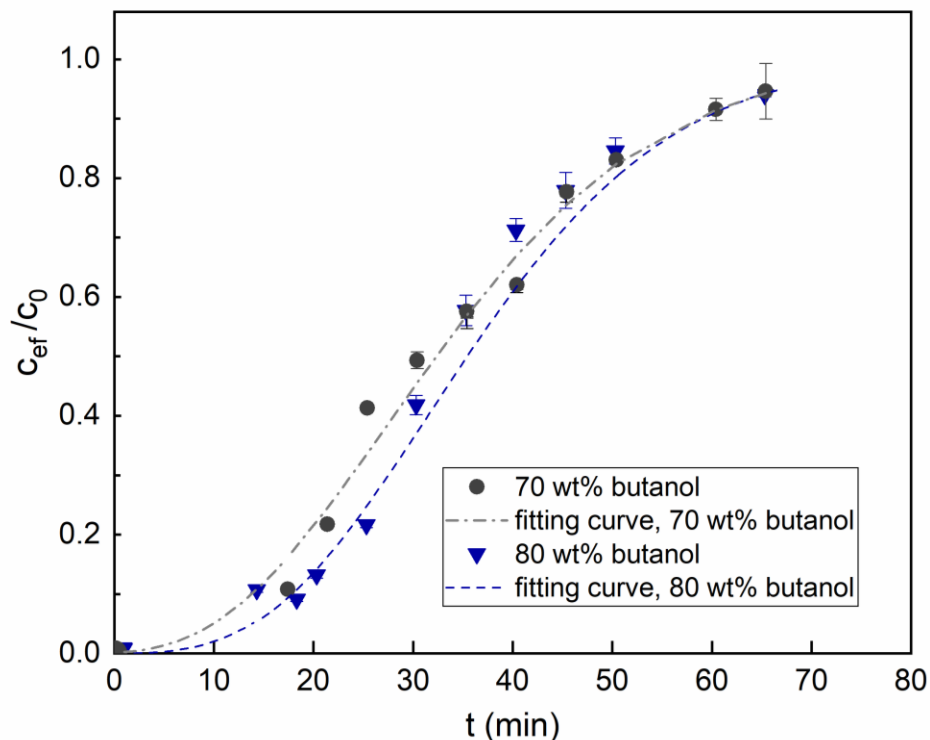


Figure 8.3 Breakthrough curves of butanol dehydration at different feed concentrations (pressure of 135 kPa, temperature of 110 °C, carrier gas flow rate 680 mL/min) and the simulation curves of the Klinkenberg model.

Table 8.3 Results of mass transfer study for water sorption in the binary system at different feed concentrations based on the Klinkenberg modeling results.

Butanol in feed (wt%)	Water in feed (wt%)	$k_{LDF} (s^{-1})$	R^2	$1/k_{LDF} (s)$	$R_p K/3k_c (s)$	$R_p^2 K/15D_e (s)$	Degrees of freedom
70	30	0.0050	0.96	200.0	0.7	199.3	9
80	20	0.0038	0.94	263.2	0.8	262.4	9

8.5 Discussion of competitive sorption between water and butanol

In this section, the kinetically driven competitive sorption of butanol and water is discussed based on the sorption features of water and butanol in the single component system and the binary

system. The kinetically driven competitive sorption between water and butanol may help to explain the basis of separation of the butanol-water mixture by the oat hull biosorbent. Such information is lacking in the literature.

Figure 8.4 shows water and butanol uptakes versus time in the binary system. The curve of butanol has a steep decrease, which suggests that the butanol sorption decreased rapidly with time when water sorption existed. The competitive sorption occurred between water and butanol for the limited site on the biosorbent. Comparing these two curves in Figure 8.4 suggests that the uptake of water was higher and faster than that of butanol in the butanol-water binary system during the sorption process. The results in the butanol-water binary system again indicate that oat hull based biosorbent was able to selectively adsorb more water than butanol. Figure 8.4 also demonstrates that water was adsorbed continually throughout the dynamics sorption process, while butanol sorption mainly occurred at the beginning of the process and then rapidly decreased to insignificance because of the competition of sorption with water.

The results presented in Chapter 7 indicate that in the single component sorption system, compared to butanol, water has a higher mass transfer rate and lower mass transfer resistance at the same conditions based on the fitting results. Water is more competitive than butanol for sorption on the oat hull biosorbent.

The sorption performance in the butanol-water binary system and the single system shows that water is more competitive than butanol for sorption on the oat hull biosorbent. Thus, the oat hull based biosorbent is able to enrich the low-grade butanol-water mixture. The results of the dynamics study in the binary and the single system also indicate different mass transfer rates between water and butanol on oat hull plays a key role for butanol dehydration. The different mass transfer rates may be because of the different mean free path of water and butanol molecules. The

mean free path, which presents the average distance a gas molecule will travel before colliding with another molecule, displays linear proportionality to the temperature and inverse proportionality to the pressure and molecular diameter. Water has smaller molecular diameter (0.28 nm) than butanol (0.46 nm). Thus, water has larger mean free path. The biosorbent mainly has mesopores (2-50 nm) and large pores (>50 nm). Water molecules may travel easier and faster due to its larger mean free path during the diffusion step. Thus, water molecules can be captured on the surface and inside the pores quickly.

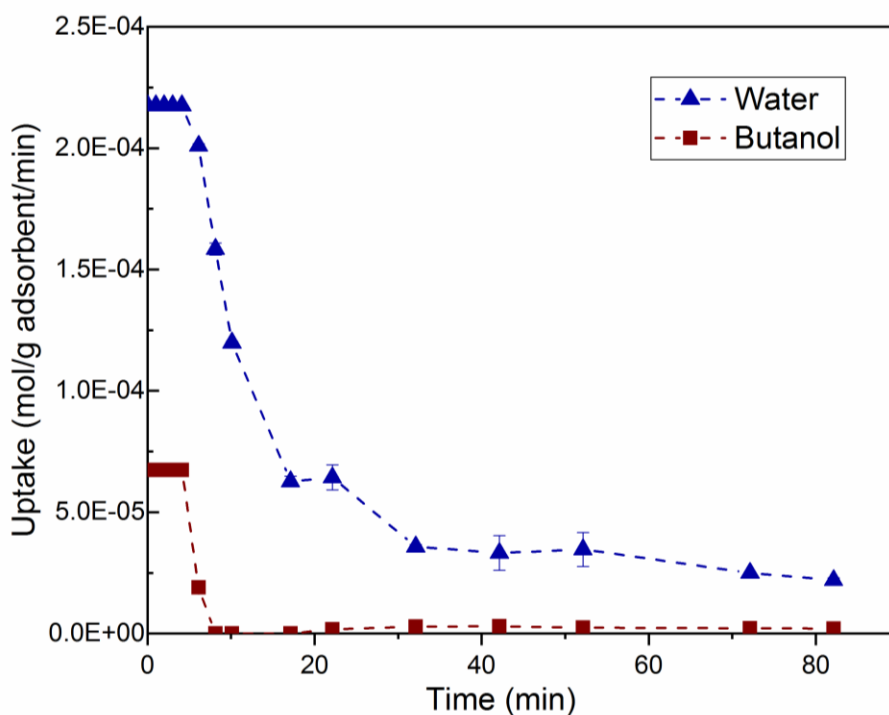


Figure 8.4 The water and butanol uptake versus time (56 wt.% butanol feed concentration, 120 °C, 135 kPa).

8.6 Discussion on sorption mechanism

It was concluded in Chapter 6 that the Dubinin-Polanyi model, which assumed the multilayer sorption and applied to the van der Waals equation, was able to describe water and butanol sorption on the biosorbent. This suggests the van der Waals forces may be dominant in water and butanol

sorption on the biosorbent, and the sorption may be multilayer. The site energy distribution analysis and thermodynamics study in Chapter 6 provides evidence that water and butanol sorption on the biosorbent is physisorption. The binding forces are weak compared with the chemisorption, which again confirms that the van der Waals forces is dominant in water sorption. The dipole-dipole attraction, one kind of van der Waals forces, may suggest the mechanism of water and butanol molecules sorption on the biosorbent since water molecules have a high polarity, and there are many polar groups such as hydroxyl and carboxyl on the biosorbent. Butanol molecules have lower polarity compared to water, and the polar groups prefer to adsorb water molecules other than alcohols with lower polarity (Sun et al., 2007). This may explain the affinity of water to the biosorbent is higher than that of butanol.

The results in Chapter 7 indicate that in the single component sorption system, compared to butanol, water has a higher mass transfer rate and lower mass transfer resistance at the same conditions. The results of the dynamics study in the binary system demonstrated in Chapter 8 also indicate the uptake of water was higher and faster than that of butanol during the dehydration of butanol. It maybe because water has larger mean free path than butanol. Water molecules will travel easier and faster during the diffusion step. The uptake of water was higher and faster than that of butanol. Thus, the oat hull based biosorbent is able to enrich the low-grade butanol-water mixture.

In summary, the dipole-dipole attraction may be the dominant mechanism of water and butanol molecules sorption on the biosorbent. This mechanism suggests the higher water affinity to the biosorbent than butanol. Further, the kinetically driven competitive sorption between water and butanol explained the basis of the separation of the butanol-water mixture by the oat hull biosorbent.

8.7 Chapter summary

In this chapter, the dynamics of water sorption on the oat hull based biosorbent were analyzed in aid of mathematical modeling. The Klinkenberg model based on the mass transfer limitation reasonably described the experimental water breakthrough curves obtained under the tested conditions. The Bohart-Adams model assuming surface adsorption being the controlling step did not provide satisfactory simulation particularly for the initial part of the breakthrough curves. This is consistent with the fact that the oat hull based biosorbent is a porous material, and water sorption is physical. Thus, the overall water sorption is limited by mass transfer resistance. This implies that the water sorption mechanism and dynamics are more likely to follow the Klinkenberg model's theory.

In addition, based on the Klinkenberg modeling results, the overall, external, and internal mass transfer resistances of water sorption on the oat hull based biosorbent were estimated. The results indicated that the water sorption rate on the biosorbent was controlled by mass transfer resistance. From the comparison of the mass transfer at different temperatures, it was concluded that the water sorption mass transfer rate increased with the increase in temperature. It is also noted that though the Klinkenberg model provided the satisfactory simulation of water breakthrough curves when butanol content in the feed is in the range of 56-80 wt.%, for extended applications of the model, it is necessary to consider the effects of butanol presence in the water sorption isotherm. This needs to be done in a future investigation.

The kinetically driven competitive sorption between water and butanol explained the basis of the separation of the butanol-water mixture by the oat hull biosorbent. Water is more competitive than butanol during dynamic sorption on the oat hull biosorbent; thus, this biosorbent is able to dehydrate butanol solutions.

CHAPTER 9. REUSABILITY STUDY OF THE OAT HULL BIOSORBENT

Contribution of this chapter to overall Ph.D. work

This chapter demonstrates the reusability study of the oat hull based biosorbent. Furthermore, the preliminary economic analysis is provided for butanol dehydration by sorption using the biosorbent.

9.1 Reusability of the biosorbent in the binary system

In order to investigate the reusability of the oat hull based biosorbent for butanol dehydration, the biosorbent was regenerated and reused in the same column without being changed. After sorption, nitrogen gas was purged to the column from the bottom under the pressure of 33 kPa at 105 °C to flash out all the adsorbates for 240 min. Then, the regenerated bed was reused for adsorbing water from the butanol-water mixture. The profile of butanol concentration in the effluent for the fresh bed and the regenerated bed (after 20 sorption-desorption cycles) at the same conditions are presented in Figure 9.1. The butanol concentration of the effluent shows that the oat hull biosorbent is able to concentrate 56 wt.% butanol solution to high purity product 99 wt.% butanol. The two curves are overlapped. It was demonstrated that the biosorbent derived from oat hull used in this study has been regenerated and reused successfully for more than 20 cycles with satisfactory performance, and it can be continually used.

A qualitatively FTIR analysis of the biosorbent was also done. The FTIR spectra of the biosorbent before and after 20 sorption-desorption cycles were nearly the same, as shown in Figure 9.2. No significant changes in the functional groups of the biosorbent were observed after the 20 sorption-desorption cycles. The biosorbent can be continuously used, indicating that the biosorbent has high stability and is reusable during the sorption process.

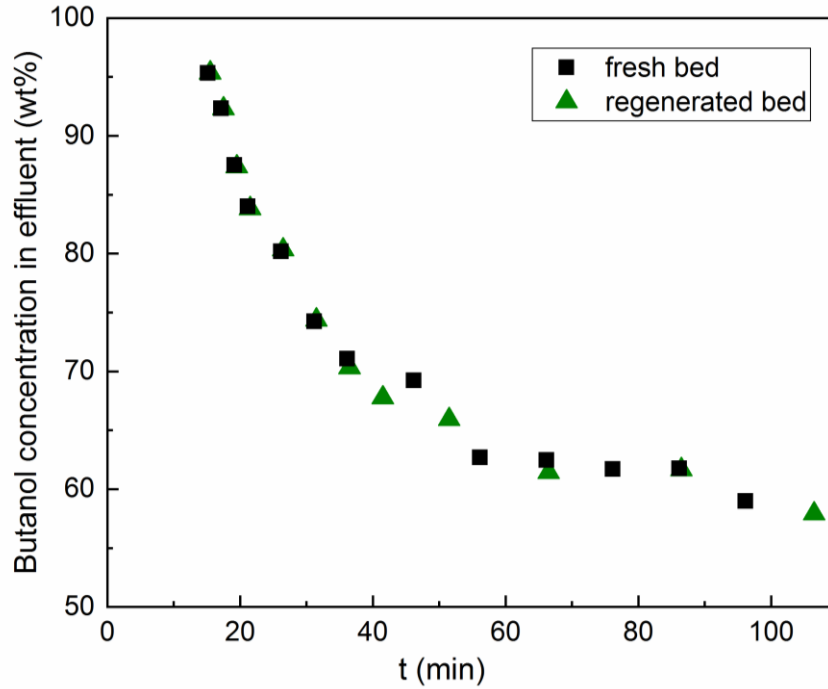


Figure 9.1 The profile of butanol concentration in effluent on the fresh and regenerated bed at 110 °C, 135 kPa, and 56 wt% butanol feed concentration.

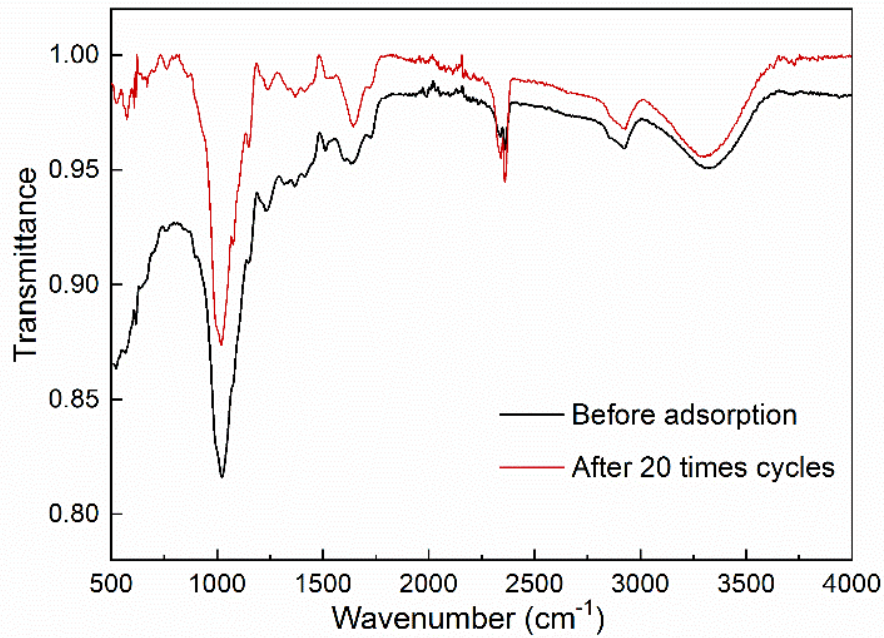


Figure 9.2 FTIR spectra of the fresh oat hull biosorbent and FTIR spectra of reused and regenerated oat hull biosorbent.

9.2 Reusability of the biosorbent in pure water or pure butanol system

For sorption experiments in pure water or pure butanol system, the saturated oat hull based biosorbent was also regenerated and reused in the packed column.

The water sorption breakthrough curves of the fresh biosorbent and reused biosorbent (after 20 sorption-desorption cycles) at the same conditions are presented in Figure 9.3a. It can be seen from the overlapped breakthrough curves that the regenerated biosorbent has a similar water sorption performance as the fresh one.

Figure 9.3b further shows the butanol sorption breakthrough curves of fresh biosorbent and reused biosorbent (after 20 cycles). The butanol sorption breakthrough curves of fresh biosorbent and reused biosorbent are also overlapped. The results demonstrate that the oat hull based biosorbent has been used for over 20 cycles for water or butanol sorption without deteriorated quality. The oat hull based biosorbent is a stable and reusable material in the application for sorption.

It was concluded that the biosorbent used in this work were regenerated and reused successfully for more than 20 sorption-regeneration cycles with satisfactory sorption performance for both butanol dehydration and pure water or butanol systems. It can be continually used.

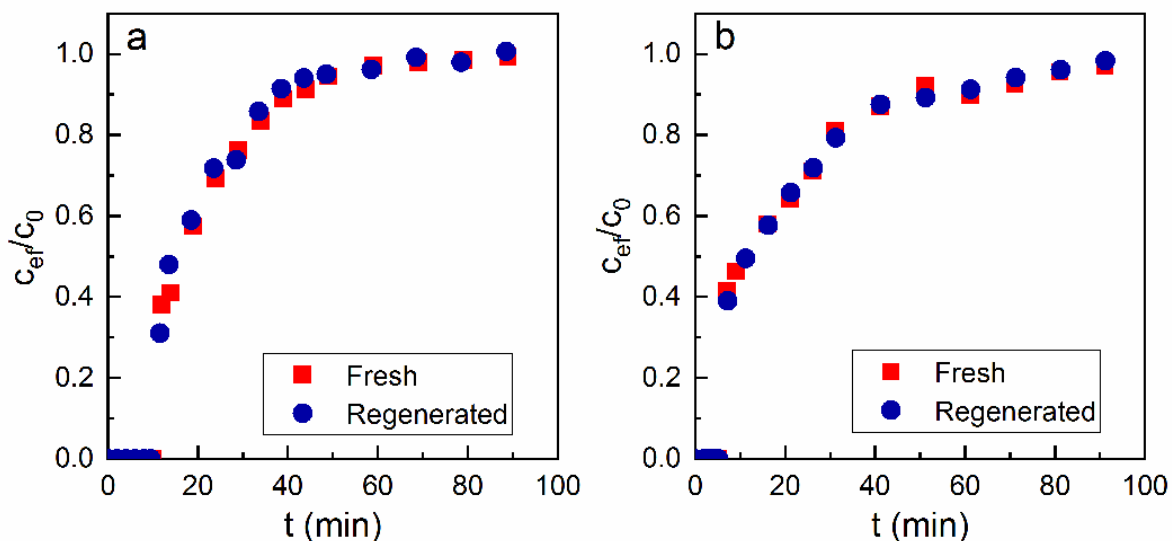


Figure 9.3 Breakthrough curves of the fresh and regenerated bed at 120 °C, 135 kPa: (a) water sorption; (b) butanol sorption.

9.3 Economic analysis of butanol dehydration

9.3.1 Butanol dehydration in a pressure swing adsorption process

Pressure swing adsorption (PSA) is used for gas separation and purification due to its low-cost operation, high product recovery rates, and operational simplicity. The pressure swing adsorption process using biosorbent is a promising method for drying biobutanol in the industry, as the biosorbent is more available and environmentally friendly.

Aspen Adsorption simulator can be used for optimal design, simulation, and analysis of gas sorption processes. It was used to simulate the butanol dehydration (drying) in a continuous PSA two-column system using the oat hull based biosorbent. In a two-column cycle, while one column is in the adsorption step, the other column performs the regeneration step. In general, it takes around 6 minutes to switch.

The simulation in the Aspen Adsorption simulator aims to build the sorption process and to optimize the process. It enables early testing of key model parameters and assumptions. The

simulation is based on the assumptions that each column is identical (same biosorbent layers and model assumptions), and the biosorbent is sent to the column which is re-used later in the cycle. The simulation is designed to produce 9800 tons butanol (99.5 wt.%) product per year. The working days are 300 days per year. The production scale is chosen by reference to the simulation of fuel ethanol production using the PSA process (Simo et al., 2008).

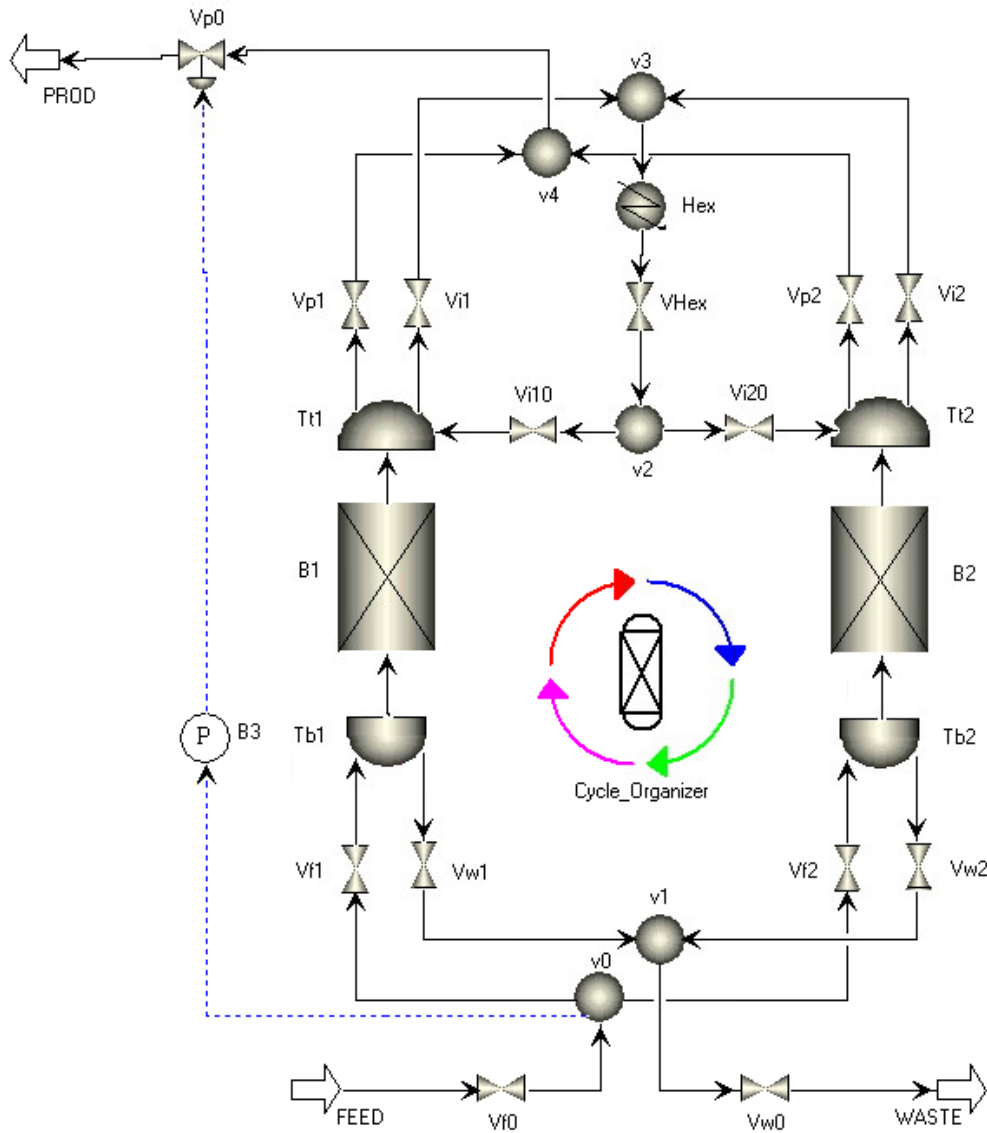


Figure 9.4 Simulation in Aspen Adsorption.

According to the experimental conditions tested in the lab-scale in this work, the selective water sorption (butanol dehydration) was carried out at 110 °C and 135 kPa. The regeneration (desorption) was carried out in the same column after sorption. Part of the product was used to flash out the adsorbates. The depressurization was carried out at 105 °C and 20 kPa. The whole pressure swing adsorption process has been separated into 6 steps (Li et al., 2016; Wu et al., 2015).

The cycle information is listed below:

Step 1: 60 sec, feed / production (column 1) + depressurization (column 2)

Step 2: 360 sec, feed / production / purge out (column 1) + purge in (column 2)

Step 3: 30 sec, feed / production / repress out (column 1) + repress in (column 2)

Step 4: 60 sec, depressurization (column 1) + feed / production (column 2)

Step 5: 360 sec, purge in (column 1) + feed / production / purge out (column 2)

Step 6: 30 sec, repress in (column 1) + feed / production / repress out (column 2)

After running the simulation, the stream information was applied in Aspen HYSYS to simulate the dehydration process and calculate the cost.

9.3.2 Total capital cost and manufacturing cost estimation

The streams information was input to Aspen HYSYS for equipment sizing and economic evaluations. Economic evaluations were carried out using Economic module in Aspen HYSYS. This module rapidly estimates the capital and operating costs. Before the estimation, it was assumed the cost index based on the updated CHE cost index. All cost calculations were based on the chemical engineering plant cost index (CEPCI) of 628.2 (for 2017). The capital cost calculation is based on this value. The estimation does not take into consideration of war, natural disasters and other force majeure accident.

Major instruments include compressor, sorption column, condenser, and pump. The purchase cost can be estimated by equipment parameters and specifications. The default material of construction for all equipment is carbon steel. The cost of equipment and the installation was used to calculate the fixed capital investment. Fixed capital investment was calculated using the Aspen and CEPCI index that includes components such as purchased equipment, the setting of equipment, piping, civil, instrumentation, electrical fittings, insulation, administrative overheads, contingencies, and escalations. The working capital is 15% of the fixed capital investment, and the total capital investment is the sum of fixed capital investment and working capital. The total capital investment is about \$2.05 million, and this value covered the investment before the plant can operate successfully and produce the desired product.

The expense during the operating period includes manufacturing expenses and general expenses. The direct manufacturing expenses include raw materials fees, utility fees, and labor fees. The indirect manufacturing expenses include packing & storage cost, all insurance, and local taxes. The manufacturing cost has been calculated according to the simulation results and the assumption above. Table 9.1 shows the details of the operating cost and utility cost estimated by the Economic module in Aspen HYSYS. The sizing and the expense evaluation are estimated using default methods and the missing data is estimated by Aspen HYSYS system. The location, vessel design code, soil conditions, and level of instrumentation will affect the capital and operating cost. These specifications can be further defined by Aspen Process Economic Analyze or by Aspen Capital Cost Estimator. The Economic module in Aspen HYSYS provides simple and initial cost estimation in the early phase of process design.

The economic evaluation was also carried out for the butanol dehydration process by PSA using 3A zeolite molecular sieves, which is one of the most popularly used adsorbents in the

industry for dehydration of gases or ethanol. 3A zeolite molecular sieves, which consisting of SiO_2 , AlO_2 groups and alkali-ions, has the pore size of 0.30 nm. 3A zeolite is capable of adsorbing water molecules (approximate molecular diameter of 0.28 nm) in the cavities of complex crystal structure. The economic analysis results of PSA using molecular sieves adsorbent was compared with that of using oat hull based biosorbent and shown in Table 9.1. Pressure swing adsorption using oat hull based biosorbent has a lower capital cost, operating cost, and utilities cost compared with the process using molecular sieves as adsorbent. The utilities cost using oat hull based biosorbent is 29% lower than using the traditional adsorbent molecular sieves. This result indicates that the production of anhydrous biobutanol by pressure swing adsorption process using the biosorbent is more economically feasible than using molecular sieves as adsorbent. However, this analysis is basic, and comprehensive analysis is necessary in order to provide more effective information in applying this technology in the real butanol industry.

Table 9.1 Summary of economic analysis for butanol dehydration by PSA using different adsorbents.

Oat hulls as biosorbent (56 wt.% butanol feed)	
Investment	Cost
Total capital investment (USD)	2,052,090
Total operating cost (USD/Year)	1,070,300
Total utilities cost (USD/Year)	63,438
Total equipment cost (USD)	263,700
Total installed cost (USD)	386,600
Molecular sieves as biosorbent (56 wt.% butanol feed)	
Investment	Cost
Total capital investment (USD)	2,147,300
Total operating cost (USD/Year)	1,132,150
Total utilities cost (USD/Year)	89,125
Total equipment cost (USD)	263,700
Total installed cost (USD)	386,600

9.4 Chapter summary

It was concluded that the biosorbent derived from oat hull used in this work was viably regenerated and reused for butanol dehydration with satisfactory performance and stability. The reusability of the biosorbent in the water sorption system reveals the oat hull material was stable, and it had been used for over 20 sorption-desorption cycles without deteriorated quality for water sorption. Oat hull is a stable and reusable material in the application for butanol dehydration. No significant changes in the functional groups of the biosorbent were observed after the 20 sorption-

desorption cycles. Furthermore, the preliminary economic analysis shows the production of anhydrous biobutanol by pressure swing adsorption process using the oat hull based biosorbent is more economical than using the traditional adsorbent molecular sieves.

CHAPTER 10. CONCLUSIONS, ORIGINAL CONTRIBUTIONS AND RECOMMENDATIONS

10.1 Overall conclusions and original contributions to knowledge development

1. A biosorbent was successfully developed from oat hulls. The biosorbent was successfully applied to dehydrate the butanol-water azeotrope and achieve high purity butanol. The sorption process developed in this work can be used as an alternative to replace the decantation and distillation cycles in the industry to break the butanol-water azeotrope and purify the butanol. It can also be transferrable to dehydrate other bioalcohols or organic vapors. The sorption equilibrium and kinetics were successfully analyzed by the Dubinin-Polanyi model and the linear driving force model.

2. The biosorbent has a porous structure mainly with mesopores. Polar groups such as hydroxyl, carboxyl, and so on exist on the biosorbent. The biosorbent demonstrated thermal stability at temperatures up to 220 °C, which is higher than the experimental temperature (110-120 °C). This biosorbent was largely consistent with the composition of oat hull used in other studies. The biosorbent before and after sorption and desorption confirm that the structure of oat hulls based biosorbent was relatively stable during sorption and desorption. Water molecules are able to diffuse into the inner structure of the biosorbent, and water molecules may reach the sorption sites of the cellulose, hemicellulose, and lignin in the biosorbent. The different batches of oat hulls tested in this work performed similarly on butanol dehydration.

This work provides information on the basic characteristics of the oat hull based lignocellulosic biosorbent. These characteristics are important to understand the sorption science.

3. The affinity of water for oat hull based biosorbent is stronger than that of butanol. In the butanol-water binary system at 110 °C, the highest concentration of effluent obtained from the feed of various butanol content (56.6–90.3 wt.%) are 95.3–99.0 wt.%, which indicates that the oat hull based biosorbent is able to dehydrate the water/butanol binary azeotrope and butanol solution with high concentration. The results indicate that the oat hull based biosorbent was able to effectively remove water from butanol.

The temperature and feed concentration at the tested range have significant effects on the dehydration performance. The higher temperature leads to a higher rate of mass transfer but lower sorption capacity. When the temperature was increased from 110 to 120 °C, the water sorption capacity decreased from 138 to 61 mg/g. The higher butanol concentration in the feed led to the lower separation factor and water sorption capacity. When the butanol concentration in the feed increased from 56.6 to 69.1 wt.%, the water sorption capacity decreased from 138 to 89 mg/g.

Data such as water sorption capacity and water sorption selectivity over butanol was determined and reported. Competitive sorption between water and butanol, and the influences of different conditions on butanol dehydration were analyzed. These results are important for future work on the development of butanol dehydration.

4. The large pore Dubinin-Polanyi model successfully simulated the water sorption equilibrium data in both the pure water sorption system and the butanol-water binary system. This indicates that water sorption is based on large pores, which is consistent with the result of pore size distribution that the oat hulls material mainly contains large pores (mesopores and macropores). The competitive sorption occurred between butanol and water for sorption sites on the biosorbent, which is supported by the value of q_0 (limiting mass for sorption) of pure water sorption is higher than that of butanol-water system.

The Dubinin-Polanyi model effectively described butanol sorption equilibrium data in the pure butanol sorption system and the butanol-water binary system. The estimated values of q_0 for butanol sorption are lower than those for water sorption in the butanol-water binary system, which implies that the biosorbent has higher water sorption affinity. The thermodynamic study provided evidence of the spontaneity and exothermic nature of the sorption process.

The information of water and/or butanol sorption affinity, model suitability and mechanisms were provided by the equilibrium isotherm investigation. These results provide fundamental information for sorbents performance and mechanisms in this field.

5. The site energy of water sorption was calculated. 98% of water sorption took place on the sites having energy lower than 10,000 J/mol. The weighted mean site energy for water sorption (2378 J/mol) in the butanol-water binary system is higher than that of butanol (2105 J/mol). In the butanol-water binary system, water sorption is more competitive than butanol. The site energy distribution analysis provides the evidence that water and butanol sorption on the biosorbent is physisorption, and the binding force is weak compared to the chemisorption, which suggests the van der Waals forces may be dominant in sorption. The dipole-dipole attraction, one kind of van der Waals forces, may be one of the major mechanisms of water and butanol sorption on the biosorbent. This result suggests water exhibits higher affinity to the biosorbent than butanol.

The approximate sorption site energy distribution provides a method to study the sorption mechanisms and energy characteristics of sorbent surfaces for heterogeneous materials.

6. The Klinkenberg model reasonably simulated the water and butanol breakthrough curves in pure water or pure butanol component sorption system at different conditions. The sorption rate was controlled by mass transfer resistances.

The dynamics study of pure butanol and pure water on the oat hull based biosorbent provided information on mass transfer resistance of water and butanol sorption on the biosorbent and the modeling results which can be applied to the similar systems.

7. The Klinkenberg model based on the mass transfer limitation reasonably described the water breakthrough curves of the butanol-water vapor sorption system, while the Bohart-Adams model assuming surface adsorption being the controlling step did not provide a satisfactory simulation. This is consistent with the fact that the oat hull based biosorbent is a porous material, and water sorption is physical. Thus, the overall water sorption is limited by mass transfer resistance. In addition, the modeling results indicated that the water sorption rate on the biosorbent was controlled by mass transfer resistance. Compared to butanol, water has more favorable sorption performance on the oat hull biosorbent; thus, this biosorbent is able to dehydrate butanol solutions.

The mass transfer resistance and the rate-limited step of water sorption from butanol-water vapor were provided based on the fitting results in this work. The kinetically driven competitive sorption of butanol and water was proposed to explain the basis of the separation of the butanol-water mixture by the oat hull biosorbent.

8. The biosorbent derived from oat hull used in this work was viably regenerated and reused for butanol dehydration for over 20 sorption-desorption cycles with satisfactory performance and high stability. The oat hull is a stable and reusable material in the application for water sorption. Furthermore, the economic analysis shows the production of anhydrous biobutanol by pressure swing adsorption process using biosorbent is economically feasible.

The reusability study of the oat hull based biosorbent and the preliminary economic analysis provided information on the feasibility of the application of this biosorbent in butanol and similar alcohols dehydration.

10.2 Recommendations for future work

Butanol recovery and drying are less developed than the development of ethanol purification. Based on the results in this thesis, lignocellulosic-based biosorbents could be a good choice for butanol dehydration. Thus, it is necessary to study the sorption characteristics of more potential lignocellulosic-based sorbents and develop more appropriate sorbents for butanol drying.

The oat hull based biosorbent could be used for dehydration of other bio-alcohols, and the capability needs to be studied in future work. Developing pellets of biosorbent with controlled shape and size could be considered in future investigations.

Coomassie blue staining and optical microscopy assist to visualize water diffusion into the inner structure of the oat hull based biosorbent. The detailed investigation in this could provide an area of future research.

The multicomponent sorption isotherm should be further investigated for butanol dehydration. The mechanisms such as the interaction of water and butanol during this process may be explained in more detail by multicomponent sorption isotherm.

The Klinkenberg model provided a satisfactory simulation of breakthrough curves when butanol content in the feed is in the range of 56-80 wt.%. To apply this model for an extended range of butanol concentration, it is necessary to consider the effect of butanol in a water sorption isotherm. However, this will bring challenges to determine an analytical solution for the model. This can form an area of future research.

In this work, the Klinkenberg model gives a satisfactory fit of the data at different conditions. However, some breakthrough curves simulated by the Klinkenberg model seem to show overprediction of sorption. It may be because the Klinkenberg model assumes a linear sorption isotherm, which may diverge with some data points of real isotherms. In addition, the overprediction could be due to the fact that the temperature of the column has a little fluctuation because of sorption heat generated in the column. Consideration could be made to decrease the divergence between model and experimental data such as considering a combined wave front model.

The optimization of conditions and more detailed economic analysis for butanol dehydration using biosorbents is worth pursuing further, since this information is very much needed when this process is applied in the industry.

REFERENCES

- Agnihotri, V. G., & Giles, C. H. (1972). The cellulose–dye adsorption process. A study by the monolayer method. *Journal of the Chemical Society, Perkin Transactions 2*, 15, 2241–2246.
- Agu, O. S., Tabil, L. G., & Dumonceaux, T. (2017). Microwave-Assisted Alkali Pre-Treatment, Densification and Enzymatic Saccharification of Canola Straw and Oat Hull. *Bioengineering (Basel, Switzerland)*, 4(2), 25.
- Aguilera, P. G., & Gutiérrez Ortiz, F. J. (2016). Prediction of fixed-bed breakthrough curves for H₂S adsorption from biogas: Importance of axial dispersion for design. *Chemical Engineering Journal*, 289, 93–98.
- Al-Asheh, S., Banat, F., & Al-Lagtah, N. (2004). Separation of Ethanol–Water Mixtures Using Molecular Sieves and Biobased Adsorbents. *Chemical Engineering Research and Design*, 82(7), 855–864.
- Aladko, E. Y., Dyadin, Y. A., Fenelonov, V. B., Larionov, E. G., Mel'gunov, M. S., Manakov, A. Y., Nesterov, A. N., & Zhurko, F. V. (2004). Dissociation Conditions of Methane Hydrate in Mesoporous Silica Gels in Wide Ranges of Pressure and Water Content. *The Journal of Physical Chemistry B*, 108(42), 16540–16547.
- Alcañiz-Monge, J., Pérez-Cadenas, M., & Lozano-Castelló, D. (2009). Influence of pore size distribution on water adsorption on silica gels. *Journal of Porous Materials*, 17(4), 409–416.
- Anderson, L. E., Gulati, M., Westgate, P. J., Kvam, E. P., Bowman, K., & Ladisch, M. R. (1996). Synthesis and optimization of a new starch-based adsorbent for dehumidification of air in a pressure-swing dryer. *Industrial & Engineering Chemistry Research*, 35(4), 1180–1187.

- Angelopoulos, P. M., Balomenos, E., & Taxiarchou, M. (2016). Thin-Layer Modeling and Determination of Effective Moisture Diffusivity and Activation Energy for Drying of Red Mud from Filter Presses. *Journal of Sustainable Metallurgy*, 2(4), 344–352.
- Annadurai, G., Juang, R. S., & Lee, D. J. (2002). Use of cellulose-based wastes for adsorption of dyes from aqueous solutions. *Journal of Hazardous Materials*, 92(3), 263–274.
- Avilés Martínez, A., Saucedo-Luna, J., Segovia-Hernandez, J. G., Hernandez, S., Gomez-Castro, F. I., & Castro-Montoya, A. J. (2012). Dehydration of Bioethanol by Hybrid Process Liquid–Liquid Extraction/Extractive Distillation. *Industrial & Engineering Chemistry Research*, 51(17), 5847–5855.
- Banerjee, S., Sharma, G. C., Gautam, R. K., Chattopadhyaya, M. C., Upadhyay, S. N., & Sharma, Y. C. (2016). Removal of Malachite Green, a hazardous dye from aqueous solutions using *Avena sativa* (oat) hull as a potential adsorbent. *Journal of Molecular Liquids*, 213, 162–172.
- Bankar, S. B., Survase, S. A., Ojamo, H., & Granström, T. (2013). Biobutanol: the outlook of an academic and industrialist. *RSC Advances*, 3(47), 24734–24757.
- Barrer, R. M., & Davies, J. A. (1970). Sorption in Decationated Zeolites. I. Gases in Hydrogen-Chabazite. *Proceedings of the Royal Society of London. Series A, Mathematical and Physical Sciences*, 320(1542), 289–308.
- Beery, K. E., Gulati, M., Kvam, E. P., & Ladisch, M. R. (1998). Effect of enzyme modification of corn grits on their properties as an adsorbent in a skarstrom pressure swing cycle dryer. *Adsorption*, 4(3–4), 321–335.

- Beery, K. E., & Ladisch, M. R. (2001a). Adsorption of water from liquid-phase ethanol-water mixtures at room temperature using starch-based adsorbents. *Industrial & Engineering Chemistry Research*, 40(9), 2112–2115.
- Beery, K. E., & Ladisch, M. R. (2001b). Chemistry and properties of starch based desiccants. *Enzyme and Microbial Technology*, 28(7), 573–581.
- Benson, T. J., & George, C. E. (2005). Cellulose based adsorbent materials for the dehydration of ethanol using thermal swing adsorption. *Adsorption*, 11(11), 697–701.
- Bharathiraja, B., Jayamuthunagai, J., Sudharsanaa, T., Bharghavi, A., Praveenkumar, R., Chakravarthy, M., & Yuvaraj, D. (2017). Biobutanol – An impending biofuel for future: A review on upstream and downstream processing techniques. *Renewable and Sustainable Energy Reviews*, 68, 788–807.
- Bohart, G. S., & Adams, E. Q. (1920). Some aspects of the behavior of charcoal with respect to chlorine.1. *Journal of the American Chemical Society*, 42(3), 523–544.
- Bolto, B., Hoang, M., & Xie, Z. (2011). A review of membrane selection for the dehydration of aqueous ethanol by pervaporation. *Chemical Engineering and Processing: Process Intensification*, 50(3), 227–235.
- Boonfung, C., & Rattanaphanee, P. (2010). Pressure swing adsorption with cassava adsorbent for dehydration of ethanol vapor. *World Academy of Science, Engineering and Technology*, 4, 716–719.
- Cai, D., Chen, H., Chen, C., Hu, S., Wang, Y., Chang, Z., Miao, Q., Qin, P., Wang, Z., Wang, J., & Tan, T. (2016). Gas stripping–pervaporation hybrid process for energy-saving product recovery from acetone–butanol–ethanol (ABE) fermentation broth. *Chemical Engineering Journal*, 287, 1–10.

- Carmo, M. J., Adeodato, M. G., Moreira, A. M., Parente, E. J. S., & Vieira, R. S. (2004). Kinetic and thermodynamic study on the liquid phase adsorption by starchy materials in the alcohol-water System. *Adsorption*, *10*(3), 211–218.
- Carmo, M. J., & Gubulin, J. C. (1997). Ethanol-water adsorption on commercial 3A zeolites: kinetic and thermodynamic data. *Brazilian Journal of Chemical Engineering*, *14*, 217–244.
- Carter, M. C., Kilduff, J. E., & Weber, W. J. (1995). Site energy distribution analysis of preloaded adsorbents. *Environmental Science & Technology*, *29*(7), 1773–1780.
- Cerofolini, G. F. (1974). Localized adsorption on heterogeneous surfaces. *Thin Solid Films*, *23*(2), 129–152.
- Chahbani, M. H., & Tondeur, D. (2000). Mass transfer kinetics in pressure swing adsorption. *Separation and Purification Technology*, *20*(2), 185–196.
- Chang, H., Yuan, X. G., Tian, H., & Zeng, A. W. (2006a). Experimental investigation and modeling of adsorption of water and ethanol on cornmeal in an ethanol-water binary vapor system. *Chemical Engineering Technology*, *29*(4), 454–461.
- Chang, H., Yuan, X. G., Tian, H., & Zeng, A. W. (2006b). Experiment and prediction of breakthrough curves for packed bed adsorption of water vapor on cornmeal. *Chemical Engineering and Processing: Process Intensification*, *45*(9), 747–754.
- Chang, R. (2000). *Physical chemistry for the chemical and biological sciences*. University Science Books.
- Chopade, V. J., Khandetod, Y. P., & Mohod, A. G. (2015). Dehydration of Ethanol-Water Mixture Using 3a Zeolite Adsorbent. *International Journal of Emerging Technology and Advanced Engineering*, *5*(11), 152–155.

- Chu, K. H. (2010). Fixed bed sorption: Setting the record straight on the Bohart–Adams and Thomas models. *Journal of Hazardous Materials*, 177(1–3), 1006–1012.
- Chu, K. H., Feng, X., Kim, E. Y., & Hung, Y.-T. (2011). Biosorption Parameter Estimation with Genetic Algorithm. *Water*, 3(1), 177–195.
- Claessens, B., Martin-Calvo, A., Gutiérrez-Sevillano, J. J., Dubois, N., Denayer, J. F. M., & Cousin-Saint-Remi, J. (2019). Macroscopic and Microscopic View of Competitive and Cooperative Adsorption of Alcohol Mixtures on ZIF-8. *Langmuir*, 35(11), 3887–3896.
- Crawshaw, J. R., & Hills, J. H. (1990). Sorption of ethanol and water by starch materials. *Industrial & Engineering Chemistry Research*, 29(2), 307–309.
- Dąbrowski, A. (2001). Adsorption — from theory to practice. *Advances in Colloid and Interface Science*, 93(1), 135–224.
- Dang, V. B. H., Doan, H. D., Dang-Vu, T., & Lohi, A. (2009). Equilibrium and kinetics of biosorption of cadmium(II) and copper(II) ions by wheat straw. *Bioresource Technology*, 100(1), 211–219.
- Davison, B. H., & Thompson, J. E. (1993). Continuous direct solvent extraction of butanol in a fermenting fluidized-bed bioreactor with immobilized *Clostridium acetobutylicum*. *Applied Biochemistry and Biotechnology*, 39–40(1), 415–426.
- Errico, M., Rong, B.-G., Tola, G., & Spano, M. (2013). Optimal Synthesis of Distillation Systems for Bioethanol Separation. Part 1: Extractive Distillation with Simple Columns. *Industrial & Engineering Chemistry Research*, 52(4), 1612–1619.
- Fahmi, A., Banat, F. A., & Jumah, R. (1999). Vapor-liquid equilibrium of ethanol-water system in the presence of molecular sieves. *Separation Science and Technology*, 34(12), 2355–2368.

- Faisal, A., Zhou, M., Hedlund, J., & Grahn, M. (2018). Zeolite MFI adsorbent for recovery of butanol from ABE fermentation broths produced from an inexpensive black liquor-derived hydrolyzate. *Biomass Conversion and Biorefinery*, 8(3), 679–687.
- Faizal, A. M., Kutty, S. R. M., & Ezechi, E. H. (2014). Modelling of Adams-Bohart and Yoon-Nelson on the Removal of Oil from Water Using Microwave Incinerated Rice Husk Ash (MIRHA). *Applied Mechanics and Materials*, 625, 788–791.
- Farhadpour, F. A., & Bono, A. (1996). Sorptive separation of ethanol-water mixtures with a bi-dispersed hydrophobic molecular sieve, silicalite: determination of the controlling mass transfer mechanism. *Chemical Engineering and Processing: Process Intensification*, 35(2), 141–155.
- Fomina, M., & Gadd, G. M. (2014). Biosorption: current perspectives on concept, definition and application. *Bioresource Technology*, 160, 3–14.
- Freundlich, H. (1909). *Kapillarchemie: eine Darstellung der Chemie der Kolloide und verwandter Gebiete*. Akademische Verlagsgesellschaft.
- Friedl, A. (2016). Downstream process options for the ABE fermentation. *FEMS Microbiology Letters*, 363(9), 1–5.
- Fulazzaky, M. A., Khamidun, M. H., & Omar, R. (2013). Understanding of mass transfer resistance for the adsorption of solute onto porous material from the modified mass transfer factor models. *Chemical Engineering Journal*, 228, 1023–1029.
- Gabruś, E., & Downarowicz, D. (2016). Anhydrous ethanol recovery from wet air in TSA systems – Equilibrium and column studies. *Chemical Engineering Journal*, 288, 321–331.
- Ghanbari, S., & Niu, C. H. (2018). Characterization of a High-Performance Biosorbent for Natural Gas Dehydration. *Energy & Fuels*, 32(11), 11979–11990.

- Ghanbari, S., & Niu, C. H. (2019). Characteristics of oat hull based biosorbent for natural gas dehydration in a PSA process. *Journal of Natural Gas Science and Engineering*, *61*, 320–332.
- Goerlitz, R., Weisleder, L., Wuttig, S., Trippel, S., Karstens, K., Goetz, P., & Niebelschuetz, H. (2018). Bio-butanol downstream processing: regeneration of adsorbents and selective exclusion of fermentation by-products. *Adsorption*, *24*(1), 95–104.
- Gorbach, A., Stegmaier, M., & Eigenberger, G. (2004). Measurement and Modeling of Water Vapor Adsorption on Zeolite 4A—Equilibria and Kinetics. *Adsorption*, *10*(1), 29–46.
- Grande, C. A. (2012). Advances in pressure swing adsorption for gas separation. *ISRN Chemical Engineering*, *2012*, 1–13.
- Groot, W. J., Soedjak, H. S., Donck, P. B., van der Lans, R. G. J. M., Luyben, K. C. A. M., & Timmer, J. M. K. (1990). Butanol recovery from fermentations by liquid-liquid extraction and membrane solvent extraction. *Bioprocess Engineering*, *5*(5), 203–216.
- Groot, W. J., van der Lans, R. G. J. M., & Luyben, K. C. A. M. (1989). Batch and continuous butanol fermentations with free cells: integration with product recovery by gas-stripping. *Applied Microbiology and Biotechnology*, *32*(3), 305–308.
- Gu, T., Tsai, G.-J., & Tsao, G. T. (1990). New approach to a general nonlinear multicomponent chromatography model. *AIChE Journal*, *36*(5), 784–788.
- Gutiérrez Ortiz, F. J., Aguilera, P. G., & Ollero, P. (2014). Modeling and simulation of the adsorption of biogas hydrogen sulfide on treated sewage-sludge. *Chemical Engineering Journal*, *253*, 305–315.

- Han, R., Wang, Y., Zhao, X., Wang, Y., Xie, F., Cheng, J., & Tang, M. (2009). Adsorption of methylene blue by phoenix tree leaf powder in a fixed-bed column: experiments and prediction of breakthrough curves. *Desalination*, 245(1–3), 284–297.
- Hu, X., & Xie, W. (2006). Fixed-Bed adsorption and fluidized-bed regeneration for breaking the azeotrope of ethanol and water. *Separation Science and Technology*, 36(1), 125–136.
- Huang, B., Liu, Q., Caro, J., & Huang, A. (2014). Iso-butanol dehydration by pervaporation using zeolite LTA membranes prepared on 3-aminopropyltriethoxysilane-modified alumina tubes. *Journal of Membrane Science*, 455, 200–206.
- Huang, H. J., Ramaswamy, S., & Liu, Y. (2014). Separation and purification of biobutanol during bioconversion of biomass. *Separation and Purification Technology*, 132, 513–540.
- Huang, Q., Niu, C. H., & Dalai, A. K. (2019). Production of anhydrous biobutanol using a biosorbent developed from oat hulls. *Chemical Engineering Journal*, 356, 830–838.
- Jain, S. K. J. S. K. (2016). *Conceptual Chemistry Volume-I For Class XII*. S. Chand.
- Jayaprakash, D. (2016). *Drying Butanol Using Biosorbents in a Pressure Swing Adsorption Process*. University of Saskatchewan, College of Graduate Studies Research.
- Jayaprakash, D., Dhabhai, R., Niu, C. H., & Dalai, A. K. (2017). Selective Water Removal by Sorption from Butanol-Water Vapor Mixtures: Analyses of Key Operating Parameters and Site Energy Distribution. *Energy and Fuels*, 31(5), 5193–5202.
- Jiao, P., Wu, J., Zhou, J., Yang, P., Zhuang, W., Chen, Y., Zhu, C., Guo, T., & Ying, H. (2015). Mathematical modeling of the competitive sorption dynamics of acetone–butanol–ethanol on KA-I resin in a fixed-bed column. *Adsorption*, 21(3), 165–176.
- Karpowicz, F., Hearn, J., & Wilkinson, M. C. (1995). The quantitative use of the Bohart-Adams equation to describe effluent vapour profiles from filter beds. *Carbon*, 33(11), 1573–1583.

- Kim, Y., Hendrickson, R., Mosier, N., Hilaly, A., & Ladisch, M. R. (2011). Cassava starch pearls as a desiccant for drying ethanol. *Industrial & Engineering Chemistry Research*, *50*(14), 8678–8685.
- Klinkenberg, A. (1954). Heat transfer in cross-flow heat exchangers and packed beds. *Industrial & Engineering Chemistry*, *46*(11), 2285–2289.
- Klinkenberg, Adriaan. (1948). Numerical Evaluation of Equations Describing Transient Heat and Mass Transfer in Packed Solids. *Industrial & Engineering Chemistry*, *40*(10), 1992–1994.
- Kourkoutas, Y., Bekatorou, A., Banat, I. M., Marchant, R., & Koutinas, A. A. (2004). Immobilization technologies and support materials suitable in alcohol beverages production: a review. *Food Microbiology*, *21*(4), 377–397.
- Kraemer, K., Harwardt, A., Bronneberg, R., & Marquardt, W. (2011). Separation of butanol from acetone–butanol–ethanol fermentation by a hybrid extraction–distillation process. *Computers & Chemical Engineering*, *35*(5), 949–963.
- Kumar, K. V., Gadipelli, S., Wood, B., Ramisetty, K. A., Stewart, A. A., Howard, C. A., Brett, D. J. L., & Rodriguez-Reinoso, F. (2019). Characterization of the adsorption site energies and heterogeneous surfaces of porous materials. *Journal of Materials Chemistry A*, *7*(17), 10104–10137.
- Kumar, K. V., Monteiro de Castro, M., Martinez-Escandell, M., Molina-Sabio, M., & Rodriguez-Reinoso, F. (2011). A site energy distribution function from Toth isotherm for adsorption of gases on heterogeneous surfaces. *Physical Chemistry Chemical Physics*, *13*(13), 5753–5759.

- Kushwaha, D., Srivastava, N., Mishra, I., Upadhyay, S. N., & Mishra, P. K. (2019). Recent trends in biobutanol production. *Reviews in Chemical Engineering*, 35(4), 475–504.
- Ladisch, M R. (1997). Biobased adsorbents for drying of gases. *Enzyme and Microbial Technology*, 20(3), 162–164.
- Ladisch, M R, & Dyck, K. (1979). Dehydration of ethanol- New approach gives positive energy balance. *Science*, 205(4409), 898–900.
- Ladisch, Michael R. (1991). Fermentation-derived butanol and scenarios for its uses in energy-related applications. *Enzyme and Microbial Technology*, 13(3), 280–283.
- Ladisch, Michael R, Voloch, M., Hong, J., Bienkowski, P., & Tsao, G. T. (1984). Cornmeal adsorber for dehydrating ethanol vapors. *Industrial & Engineering Chemistry Process Design and Development*, 23(3), 437–443.
- Lee, B.-G., & Rowell, R. M. (2004). Removal of Heavy Metal Ions from Aqueous Solutions Using Lignocellulosic Fibers. *Journal of Natural Fibers*, 1(1), 97–108.
- Lee, J. Y., Westgate, P. J., & Ladisch, M. R. (1991). Water and ethanol sorption phenomena on starch. *AIChE Journal*, 37(8), 1187–1195.
- LeVan, M. D., & Vermeulen, T. (1981). Binary Langmuir and Freundlich isotherms for ideal adsorbed solutions. *The Journal of Physical Chemistry*, 85(22), 3247–3250.
- Li, D., Zhou, Y., Shen, Y., Sun, W., Fu, Q., Yan, H., & Zhang, D. (2016). Experiment and simulation for separating CO₂/N₂ by dual-reflux pressure swing adsorption process. *Chemical Engineering Journal*, 297, 315–324.
- Li, Y., Shen, J., Guan, K., Liu, G., Zhou, H., & Jin, W. (2016). PEBA/ceramic hollow fiber composite membrane for high-efficiency recovery of bio-butanol via pervaporation. *Journal of Membrane Science*, 510, 338–347.

- Lin, X., Wu, J., Fan, J., Qian, W., Zhou, X., Qian, C., Jin, X., Wang, L., Bai, J., & Ying, H. (2012). Adsorption of butanol from aqueous solution onto a new type of macroporous adsorption resin: Studies of adsorption isotherms and kinetics simulation. *Journal of Chemical Technology and Biotechnology*, 87, 924–931.
- Liu, F., Liu, L., & Feng, X. (2005). Separation of acetone–butanol–ethanol (ABE) from dilute aqueous solutions by pervaporation. *Separation and Purification Technology*, 42(3), 273–282.
- Lodi, G., De Guido, G., & Pellegrini, L. A. (2018). Simulation and energy analysis of the ABE fermentation integrated with gas stripping. *Biomass and Bioenergy*, 116, 227–235.
- Lowell, S., & Shields, J. E. (1984). *Powder Surface Area and Porosity*. Springer, Dordrecht.
- Luyben, L. W. (2008). Control of the heterogeneous azeotropic n-butanol/water distillation system. *Energy & Fuels*, 22, 4249–4258.
- Malek, A., & Farooq, S. (1997). Kinetics of Hydrocarbon Adsorption on Activated Carbon and Silica Gel. *AIChE Journal*, 43(3), 761–776.
- Mariano, A. P., & Filho, R. M. (2012). Improvements in Biobutanol Fermentation and Their Impacts on Distillation Energy Consumption and Wastewater Generation. *BioEnergy Research*, 5(2), 504–514.
- Mariano, A. P., Keshtkar, M. J., Atala, D. I. P., Filho, F. M., Maciel, M. R. W., Filho, R. M., & Stuart, P. (2011). Energy Requirements for Butanol Recovery Using the Flash Fermentation Technology. *Energy & Fuels*, 25(5), 2347–2355.
- Menkiti, M. C., Aniagor, C. O., Agu, C. M., & Ugonabo, V. I. (2018). Effective Adsorption of Crystal Violet Dye from an Aqueous Solution Using Lignin-Rich Isolate from Elephant Grass. *Water Conservation Science and Engineering*, 3(1), 33–46.

- Missouri Dairy Resource App.* (n.d.). University of Missouri. Retrieved August 7, 2018, from <http://agebb.missouri.edu/dairy/byprod/index.htm>
- Mitchell, W. (1998). Physiology of Carbohydrate to Solvent Conversion by Clostridia. *Advances in Microbial Physiology*, 39, 31–130.
- Molecular Sieve Price.* (n.d.). Alibaba.Com. Retrieved April 25, 2019, from <https://www.alibaba.com/showroom/molecular-sieve-price.html>
- Mu, T. H., & Sun, H. N. (2019). *Chapter 22 - Sweet Potato Leaf Polyphenols: Preparation, Individual Phenolic Compound Composition and Antioxidant Activity* (pp. 365–380). Academic Press.
- Ouchi, T., Hamamoto, Y., Mori, H., Takata, S., & Etoh, A. (2014). Water vapor adsorption equilibrium and adsorption/desorption rate of porous alumina film adsorbent synthesized with anodization on heat transfer plate. *Applied Thermal Engineering*, 72(2), 219–228.
- Oudshoorn, A., van der Wielen, L. A. M., & Straathof, A. J. J. (2009a). Adsorption equilibria of bio-based butanol solutions using zeolite. *Biochemical Engineering Journal*, 48(1), 99–103.
- Oudshoorn, A., van der Wielen, L. A. M., & Straathof, A. J. J. (2009b). Assessment of Options for Selective 1-Butanol Recovery from Aqueous Solution. *Industrial & Engineering Chemistry Research*, 48, 7325.
- Outram, V., Lalander, C. A., Lee, J. G. M., Davies, E. T., & Harvey, A. P. (2017). Applied in situ product recovery in ABE fermentation. *Biotechnology Progress*, 33(3), 563–579.
- Pang, Z. W., Lu, W., Zhang, H., Liang, Z. W., Liang, J. J., Du, L. W., Duan, C. J., & Feng, J. X. (2016). Butanol production employing fed-batch fermentation by *Clostridium acetobutylicum* GX01 using alkali-pretreated sugarcane bagasse hydrolysed by enzymes from *Thermoascus aurantiacus* QS 7-2-4. *Bioresource Technology*, 212, 82–91.

- Paschoal, G. B., Muller, C. M. O., Carvalho, G. M., Tischer, C. A., & Mali, S. (2015). Isolation and characterization of nanofibrillated cellulose from oat hulls. *Química Nova*, 38, 478–482.
- Perry, R. H., & Green, D. W. (2008). *Perry's chemical engineers' handbook* (Eighth edi). New York, McGraw-Hill.
- Pruksathorn, P., & Vitidsant, T. (2009). Production of pure ethanol from azeotropic solution by pressure swing adsorption. *Korean Journal of Chemical Engineering*, 26(4), 1106–1111.
- Purnomo, C. W., & Prasetya, A. (2007). The Study of Adsorption Breakthrough Curves of Cr (VI) on Bagasse Fly Ash (BFA). *World Congress on Engineering and Computer Science 2007*, 2, 24–26.
- Pyrgakis, K. A., de Vrije, T., Budde, M. A. W., Kyriakou, K., López-Contreras, A. M., & Kokossis, A. C. (2016). A process integration approach for the production of biological isopropanol, butanol and ethanol using gas stripping and adsorption as recovery methods. *Biochemical Engineering Journal*, 116, 176–194.
- Quintero, J. A., & Cardona, C. A. (2009). Ethanol dehydration by adsorption with starchy and cellulosic materials. *Industrial and Engineering Chemistry Research*, 48(14), 6783–6788.
- Qureshi, N., & Blaschek, H. P. (2000). Butanol Production Using *Clostridium beijerinckii* BA101 Hyper-Butanol Producing Mutant Strain and Recovery by Pervaporation. *Applied Biochemistry and Biotechnology*, 84, 225–235.
- Qureshi, N., & Blaschek, H. P. (2001). Recovery of butanol from fermentation broth by gas stripping. *Renewable Energy*, 22(4), 557–564.

- Qureshi, N., Hughes, S., Maddox, I. S., & Cotta, M. A. (2005). Energy-efficient recovery of butanol from model solutions and fermentation broth by adsorption. *Bioprocess and Biosystems Engineering*, 27(4), 215–222.
- Qureshi, N., Saha, B. C., Dien, B., Hector, R. E., & Cotta, M. A. (2010). Production of butanol (a biofuel) from agricultural residues: Part I – Use of barley straw hydrolysate. *Biomass and Bioenergy*, 34(4), 559–565.
- Rakshit, S. K., Ghosh, P., & Bisaria, V. S. (1993). Ethanol separation by selective adsorption of water. *Bioprocess Engineering*, 8(5), 279–282.
- Ranjbar, Z., Tajallipour, M., Niu, H. C., & Dalai, A. (2013). Water removal from ethanol vapor by adsorption on canola meal after protein extraction. *Industrial & Engineering Chemistry Research*, 52(52), 14429–14440.
- Rathour, R. K., Ahuja, V., Bhatia, R. K., & Bhatt, A. K. (2018). Biobutanol: New era of biofuels. *International Journal of Energy Research*, 42(15), 4532–4545.
- Rebar, V., Fischbach, E. R., Apostolopoulos, D., & Kokini, J. L. (1984). Thermodynamics of water and ethanol adsorption on four starches as model biomass separation systems. *Biotechnology and Bioengineering*, 26(5), 513–517.
- Ruthven, D. M. (1984). *Principles of Adsorption and Adsorption Processes*. John Wiley & Sons.
- Ruthven, D. M., Farooq, S., & Knaebel, K. . (1993). *Pressure Swing Adsorption*. Wiley.
- Sapan, C. V, Lundblad, R. L., & Price, N. C. (1999). Colorimetric protein assay techniques. *Biotechnology and Applied Biochemistry*, 29(2), 99–108.
- Saravanan, V., Waijers, D. A., Ziari, M., & Noordermeer, M. A. (2010). Recovery of 1-butanol from aqueous solutions using zeolite ZSM-5 with a high Si/Al ratio; suitability of a column process for industrial applications. *Biochemical Engineering Journal*, 49(1), 33–39.

- Sarchami, T., Munch, G., Johnson, E., Kießlich, S., & Rehmman, L. (2016). A Review of Process-Design Challenges for Industrial Fermentation of Butanol from Crude Glycerol by Non-Biphasic *Clostridium pasteurianum*. *Fermentation*, 2(2), 13.
- Sarchami, T., & Rehmman, L. (2015). Optimizing Acid Hydrolysis of Jerusalem Artichoke-Derived Inulin for Fermentative Butanol Production. *BioEnergy Research*, 8(3), 1148–1157.
- Serna-Guerrero, R., & Sayari, A. (2010). Modeling adsorption of CO₂ on amine-functionalized mesoporous silica. 2: Kinetics and breakthrough curves. *Chemical Engineering Journal*, 161(1–2), 182–190.
- Setlhaku, M., Heitmann, S., Górak, A., & Wichmann, R. (2013). Investigation of gas stripping and pervaporation for improved feasibility of two-stage butanol production process. *Bioresource Technology*, 136, 102—108.
- Shah, Y. R., & Sen, D. J. (2011). Bioalcohol as green energy - A review. *International Journal of Current Science Research.*, 1(2), 57–62.
- Shen, X., Guo, X., Zhang, M., Tao, S., & Wang, X. (2015). Sorption mechanisms of organic compounds by carbonaceous materials: Site energy distribution consideration. *Environmental Science and Technology*, 49(8), 4894–4902.
- Simo, M., Sivashanmugam, S., Brown, C. J., & Hlavacek, V. (2009). Adsorption/Desorption of Water and Ethanol on 3A Zeolite in Near Adiabatic Fixed Bed. *Industrial & Engineering Chemistry Research*, 48(20), 9247–9260.
- Simo, M, Brown, C. J., & Hlavacek, V. (2006). Modeling of Industrial Psa Process for Fuel Ethanol. *AIChE Annual Meeting*.

- Simo, Marian, Brown, C. J., & Hlavacek, V. (2008). Simulation of pressure swing adsorption in fuel ethanol production process. *Computers & Chemical Engineering*, 32(7), 1635–1649.
- Sircar, S. (2002). Pressure swing adsorption. *Industrial & Engineering Chemistry Research*, 41, 1389–1392.
- Sircar, S., & Hufton, J. R. (2000). Why does the linear driving force model for adsorption kinetics work? *Adsorption*, 6(2), 137–147.
- Smitha, B., Suhanya, D., Sridhar, S., & Ramakrishna, M. (2004). Separation of organic–organic mixtures by pervaporation—a review. *Journal of Membrane Science*, 241(1), 1–21.
- Staggs, K. W., & Nielsen, D. R. (2015). Improving n-butanol production in batch and semi-continuous processes through integrated product recovery. *Process Biochemistry*, 50(10), 1487–1498.
- Sun, N., Okoye, C., Niu, C. H., & Wang, H. (2007). Adsorption of water and ethanol by biomaterials. *International Journal of Green Energy*, 4(6), 623–634.
- Sun, X. F., Gan, Z., Jing, Z., Wang, H., Wang, D., & Jin, Y. (2015). Adsorption of methylene blue on hemicellulose-based stimuli-responsive porous hydrogel. *Journal of Applied Polymer Science*, 132(10), 41606.
- Tajallipour, M., Niu, C., & Dalai, A. (2013). Ethanol Dehydration in a Pressure Swing Adsorption Process Using Canola Meal. *Energy & Fuels*, 27(11), 6655–6664.
- Tassist, A., Lounici, H., Abdi, N., & Mameri, N. (2010). Equilibrium, kinetic and thermodynamic studies on aluminum biosorption by a mycelial biomass (*Streptomyces rimosus*). *Journal of Hazardous Materials*, 183(1–3), 35–43.

- Thirmal, C., & Dahman, Y. (2012). Comparisons of existing pretreatment, saccharification, and fermentation processes for butanol production from agricultural residues. *The Canadian Journal of Chemical Engineering*, 90(3), 745–761.
- Thurgood, C. P., & Cells, F. (2007). Estimation of Parameters for the Bohart-Adams Model. *AIChE Annual Meeting*, 9.
- Vagenas, G. K., & Karathanos, V. T. (1991). Prediction of moisture diffusivity in granular materials, with special applications to foods. *Biotechnology Progress*, 7(5), 419–426.
- Van der Bruggen, B. (2015). Freundlich Isotherm. In *Encyclopedia of Membranes*. Springer Berlin Heidelberg.
- van der Merwe, A. B., Cheng, H., Görgens, J. F., & Knoetze, J. H. (2013). Comparison of energy efficiency and economics of process designs for biobutanol production from sugarcane molasses. *Fuel*, 105, 451–458.
- Van Hecke, W., Joossen-Meyvis, E., Beckers, H., & De Wever, H. (2018). Prospects & potential of biobutanol production integrated with organophilic pervaporation – A techno-economic assessment. *Applied Energy*, 228, 437–449.
- Vane, L. M. (2008). Separation technologies for the recovery and dehydration of alcohols from fermentation broths. *Biofuels, Bioproducts and Biorefining*, 2(6), 553–588.
- Wakao, N., & Funazkri, T. (1978). Effect of fluid dispersion coefficients on particle-to-fluid mass transfer coefficients in packed beds: Correlation of sherwood numbers. *Chemical Engineering Science*, 33(10), 1375–1384.
- Worch, E. (2012). *Adsorption Technology in Water Treatment: Fundamentals, Processes, and Modeling*. De Gruyter.

- World oats production holds steady*. (2018). Grain Central.
<https://www.graincentral.com/markets/export/world-oats-production-holds-steady/>
- Wu, B., Zhang, X., Xu, Y., Bao, D., & Zhang, S. (2015). Assessment of the energy consumption of the biogas upgrading process with pressure swing adsorption using novel adsorbents. *Journal of Cleaner Production*, *101*, 251–261.
- Wu, H., Zhou, T., Li, X., Zhao, C., & Jiang, Z. (2015). Enhancing the separation performance by introducing bioadhesive bonding layer in composite pervaporation membranes for ethanol dehydration. *Chinese Journal of Chemical Engineering*, *23*(2), 372–378.
- Xu, Y., Huang, Y., Wu, B., Zhang, X., & Zhang, S. (2015). Biogas upgrading technologies: Energetic analysis and environmental impact assessment. *Chinese Journal of Chemical Engineering*, *23*(1), 247–254.
- Xue, C., Zhao, J. B., Chen, L. J., Bai, F. W., Yang, S. T., & Sun, J. X. (2014). Integrated butanol recovery for an advanced biofuel: Current state and prospects. *Applied Microbiology and Biotechnology*, *98*(8), 3463–3474.
- Xue, C., Zhao, J., Liu, F., Lu, C., Yang, S. T., & Bai, F. W. (2013). Two-stage in situ gas stripping for enhanced butanol fermentation and energy-saving product recovery. *Bioresource Technology*, *135*, 396–402.
- Yan, B., & Niu, C. H. (2017). Pre-treating biosorbents for purification of bioethanol from aqueous solution. *International Journal of Green Energy*, *14*(3), 245–252.
- Yang, H., Yan, R., Chen, H., Lee, D. H., & Zheng, C. (2007). Characteristics of hemicellulose, cellulose and lignin pyrolysis. *Fuel*, *86*(12–13), 1781–1788.
- Yang, R. T. (1987). *CHAPTER 2 - Adsorbents and Adsorption Isotherms* (pp. 9–48). Butterworth-Heinemann.

Zhang, S., Wang, Z., Zhang, Y., Pan, H., & Tao, L. (2016). Adsorption of Methylene Blue on Organosolv Lignin from Rice Straw. *Procedia Environmental Sciences*, 31, 3–11.

Zhou, Y., Lee, S. Y., & Ghosh, T. K. (1998). Water vapor adsorption-desorption characteristics of a mixed adsorbent. *Chemical Engineering Communications*, 169(1), 57–78.

APPENDIX A. FREUNDLICH MODELING RESULTS OF WATER AND BUTANOL SORPTION

The Freundlich model, which is derived by Freundlich (Freundlich, 1909), has been widely used to describe adsorption isotherms due to its relative simplicity. The Freundlich model is empirical. Conventionally, it is applied as an effective representation of the experimental data, without implying the inherent validity of particular physical model (LeVan & Vermeulen, 1981). Usually, the Freundlich isotherm is suitable to be applied for nonideal sorption of heterogeneous surfaces, and it assumes that there are different types of available sites (Mu & Sun, 2019).

The Freundlich equation is expressed as follows:

$$q = K_f P_i^{\frac{1}{n}} \quad (\text{A. 1})$$

In this equation, q is quantity adsorbed per unit mass of biosorbent, P_i is the partial pressure of the adsorbate in the gas, K_f is the Freundlich coefficient, and $1/n$ is empirical constant. Usually, K_f value corresponds to sorption capacity, and $1/n$ corresponds to sorption intensity (Van der Bruggen, 2015). The $1/n$ value can be used to describe the linearity of sorption within the tested concentration range. Normally, the value of $1/n$ values is smaller than 1.

The Freundlich model was used to describe the pure water and pure butanol sorption on the oat hull based biosorbent. Figure A.1 demonstrates the experimental data and the fitting curves of the Freundlich model. For comparison, the sorption isotherm of water vapor is also presented together with that of butanol vapor on oat hull based adsorbent at the same conditions in Figure A.1. The fitting curve for water sorption is above that of butanol within the range of conditions tested in this study, which again implies water sorption capacity of the biosorbent is higher compared with butanol sorption capacity. The fitting results and parameters obtained from model fitting are listed in Table A.1. It can be concluded from the values of R^2 (0.98, 0.99) that this model

is able to describe pure butanol and pure water sorption in this study. The values of parameter $1/n$ are close to 1, which implies the sorption in a single system is close to linear isotherm within the conditions measured in this study.

Freundlich model is able to describe water and butanol sorption data in a pure component sorption system. However, the Freundlich model is an empirical sorption model, and it can't predict the maximum sorption. Dubinin-Polanyi model provided more information such as the limiting mass of sorption by simulation.

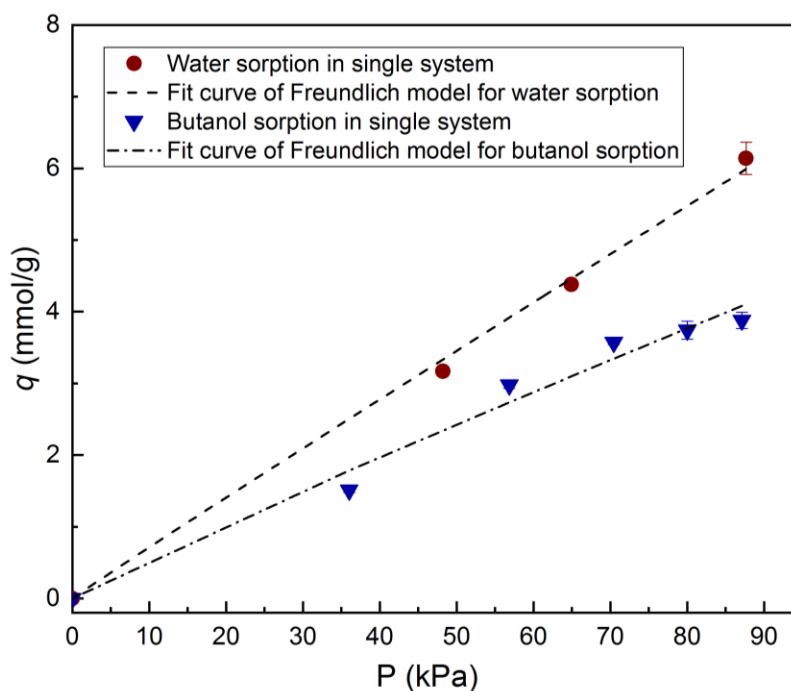


Figure A.1 Fit curves of the Freundlich model for pure water and pure butanol sorption on the biosorbent.

Table A.1 Fitting results of the Freundlich model for pure butanol and pure water sorption.

	K_f	$1/n$	R^2	RSS ((g/g) ²)	P value
<i>Single butanol system</i>	0.062	0.94	0.98	0.02	1.8E-5
<i>Single water system</i>	0.075	0.98	0.99	0.06	1.0E-5

APPENDIX B. THE MEAN FREE ENERGY

The mean free energy of adsorption can be calculated using the Dubinin-Radushkevich (D-R) model. The micropore Dubinin-Polanyi model Eq. 6.1 is similar to the Dubinin and Radushkevich model. Thus, the mean free energy can be obtained by the following expression (Crawshaw & Hills, 1990; Dang et al., 2009; Ranjbar et al., 2013):

$$\bar{E} = \frac{1}{\sqrt{2\kappa_1/\beta}} \quad (\text{B.1})$$

The values of κ_1/β for water and butanol sorption on the biosorbent were estimated by the model fitting of the micropore Dubinin-Polanyi model. The results can be seen in Tables 6.1-6.4. The calculated mean free energy for water and butanol sorption on the oat hull based biosorbent can be seen in Table B.1.

Table B.1 Fitting results of the Freundlich model for pure butanol and pure water sorption.

Water sorption	κ_1/β	\bar{E} (kJ/mol)
<i>Single water system</i>	8.77E-8	2.4
<i>Binary system</i>	5.85E-8	2.9
Butanol sorption	κ_1/β	\bar{E} (kJ/mol)
<i>Single butanol system</i>	5.49E-8	3.0
<i>Binary system</i>	9.89E-8	2.2

The mean free energy is an indicator to distinguish chemisorption and physical sorption. When the value of the mean free energy is higher than 16 kJ/mol, it is chemisorption. If the value of the mean free energy is lower than 8 kJ/mol, it is considered to be physical sorption. The results suggested that the water and butanol sorption process on oat hull based biosorbent is physical. This

result is consistent with the results obtained in other water sorption studies on corn meal (Chang et al, 2006) and canola meal (Ranjbar et al., 2013).

APPENDIX C. ECONOMIC ANALYSIS FOR BUTANOL DEHYDRATION BY DISTILLATION

In biobutanol facilities, the two distillation columns combined with a decanter are responsible for the separation of the butanol-water system because a heterogeneous azeotrope (with 79.9 wt.% butanol in upper phase, 7.7 wt.% butanol in lower phase) of butanol and water forms during the distillation. Aspen Hysys was applied to simulate the distillation process after the decantation using the feed of 80 wt.% butanol and 20 wt.% water. The adsorption process based on the same production scale was also simulated to compare with distillation. Economic evaluations were carried out using Economic module in Aspen Hysys. The economic analysis results of the distillation process can be compared with that of the sorption process. The economic analysis results were shown in Table C.1 and C.2.

Table C.1 Summary of economic analysis for butanol dehydration by adsorption.

Oat hull as biosorbent (80 wt.% butanol feed)	
Investment	Cost
Total capital investment (USD)	2,034,140
Total operating cost (USD/Year)	959,126
Total utilities cost (USD/Year)	42,413
Total equipment cost (USD)	263,700
Total installed cost (USD)	386,600

Table C.2 Summary of economic analysis for butanol dehydration by distillation.

Investment	Cost
Total capital investment (USD)	2,642,710
Total operating cost (USD/Year)	1,263,500
Total utilities cost (USD/Year)	185,492
Total equipment cost (USD)	263,600
Total installed cost (USD)	493,500

It can be seen in Table C.1 and C.2, the butanol dehydration process by adsorption process using oat hull based biosorbent has a lower capital cost, operating cost, and utilities cost compare with distillation. Production of anhydrous biobutanol by pressure swing adsorption process using biosorbent is economically feasible.